The p53 homolog p73 takes hold of the male germ line – a novel function of TAp73 in protecting sperm cell adhesion, migration and maturation within the seminiferous epithelium of the testis

---

PhD Thesis

Dissertation
for the award of the degree
"Doctor of Natural Sciences (Dr. rer. nat.)"
in the "Molecular Biology of Cells" Program
at the Georg August University Göttingen,
Faculty of Biology

submitted by

Lena Holembowski

born in

Lohr a. Main, Germany

Göttingen 2012

PhD Thesis committee:

Prof. Dr. Ute Martha Moll, School of Medicine, University of Stony Brook

Prof. Dr. Matthias Dobbelstein, Faculty of Medicine, University of Göttingen

Prof. Dr. Wolfgang Brück, Faculty of Medicine, University of Göttingen

Prof. Dr. Michael Kessel, Max Planck Institute for Biophysical Chemistry, Göttingen

Date of oral exam: December 13, 2012

AFFIDAVIT

Herewith I declare that I prepared the PhD Thesis: "The p53 homolog p73 takes hold of the male germ line – a novel function of TAp73 in protecting sperm cell adhesion, migration and maturation within the seminiferous epithelium of the testis" on my own and with no other sources and aids than quoted.

Göttingen, 17.11.2012

ACKNOWLEDGMENTS

What is a project without those many people supporting it and bringing it to life? I want to thank…

First of all, my supervisor, Prof. Ute Martha Moll. For giving me the opportunity to do my PhD in her lab and help starting the small group. For her guidance, advice and support, even over long distances, and always making sure I have a running project.

Second, but nevertheless as much, I want to thank my "local contact" person and supervisor Prof. Matthias Dobbelstein. For providing the lab space, giving constant advice and support. For never running out of ideas and having a second view on the project.

Sonja Holzmann, who introduced me into the world of mice and helped getting started into the lab and the project.

Christina Bach, Christin Fischer and Kirsten Pöhlker from the GGNB office for all their organizational help throughout the PhD.

Those, who provided financial support: the Göttingen Graduate School for Neurosciences, Biophysics, and Molecular Biosciences (GGNB) and the deutsche Krebshilfe.

Those, who contributed to this work: Dr. Dietmar Riedel for providing electron microscopy data, Dr. Andrew Wolfe for ELISA measurements, Yvonne Begus-Nahrmann for help and useful tips on mouse experiments, Sona Pirkuliyeva and Kristina Gamper for sharing data.

Frederik Köpper and Alexandra Hackmann for helpful input "how to best formulate and format a thesis".

All present and former members of the Department of Molecular Oncology. Thank you for answering the many questions, for your readiness to help, for sharing your experience and thoughts. Thank you for the great time and sharing so many laughs and stories together (who says science has to be serious all the time?)!

> *Ulrike Keitel, Ramona Schulz, Hannes Landmann, Felix Streller and Xin Zhang for having a great time in the office at the end of the floor and sharing many fruitful discussions.*
>
> *Priyanka Saini, Sai Upadhyayula and Veena Jagannathan for introducing me into the Indian culture and cuisine.*
>
> *Patricia Räke-Kügler, Claudia Buabe, Kamila Sabagh and Kathrin Fricke for support concerning lab organization and bureaucracy.*
>
> *Konstantina Marinoglou, Franziska Schmidt and Magali Hennion for sharing many nice evenings together.*

Antje Dickmanns and Magdalena Wienken for always providing me space at our bench.

Anna Binkowski, Cathrin Hippel, Daniela Kramer, Frederik Köpper, Monika Bug, Muriel Lize, Sonja Krönung and Ulrike Beyer for sharing time at coffee or lunch break and many interesting and philosophic discussions.

I am really happy that I could spend this time with you guys!

Franziska Hof, Anne and Christian Ruschel, Ulrich Friedrich and Thomas Künzel for the shared, valuable thoughts and spent time together. It´s great to have you!

My sisters Johanna and Lisa Holembowski, for being more than sisters and sharing all those emotions and thoughts. I cannot say how much you mean to me.

Christian Metje, for always being there. Thank you for all your love.

Last, not least, my parents. Thank you, for your support, helping me in any situations and always believing in me. I love you.

TABLE OF CONTENTS

TABLE OF CONTENTS I
LIST OF FIGURES V
LIST OF TABLES VII
ABBREVIATIONS IX

1 ABSTRACT 1

2 INTRODUCTION 3

2.1 Reproduction 3
2.1.1 Structure of the male germ line in mice 3
2.1.2 Spermatogenesis 5
2.1.3 Sertoli cells 9
2.1.3.1 Sertoli cells and the spermatogonial niche 9
2.1.3.2 The blood testis barrier 10
2.1.3.3 Sertoli germ cell junctions 11
2.1.3.4 The secretory function of Sertoli cells 12
2.1.4 Hormonal regulation 13
2.1.5 Infertility models 15

2.2 The p53 family 16
2.2.1 Evolution and structure of the p53 family 17
2.2.2 The transcription factors p53, p63 and p73 19
2.2.3 Functions of the p53 family members 20
2.2.4 Mouse models of p73 22

2.3 The p53 family and reproduction 23
2.3.1 p53 and the germ line 24
2.3.2 p63 and the germ line 25
2.3.3 p73 and the germ line 26

2.4 Scope of the thesis 27

3 MATERIALS 29

3.1 Technical devices and equipment 29

3.2 Consumables 31

3.3 Chemicals 33

3.4 Buffers and solutions 35

3.5 Enzymes and PCR solutions 38

3.6 Kits 39

3.7 Cell culture solutions 39
3.7.1 Cell culture components 39
3.7.2 Solutions for Sertoli cell preparation 40
3.7.3 Sertoli cell culture media 40

3.8 Antibodies 41

3.9 Oligonucleotides 42
3.9.1 Oligonucleotides for mouse genotyping PCR 42
3.9.2 Oligonucleotides for quantitative PCR 42

3.10 Mouse strains 44

3.11 Software 44

4 METHODS 46

4.1 Mouse histology 46
4.1.1 Tissue preparation 46
4.1.1.1 Fixation and processing for histologic staining 46
4.1.1.2 Fixation and processing for electron microscopy (EM) 47
4.1.2 Haematoxylin and Eosin (H&E) staining 47
4.1.3 Immunohistochemistry staining (IHC) 48
4.1.4 Immunofluorescence staining (IF) 50
4.1.5 TUNEL assay 50
4.1.6 *In vivo* Biotin assay 51
4.1.7 Quantitation of histologic stainings 51
4.1.7.1 H&E staining – sperm cell mass 52
4.1.7.2 GCNA1 staining – number of spermatogonia 52
4.1.7.3 Ki67 staining – quantitation of proliferation 52
4.1.7.4 H3Ser10 staining – quantitation of meiotic rate 52
4.1.7.5 WT1 staining – Sertoli cell number 52
4.1.7.6 Vimentin – Sertoli cell arms 53
4.1.7.7 Timp1 staining – intensity 53
4.1.7.8 Biotin staining – infiltration 53

4.2 Primary cell culture of Sertoli cells 53
4.2.1 Preparation and culturing of Sertoli cells 53
4.2.2 Immunofluorescence staining 54

4.3 Molecular biology 55
4.3.1 Isolation of genomic DNA from murine tails 55
4.3.2 Polymerase chain reaction (PCR) 55
4.3.3 DNA gel electrophoresis 57
4.3.4 Isolation of total RNA 57
4.3.5 Determination of RNA concentrations 58

4.3.6 Quantification of messenger RNA (mRNA) by PCR ... 58
4.3.6.1 Reverse transcriptase PCR (RT-PCR) ... 58
4.3.6.2 Quantitative real-time PCR (qPCR) ... 59
4.3.7 Whole genome microarray ... 61

4.4 Measurement of serum hormone levels ... 61

4.5 Statistical analysis ... 62

5 RESULTS ... 63

5.1 TAp73 depletion leads to sperm cell loss in testis ... 63
5.1.1 With completion of the first wave of spermatogenesis, p73KO mice show a strong loss of sperm cells throughout the seminiferous epithelium ... 63
5.1.2 TAp73 but not ΔNp73 is necessary for sperm development ... 65
5.1.3 During spermatogenesis, the late developing stages of sperm cells are lost in p73KO and TAp73KO mice ... 68

5.2 Basal proliferation, meiosis and hormonal regulation are not affected in p73KO and TAp73KO testis ... 70
5.2.1 Basal spermatogonia of p73KO mice retain mitotic ability ... 71
5.2.2 The meiotic rate is not changed in p73KO testis ... 71
5.2.3 No impairment of the hormonal axis of p73 and TAp73KO mice ... 73

5.3 Premature sloughing of sperm cells and detachment from the Sertoli-sperm cell cluster ... 74
5.3.1 Mature sperm cells are depleted from p73KO and TAp73KO epididymis whereas immature sperm cells are present ... 75
5.3.2 Sertoli cell number is unchanged in p73KO and TAp73KO testis ... 77
5.3.3 Sertoli cell morphology of TAp73KO mice is impaired ... 77

5.4 Adhesion- and migration-related genes are upregulated in TAp73KO mice, thereby interfering with Sertoli-sperm cell interaction ... 82
5.4.1 TAp73 functions as transcriptional inhibitor in the male germ line ... 82
5.4.2 TAp73KO leads to upregulation of proteinase inhibitors and adhesion-related molecules in the testis ... 83
5.4.3 The structure of the apical ectoplasmic specialization (ES) is impaired in TAp73KO mice ... 88

5.5 Adhesion- and migration-related genes are differentially expressed in sperm and Sertoli cells, and p73 affects gene expression in both cell types ... 90
5.5.1 Timp1 and Serpina3n expression in sperm and primary Sertoli cells ... 90
5.5.2 Integrins and metallopeptidases are differentially expressed in sperm and Sertoli cells ... 92
5.5.3 TAp73 is mainly expressed in sperm cells ... 92

5.6 The blood testis barrier is impaired in TAp73KO mice ... 94
5.6.1 TAp73KO testes have unilateral adhesions at basal Sertoli junctions ... 95
5.6.2 The blood testis barrier of TAp73KO mice is defective ... 95

6 DISCUSSION ... 99

6.1 A new developmental function for TAp73 – protection of spermatogenesis and fertility ... 100

6.2 TAp73 depletion leads to hypospermatogenesis 103

6.3 Premature sloughing of sperm cells as result of TAp73 loss 103

6.4 TAp73 – a transcriptional inhibitor in testis development? 106

6.5 TAp73 regulates adhesion and migration of sperm in the testis 107

6.6 TAp73 – a new player in spermatogenesis 111

7 REFERENCES 113

APPENDIX 128

LIST OF FIGURES

Fig. 2.1 Organization of the testis structure 4

Fig. 2.2 Structure of the epididymis 5

Fig. 2.3 Sperm cell stages 7

Fig. 2.4 Germ cell development 8

Fig. 2.5 Hormonal control of spermatogenesis 14

Fig. 2.6 The p53 family: gene loci and domain structure 18

Fig. 5.1 Testes of developing p73KO mice show normal morphology. Only with adulthood a strong sperm cell loss is visible in p73KO mice compared to WT. 64

Fig. 5.2 TAp73KO mice resemble the observed phenotype for p73KO mice, while ΔNp73 mice show normal testicular morphology. 66

Fig. 5.3 TAp73 is the major isoform of p73 expressed in testis. 67

Fig. 5.4 Testes of TAp73KO mice show reduced numbers of developing sperm cells, especially round and elongated spermatids. 70

Fig. 5.5: Number of spermatogonia in KO mice is unchanged 70

Fig. 5.6 Loss of sperm cells in KO mice is not a result of decreased proliferation or impaired meiosis. 73

Fig. 5.7 The hormonal axis is not affected in p73 and TAp73KO mice. 74

Fig. 5.8 Epididymes of TAp73KO mice display reduced numbers of mature sperm as well as increased numbers of apoptotic and immature sperm. 76

Fig. 5.9 TAp73KO mice display no change in Sertoli cell numbers. 78

Fig. 5.10 Sertoli cell morphology is impaired in TAp73KO mice. 79

Fig. 5.11 Sperm cells are not retained properly by KO Sertoli cells 80

Fig. 5.12 TAp73 exhibits inhibitory functions within the male germ line. 83

Fig. 5.13 The tissue inhibitor of metalloproteinases Timp1 and the serine peptidase inhibitor Serpina3n are strongly upregulated in p73KO and TAp73KO testis. 86

Fig. 5.14 Adhesion- and migration related genes are upregulated in TAp73KO mice. 86

Fig. 5.15 Adhesion- and migration related genes are upregulated in TAp73KO mice. 87

Fig. 5.16 The structure of the apical ectoplasmic specialization (ES) is impaired in TAp73KO mice. 89

Fig. 5.17 Primary Sertoli cell culture as a model system to study mRNA expression levels in Sertoli cells independent from sperm cells. 90

Fig. 5.18 While Timp1 is highly expressed in TAp73KO Sertoli cells, Serpina3n does not show cell specific expression. 91

Fig. 5.19 Differential mRNA expression of adhesion- and migration related target genes in TAp73KO Sertoli and sperm cells. 93

Fig. 5.20 TAp73 is primarily expressed in sperm cells. Upregulation of target genes in TAp73KO Sertoli cells is lost after frequent passaging. 94

Fig. 5.21 Failure of Sertoli-Sertoli cell adhesion in TAp73KO mice 96

Fig. 5.22 TAp73KO mice reveal a defect of the BTB 98

Fig. 6.1 The p53 family protects the germ line 101

Fig. 6.2 TAp73 balances spermatogenesis 110

LIST OF TABLES

Table 3.1: Technical Devices and equipment 29

Table 3.2: Consumables 31

Table 3.3: Chemicals 33

Table 3.4: Enzymes and PCR solutions 38

Table 3.5: Kits 39

Table 3.6: Cell culture components 39

Table 3.7: Primary antibodies 41

Table 3.8: Secondary antibodies and streptavidin conjugates 41

Table 3.9: Primers for PCR 42

Table 3.10: Oligonucleotides for quantitative PCR 42

Table 3.11: Mouse strains 44

Table 3.12: Software 44

Table 4.1: Ascending alcohol series prior to embedding 47

Table 4.2: Descending alcohol series – H&E 48

Table 4.3: Ascending alcohol series – H&E 48

Table 4.4: Ascending alcohol series – IHC 49

Table 4.5: PCR reaction mix 56

Table 4.6: PCR program (p73/TAp73) 56

Table 4.7: RT-PCR mix 1-3 59

Table 4.8: Master mix for qPCR reaction 60

Table 4.9: Cycler program for qPCR 60

Table 5.1: No difference in testis size and weight of adult p73KO and WT mice. 63

Table 5.2: Summary of analyzed p73KO, ΔNp73KO and TAp73KO mice, examining H&E stained testis sections. 67

Table 5.3: Summary of stainings applied to p73KO and TAp73KO testis and epididymis of adult mice. 75

Table 5.4: Adhesion- and migration-associated genes are deregulated in TAp73KO testis. . 84

ABBREVIATIONS

°C	Degree Celsius
µg	Microgram
µL	Microliter
µm	Micrometer
µM	Micromolar
aa	Amino acids
Adam	A disintegrin and metalloprotease domain
AJ	Adherens junction
AR	Androgen receptor
aRNA	Amplified RNA
ATM	Ataxia telangiectasia mutated homologue
Bax	Bcl-2 associated X protein
Bcl-2	B-cell lymphoma 2
bp	Base pair
BTB	Blood testis barrier
c-Abl	c-Abelson murine leukemia viral oncogene homolog
CAR	coxsackievirus and adenovirus receptor
CBP	CREB-binding protein
cDNA	Complementary DNA
CNS	Central nervous system
CRc	Cajal-Retzius cells
Crem	Cyclic AMP responsive element modulator
C-terminal/terminus	Carboxy-terminal/terminus
DAB	3,3`-Diaminobenzidin-tetrahydrochloride
DAPI	4',6-diamidino-2-phenylindole
DBD	DNA-binding domain
DDX4	DEAD box helicase protein 4
Dmc1h	Disrupted meiotic cDNA1 homologue
DNA	Desoxyribonucleic acid
dNTP	Deoxynucleotide triphosphate
dpc	Day post-coitum
(d)pp	(Day) post-partum
DSBs	Double strand breaks
EEC	Ectrodactyly-ectodermal dysplasia-facial clefts syndrome
EGF	Epidermal growth factor
EGFP	Enhanced green fluorescent protein
ELISA	Enzyme-linked immunosorbent assay
EM	Electron microscopy
ER	Endoplasmic reticulum
ERM	Ets related molecule
ERV	Endogenous retrovirus
ES	Ectoplasmic specialization

EthBr	Ethidium bromide
EtOH	Ethanol
FAC	Focal adhesion complex
FCS	Fetal calf serum
FGF	Fibroblast growth factor
FORKO	Follitropin receptor knockout
FSH	Follicle stimulating hormone
g	Gravitational force
GADD45	Growth arrest and DNA damage protein 45
GCNA1	Germ cell nuclear antigen 1
GDNF	Glial cell-line derived neurotrophic factor
GFRα1	GDNF-receptor alpha 1
GnRH	Gonadotropin releasing hormone
GOI	Gene of interest
h	Hour
HAT	Histone acetyl transferase
H&E	Haematoxylin & Eosin
IF	Immunofluorescence
IFN	Interferon
IGF	Insulin-like growth factor
Igfbp3	Insulin-like growth factor binding protein 3
IHC	Immunohistochemistry
IL	Interleukin
IVF	*In vitro* fertilization
JAM	Junctional adhesion molecule
jsd	Juvenile spermatogonial depletion
KO	Knockout
LH	Luteinizing hormone
LIF	Leukaemia inhibitory factor
LTR	Long terminal repeat
M	Molar
MEFs	Mouse embryo fibroblasts
mg	Milligram
min	Minute
mL	Milliliter
mm	Millimeter
mM	Millimolar
Mmd2	Murine double minute 2
MMP	Matrix metalloproteinase
mRNA	Messenger RNA
MYCN	Myc myelocytomatosis viral related oncogene
n	Sample size/Number of mice
ng	Nanogram
NGF	Neural growth factor
nm	Nanometer
nM	Nanomolar

n.s.	Not significant
N-terminal	Amino-terminal
OD	Oligomerization domain
PA(I)	Plasminogen activator (inhibitor)
PBS	Phosphate buffered saline
PCR	Polymerase chain reaction
PI_3K	Phosphatidyl-inositol-3 kinase
PKB	Protein kinase B
PLZF	Promyelocytic Leukaemia Zinc-Finger
POI	Protein of interest
qPCR	Quantitative real-time PCR
RE	Responsive element
RNA	Ribonucleic acid
Rpm	Rounds per minute
RT	Room temperature; Reverse transcriptase
SAC	Spindle assembly checkpoint
SAM	Sterile alpha motif
SCC	Squamous cell carcinoma
SCF	Stem cell factor
SCO	Sertoli cell only syndrome
sec	Second
Serpin	Serine protease inhibitor
SNP	Single nucleotide polymorphism
Sox8	SRY-related HMG-box protein 8
SSC	Spermatogonial stem cells
SV40	Simian vacuolating virus 40
SVZ	Subventricular zone
TAD	Transactivation domain
TAF-4b	Transcription initiation factor TFIID subunit 4B
TBC	Tubulobulbar complex
TdT	Terminal deoxynucleotidyltransferase
TGF	Transforming growth factor
TID	Transcription inhibitory domain
Timp1	Tissue inhibitor of metalloproteinases 1
TJ	Tight junctions
TNFα	Tumor necrosis factor alpha
Tris	Trisamine
TSH	Thyroid stimulating hormone
TUNEL	TdT UTP nick end labeling
U	Unit
UV	Ultraviolet
VEGF	Vascular endothelial growth factor
WT	Wildtype
WT1	Wilms tumor protein 1
ZO-1/2	Zonula occludens protein 1/2

1 ABSTRACT

The p53 family of transcription factors possesses diverge functions in tumorigenesis and development. The evolutionarily conserved role of the family member p63 to protect the genetic stability of germ cells and influence germ cell development is thought to be the ancestral protein function. Using p53, p63 and p73 knockout (KO) mice, the impact of these transcription factors on the female and male germ line was previously investigated. While mice deficient for p53 and p63 are fertile, loss of either all p73 isoforms or of the transcriptionally active TAp73 isoform alone was shown to cause infertility. Concerning its cause, female TAp73KO mice were reported to be infertile due to impaired ovulation, oocyte spindle defects and abnormal blastocyst development. However, the effect of TAp73 loss in the male germ line is unknown.

Here we identify a hitherto unknown function of the transcription factor TAp73 in the development and maintenance of the adult male germ line. Working with total p73KO and isoform-specific KO mice, we find that TAp73, but not ΔNp73 deficiency, leads to a strong loss of developing sperm cells in the testicular tubules of mice 6 weeks and older. Whereas the basal spermatogonia and pachytene spermatocytes of the germ cell epithelium are unaffected (normal cell number and cell proliferation), the numbers of late spermatocytes and spermatids are strongly reduced in global p73- and TAp73-deficient testis. Concomitantly, a higher amount of apoptotic and immature sperm cells accumulate in the lumen of the epididymis of both KO mice, indicating aberrant premature sloughing of sperm cells from the seminiferous epithelium. This finding is reinforced by the observation that the sperm cell nurse cells, the Sertoli cells, display shortened cytoplasmic arms and abnormal vacuolated morphology by electron microscopy. Moreover, the seminiferous epithelium is loosened with loss of tight packaging of sperm cells and strongly disorganized Sertoli-sperm cell junctions. This impaired epithelial structure with aberrant loss of sperm cells appears to be the result of a defective blood testis barrier (BTB), as revealed by *in vivo* BTB permeability assay and aberrant Sertoli-Sertoli tight junctions. Functional loss of the BTB disturbs the epithelial polarity, the microenvironment of developing sperm cells and their upward migration via attachment-reattachment cycles in the germ cell nursing pockets of Sertoli cells. The molecular explanation for imbalanced junctional restructuring was obtained by quantitative whole genome expression profiling of TAp73 target genes comparing wildtype (WT) versus TAp73KO testes tissue. Loss of TAp73 induces upregulation of adhesion- and migration-

related genes including integrins and protease inhibitors like Timp1 and Serpins, known to be involved in disassembly and reassembly of cell-cell junctions in the testis. TAp73 is primarily expressed in the sperm cell fraction and seems to act on Sertoli cells in a paracrine fashion, as revealed by isolated primary Sertoli cell culture, where upregulation of TAp73 target genes declined over time in long-term cultures.

In conclusion, we identify for the first time an indispensable role of TAp73 in adult spermatogenesis. Specifically, TAp73 orchestrates a transcriptional program of adhesion and migration-related genes, ensuring the cohesion of the seminiferous epithelium and preventing premature sloughing of sperm. Together, this enables proper germ cell maturation. Conversely, TAp73 loss leads to severe attachment defects of developing sperm within the seminiferous epithelium, explaining the infertility of p73KO and TAp73KO mice.

2 INTRODUCTION

2.1 Reproduction

Germ cells are the key of sexual reproduction. Compared to other cell types, they have a unique genomic pattern, displaying half the number of chromosomes present in the parent cell. By fusion of a haploid sperm cell with a haploid oocyte, a diploid zygote is formed, giving rise to the generation of new offspring with the identical chromosomal number as the parent.
However, the development of germ cells has to be controlled tightly, since they will be the basis for the following generation of each species. The process from stem cell to mature germ cell has to take place correctly in a certain environment and germ cells have to be protected against exogenous damage and mutations to assure genomic stability for the following offspring. Therefore complex organ systems have been developed in mammals, producing genetically stable germ cells.
Since this thesis is addressing the male germ line, the focus is laid on the testis environment and development of sperm cells. Most of the genes and processes involved in sperm production are described to be conserved between humans and mice. Mice can therefore be used as a convenient model system for analyzing the male germ line.

2.1.1 Structure of the male germ line in mice

The testes of mammals are paired organs, giving rise to a 100 millions of spermatozoa per day (Xia *et al.*, 2005b). The seminiferous tubules and the interstitial space of the testis are surrounded by a connective tissue capsule, the tunica albuginea. Germ cells are produced in the seminiferous epithelium of these tubules (refer to **2.1.2**), which also harbours the germ cell supporting Sertoli cells (refer to **2.1.3**) (Roosen-Runge, 1962). The tubules are enclosed by contractile myoid cells, also called peritubular cells, building the tunica propria together with layers of collagen and elastic fibers as well as immune cells like monocytes and mast cells (Clermont, 1958, Hermo *et al.*, 1976). The interstitial space between the seminiferous tubules consists of the testosterone producing Leydig cells (refer to **2.1.4**), macrophages, nerves as well as lymphatic and blood channels (Christensen *et al.*, 1965, Borg *et al.*, 2010). Besides macrophages, which are important for immune and inflammatory responses, dendritic cells, T cells and natural killer cells can be found in the interstitial area (Hutson, 1994, Tompkins *et al.*, 1998). The structure of the murine testis and the involved cell types are shown in *Figure 2.1* (Cooke *et al.*, 2002). After passing the developmental processes in

the seminiferous epithelium of the testicular tubules, spermatozoa are released in the tubular lumen. They travel to the rete testis and are transported to the head of the epididymis via the efferent duct system.

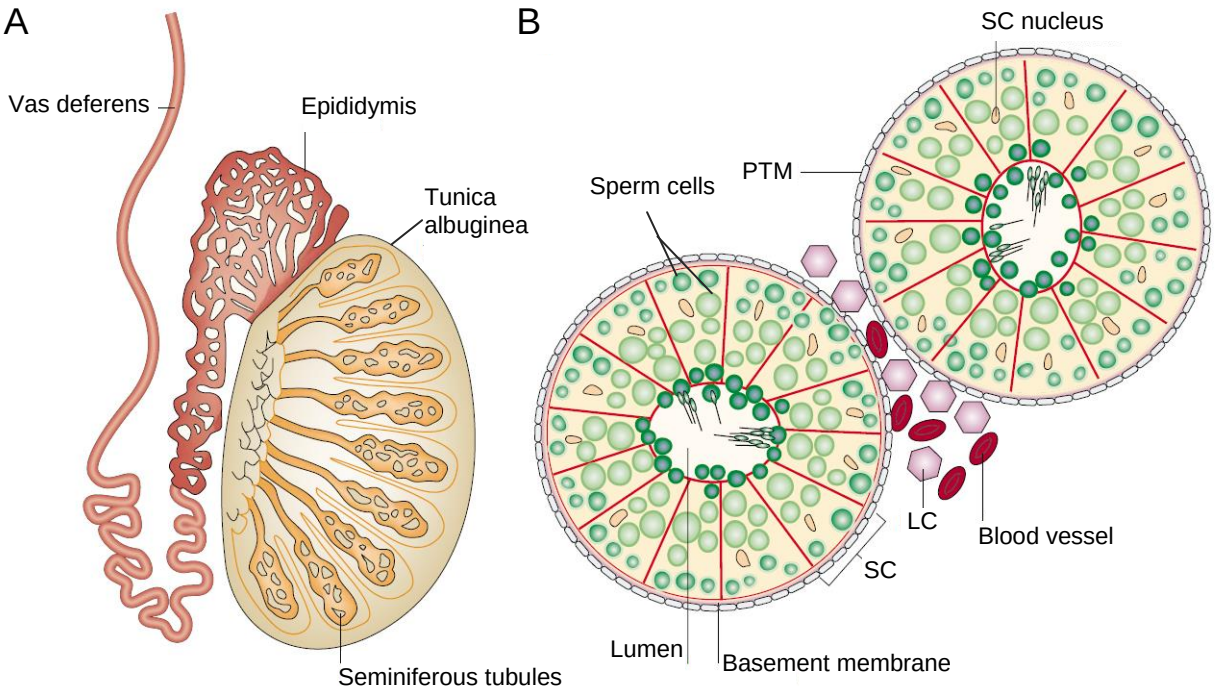

Fig. 2.1 Organization of the testis structure

A) The testis is surrounded by a connective tissue capsule, the tunica albuginea. The seminiferous tubules are winding themselves through the entire testis. They harbour the sperm cells and transport the released spermatozoa towards the rete testis into the epididymis. The epididymis is located close to the testis, spanning itself over the entire length of the testis. Like the testis it consists of highly convoluted tubules. Sperm cells undergo further maturation while travelling through the epididymis and are released into the vas deferens upon ejaculation.
B) The cellular structure of the testis is depicted. Seminiferous tubules are limited by the basement membrane and the surrounding PTMs (peritubular myoid cells), which together build the tunica propria. The seminiferous epithelium of the tubules consists of Sertoli cells (SC - yellow cells, outlined with red), spanning through the entire epithelium, and of the developing sperm cells at different maturation stages (green cells) embedded in the SCs. Tails of spermatozoa are reaching into the tubular lumen (dark green cells). After release from the seminiferous epithelium into the seminiferous fluid they will be transported towards the epididymis. Another type of somatic cells, the Leydig cells (LC - purple cells) are located next to blood vessels in the interstitial space between the tubules.
(modified after Cooke and Saunders, 2002)

The epididymis is located directly next to the testis, wrapping itself around its total length (*Figure 2.1*). It can be separated into three parts, the head of the organ (caput), the body (corpus) and the tail (cauda) (*Figure 2.2*, after (Borg *et al.*, 2010)). The histology of the epididymis shows that it is a long and highly convoluted tubule itself and can be classified into seven internal regions, according to their epithelial morphology and present tissue septae

(Soranzo *et al.*, 1982, Takano, 1980). After further maturation steps mature spermatozoa are released in the vas deferens during the ejaculation process.

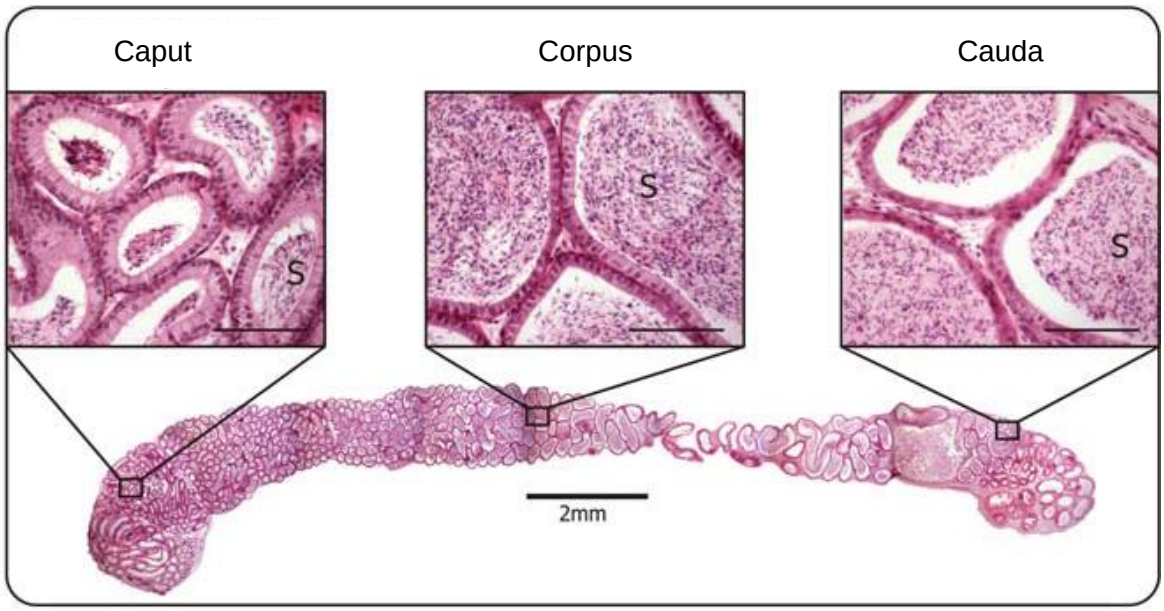

Fig. 2.2 Structure of the epididymis

The epididymis can be divided into three main parts: caput, corpus and cauda epididymidis. Spermatozoa travelling through the rete testis enter the epididymis at the head (caput). While travelling through the caput and corpus epididymidis, spermatozoa undergo further post-testicular maturation steps. The tail of the epididymis (cauda) is thought to mainly function as storage for the mature, still immotile sperm cells. (modified after Borg et al., 2010)

2.1.2 Spermatogenesis

Mice reach fertility at around 6 to 7 weeks of age. At this time point the first wave of spermatogenesis is completed and mature spermatozoa are present (Bellve *et al.*, 1977, Kramer *et al.*, 1981). From now on sperm cells will be produced continuously in the adult testis. The complex process of spermatogenesis can be divided into 3 phases: the spermatogonial and meiotic phases (Ia and Ib), spermiogenesis (II) and spermiation (III) (Cooke *et al.*, 2002).

The spermatogonial phase is necessary to maintain the stem cell pool of the testis throughout life. Spermatogonia are localized close to the basement membrane of the seminiferous tubule, accompanied by Sertoli cells. They undergo mitotic divisions to replace themselves frequently (self-proliferation) and to provide a constant supply of a basic population for the following meiotic steps to finally produce mature spermatozoa. Dependent on functional criteria, they can be classified into spermatogonial stem cells (As), able to colonize a recipient

testis after transplantation, and differentiated spermatogonia. The latter ones are divided into type A and B spermatogonia, according to their morphology and gene expression pattern. Type A spermatogonia divide asymmetrically into type A and B spermatogonia (de Rooij, 2001, Oatley *et al.*, 2006). With type B spermatogonia, meiosis is initiated.

Meiosis can be divided into two cell divisions and, compared to mitosis, the final outcome is the bisection of the chromosomal number from diploid to haploid. Meiosis I starts with the separation of the homologous chromosome pairs and meiosis II separates the sister chromatids of one chromosome. Therefore 4 haploid gametes will evolve out of one spermatogonium. Meiosis I consists of 5 phases based on cytological features and chromosome dynamics: prophase, metaphase, anaphase, telophase and cytokinesis (Baarends *et al.*, 2001). The prophase takes 90% of the time during meiosis I and can further be divided into 5 stages, called leptotene, zygotene, pachytene, diplotene and diakinesis. During these stages highly condensed homologous chromosomes (each build of two sister chromatids) will assemble longitudinally to each other and will be joined by the synaptonemal complex (SC). Now crossing over between homologous chromatids can occur and recombination events will increase the genetic variability. This bivalent structure, containing four chromatids, is also called chiasmata or tetrad stage and additionally helps positioning the chromosomes at the meiotic spindle (Cobb *et al.*, 1998, Cohen *et al.*, 2006). By reaching the leptotene stage, germ cells are now called spermatocytes I and start moving towards the luminal part of the seminiferous epithelium. After attachment of paired chromosomes to the spindle (metaphase), movement of single chromosomes to opposite poles of the spindle (anaphase), uncoiling of chromosomes into loose chromatin (telophase), and separating of the two poles into two new daughter cells (cytokinesis), the gametes are now called spermatocytes II. These cells still contain a diploid DNA content, but only a haploid number of chromosomes, each cell possessing different genetic information. With completing the second meiotic division, which is comparable to the mitotic process, spermatids finally contain a haploid DNA content with a haploid chromosomal number (Handel *et al.*, 1999). These initial meiotic steps are crucial for the production of viable gametes and any failure will result in the absence of sperm or the production of aneuploidic sperm cells.

Round postmeiotic spermatids will subsequently undergo spermiogenesis. Experiencing extensive morphological changes, they gain polarity, develop into elongated spermatids and finally into spermatozoa. Structural processes of spermiogenesis include the formation of the acrosome, which contains the enzymes necessary for the sperm to penetrate the oocyte, condensation and elongation of the nucleus, development of a flagellum and the elimination of cytoplasm (Ward *et al.*, 1991, Cooke *et al.*, 2002). The excess cytoplasm together with

packed RNA and organelles is also called residual bodies and is phagocytosed by Sertoli cells. Astonishingly, the size of the spermatid head decreases to around 5% of a somatic cell nucleus. Nuclear condensation is thereby achieved by removing the histones and replacing them first with transition proteins Tnp1 and Tnp2 and finally with the protamines PRM1 and PRM2, which are unique for spermatids. The tightly packed chromatin is transcriptionally inactive (Brewer *et al.*, 1999, Ward *et al.*, 1991). The reshaping of the sperm cell will ensure its future motility and ability to fuse with the oocyte.

When we look at the seminiferous epithelium of the murine testis, we find a certain positioning and defined association of sperm cells in the already described stages; the spermatogonia at the very basal level, meiotic cells in the next layer, round spermatids following and close to the lumen elongated spermatids and spermatozoa (Leblond *et al.*, 1952, Oakberg, 1956). Therefore sperm cells migrate from basal to luminal, while developing from stem cells to spermatozoa (*Figure 2.3, after (Cooke et al., 2002)*). Differentiating sperm cells remain connected to each other by cytoplasmic bridges. In more detail twelve stages of sperm cells (I-XII) are described in mice, according to the histology of the cell. The occurrence of these twelve cell stages over time in a given area of the tubule are defined as the “cycle of the seminiferous epithelium” (Leblond *et al.*, 1952, Oakberg, 1957).

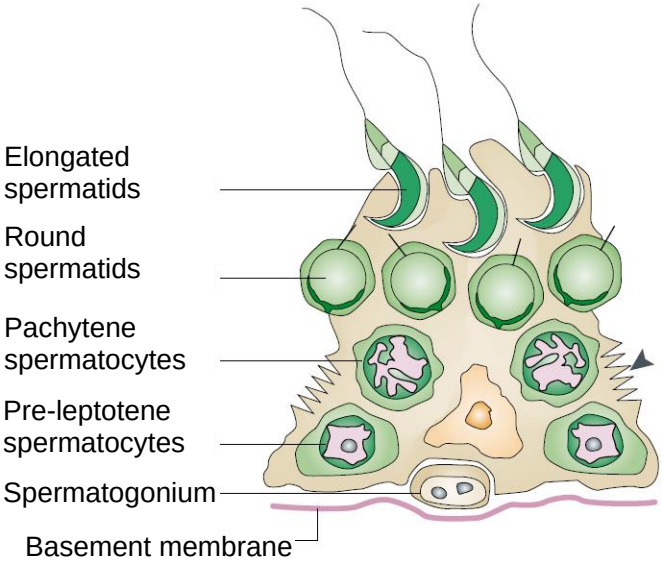

Fig. 2.3 Sperm cell stages

One columnar Sertoli cell can wrap its cytoplasmic arms around several sperm cells of different stages. Sperm cells undergo maturation from spermatogonia to elongated spermatids. They migrate from basal to luminal while undergoing meiosis and spermiogenesis. Tight junctions (arrowhead) between adjacent Sertoli cells divide the seminiferous epithelium into two compartments: the stem cell compartment (stem and pre-meiotic cells) and the developmental compartment (meiotic and spermiogenic cells). (modified after Cooke and Saunders, 2002)

The first wave of sperm production is synchronous throughout the testis. If we therefore look at a particular cross-section of a tubule on histological level all germ cells will show the same developmental stage. In mice differentiated spermatogonia appear postnatal at day 8 pp (post-partum). Meiosis I starts 10 days after birth and secondary spermatocytes can be seen by day 18 pp. Round spermatids are already found at day 20 pp, but spermiogenesis only

starts at day 30 pp. Around 5 to 7 weeks after birth spermatozoa can be found and are from now on produced periodically throughout life time (*Figure 2.4*, after (Barakat *et al.*, 2008)) (Bellve *et al.*, 1977, Nebel *et al.*, 1961).

Mature, but immotile spermatozoa are finally released from the seminiferous epithelium into the tubular lumen by spermiation. Through progressive loss of adhesive cell junctions sperm cells are able to detach from the Sertoli cells. At this point sperm cells are structurally complete, but functionally immature (O'Donnell *et al.*, 2011).

Spermatozoa move towards the rete testis and into the caput epididymidis by peristaltic contraction achieved by the tunica propria. In the epididymis post-testicular sperm maturation takes place. This includes remodelling of the membrane lipid composition, removal and addition of proteins to the sperm and post-translational modifications like glycosylation and phosphorylation (Aitken *et al.*, 2007, Baker *et al.*, 2005, Schlegel *et al.*, 1986). Sperm cells obtain their functional competence while travelling through the whole length of the epididymis. The cauda epididymidis is described to mainly function as storage of mature, still immotile spermatozoa (Jones, 1999). Only by ejaculation and residence in the female reproductive tract they gain motility, undergoing a process called capacitation, and are able to fertilize the egg through the acrosome reaction (Austin, 1952).

Fig. 2.4 Germ cell development

First wave of spermatogenesis –
the following stages are depicted:

0 dpp: gonocytes
4 dpp: spermatogonia, type A
6 dpp: spermatogonia, type B
8 dpp: pre-leptotene spermatocytes
10 dpp: zygotene spermatocytes
16 dpp: pachytene spermatocytes
26 dpp: round spermatids
42 dpp: elongated spermatids

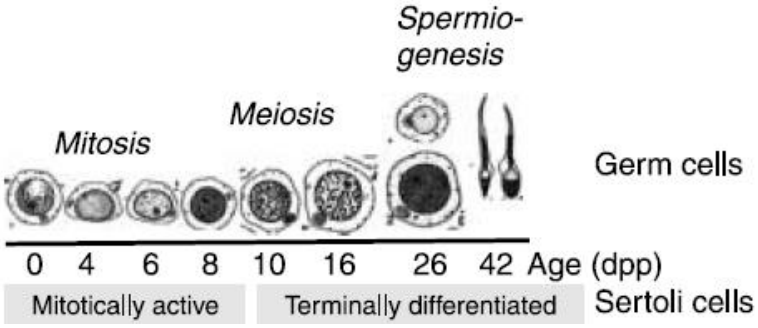

Prenatal Sertoli cells are mitotically active and cease to divide, when spermatogenesis starts around day 8-10. They get terminally differentiated and form Sertoli–Sertoli cell tight junctions. (modified after Barakat et al., 2008)

2.1.3 Sertoli cells

Sertoli cells were first described in 1865, by Enrico Sertoli. Sertoli cells sit on the basement membrane of the testicular tubules, their cytoplasmic arms reaching through the entire seminiferous epithelium. By enveloping all surrounding germ cells they are thought to have a crucial nursing role, providing physical support, nutrients and paracrine signals for the development of the sperm cells (Griswold, 1998). An adult Sertoli cell is able to get in contact with five different sperm cell types, supporting 30 to 50 germ cells in total. Developing sperm cells migrate from the basement membrane to the apical lumen of the tubule, all time staying in contact with the Sertoli cells. This process is facilitated by restructuring the Sertoli cell cytoskeleton and Sertoli-germ cell junctions. Sertoli cells also trigger spermiation, the release of these immature spermatozoa into the lumen (Mruk *et al.*, 2004). They are thought to only possess constant mitotic activity during the maturation stages in testis development (Kluin *et al.*, 1984). With puberty, the round-shaped progenitor cells elongate and mature Sertoli cells form tight junctions between them (*Figure 2.3* and *2.4*). However, even differentiated Sertoli cells were described to loose proliferative capacity upon adulthood, adult Sertoli cells transplanted into Sertoli defective testes were able to restore the acceptor Sertoli cell pool and spermatogenesis in infertile mice (Shinohara *et al.*, 2003). Additionally, during primary cell culture, adult Sertoli cells were reentering the cell cycle and could be maintained for several months under optimized conditions before going into senescence (Ahmed *et al.*, 2009, Chui *et al.*, 2011). Therefore, mature Sertoli cells were described to be terminally differentiated, quiescent cells that contain subpopulations with stem cell-like character and proliferative capacity (Hayrabedyan *et al.*, 2012).

2.1.3.1 Sertoli cells and the spermatogonial niche

Spermatogonial stem cells (SSCs) are the basis of spermatogenesis. To maintain fertility throughout life time, a balance between self-renewal and differentiation of the SSCs has to be ensured. Therefore SSCs reside in a specific microenvironment, the so called stem cell niche. On the one hand maintenance of self-renewal is dependent on intrinsic gene expression within the stem cells. For example the transcription factor Plzf (Promyelocytic Leukaemia Zinc-Finger) acts as transcriptional repressor to support self-renewal (Buaas *et al.*, 2004, Costoya *et al.*, 2004). And TAF-4b, a germ cell specific subunit of the RNA polymerase complex (TFIID), is essential for spermatogonial stem cell proliferation (Falender *et al.*, 2005). On the other hand self-renewal and differentiation of SSCs are strongly dependent on extrinsic signals, mainly coming from the Sertoli cells. By building tight

junctions between themselves, Sertoli cells divide the seminiferous epithelium into a basal compartment harbouring spermatogonia and an adluminal compartment containing the meiotic and spermiogenic germ cells (also refer to **2.1.3.2**). The basal compartment serves as niche for the SSCs and only there self-renewal and maintenance is possible. During early postnatal development, while Sertoli cells are maturing, the SSC niche develops (Ogawa *et al.*, 2005, Dadoune, 2007). Sertoli cells secrete several soluble factors, influencing SSC self-renewal or differentiation. GDNF (glial cell-line derived neurotrophic factor) is a member of the TGF-β family and is produced and secreted by Sertoli cells. It binds to GDNF receptors on SSCs, like GFRα1 or c-RET tyrosine kinase receptor, which in turn will activate the PI_3-kinase (phosphatidyl-inositol-3) or Src tyrosine kinase pathway, ensuring cell survival. GDNF stimulates SSC proliferation and is important for maintenance of the self-renewal ability of SSCs during the perinatal period of development (Meng *et al.*, 2000, Naughton *et al.*, 2006, Sariola *et al.*, 2003). Differentiation of SSCs beyond type A spermatogonial stages is enabled by another Sertoli cell product, the stem cell factor SCF (steel locus). Upon spermatogenesis SCF is produced, activating the c-KIT tyrosine kinase - PI_3K/PKB/AKT survival pathway (Blume-Jensen *et al.*, 2000, Ohta *et al.*, 2000). It is hypothesized that GDNF signalling activates the transcriptional repressor Plzf in undifferentiated spermatogonia and that SCF signalling might neutralize this repression to drive differentiation (Berruti, 2006). The transcription factor ERM (Ets related molecule) is expressed in Sertoli cells during the pubertal period and is required for maintenance of self-renewal and spermatogenesis in adult mice throughout life (Chen *et al.*, 2005).

2.1.3.2 The blood testis barrier

The blood testis barrier (BTB) acts as a boundary between proliferating diploid spermatogonia at the basement membrane and differentiating haploid spermatocytes and spermatids migrating towards the tubular lumen. It therefore creates a specific microenvironment necessary for the SSCs (refer to **2.1.3.1**) and protects the developing sperm cells against harmful agents and an auto immune response against the unique antigens of the testis. Different junctional complexes are part of the BTB: gap junctions, desmosomal-like junctions, tight junctions, and the so called basal ectoplasmic specialization (ES) as well as the basal tubulobulbar complex (TBC). In contrast to other somatic cells, tight junctions of Sertoli cells are found closest to the basement membrane and help to maintain an impermeable barrier and cell polarity. In murine testis, the transmembrane proteins of the occludin-, claudin- and JAM-family are linked to the cytoskeleton via the adaptors ZO-1/ZO-2 (Xia *et al.*, 2005b). Coexisting with tight junctions the basal ES can be found at the BTB. The

basal ES exists as homotypic interactions between adherens junction (AJ) transmembrane proteins like cadherins (calcium-dependent junctions) and nectin-2. Thereby N- or E-cadherin interact with γ-catenin or β-catenin that are linked to the actin cytoskeleton via α-catenin. Nectin-2 is linked to the actin filament bundles (filamentous actin = F-actin) via afadin (Lee *et al.*, 2003, Ozaki-Kuroda *et al.*, 2002, Takai *et al.*, 2003). When entering meiosis, developing spermatocytes have to pass the BTB and migrate to the upper layers of the seminiferous epithelium (Russell, 1977). This is possible by transient opening (dissolving) of the junctions and closing (regenerating) them directly after spermatocytes have passed. The engagement and disengagement theory states that remodelling processes and coordination between proteins of the ES and TJ enable the movement of pre-leptotene spermatocytes across the BTB (Yan *et al.*, 2005). Additionally, integrins have been discussed being part of the BTB. They are heterodimeric transmembrane receptors, composed of α and β subunits. Several of these subunits, like α6 β1 integrin, have been found in testis, but it is not yet sure if they are primarily located to cell-matrix (FAC – focal adhesion complex, hemidesmosomes) or cell-cell (i.e. basal ES) junctions (Giebel *et al.*, 1997, Salanova *et al.*, 1995).

2.1.3.3 Sertoli germ cell junctions

Developing spermatocytes and spermatids are attached to Sertoli cells via AJs and desmosome-like (hybrid junction between gap junctions and desmosomes) junctions. When germ cells migrate from basal to luminal, extensive junction-restructuring events between Sertoli and sperm cells take place during the seminiferous cycle. Exchange of ions and small molecules between Sertoli and germ cells is enabled by gap junctions, channels consisting of connexin subunits (Mruk *et al.*, 2004). The tightest adhesion between Sertoli cells and germ cells is observed at the apical junction (Wolski *et al.*, 2005). It connects the head of the spermatozoa and elongated spermatids with Sertoli cells, the sperm tail reaching into the lumen of the tubule. These junctions are adherens-like junctions and specific for the testis, called apical ectoplasmic specialization (apical ES). Like the basal ES, which is part of the BTB (refer to **2.1.3.2**), they consist of a similar pool of junctional proteins and have a certain cytoskeletal structure. The apical ES is an actin-based hybrid anchoring junction sharing structures of tight junctions, adherens junctions and focal contacts (Yan *et al.*, 2007). In contrast to the basal ES the apical ES does not include TJ as such. However, TJ transmembrane proteins like the junctional adhesion molecule-B and C (JAM-B/C) and the coxsackievirus and adenovirus receptor CAR have been found at the apical ES, which might influence spermatid polarization and orientation (Coyne *et al.*, 2005, Gliki *et al.*, 2004, Mirza *et al.*, 2006). Also different to the basal ES, you find heterotypic actin-based adherens

junctions with nectin-2 on Sertoli cells connecting to nectin-3 on sperm cells (Takai *et al.*, 2003). Another intensively studied junction is the α6β1-integrin-laminin333 complex. Laminin is a heterotrimeric glycoprotein of three chains, usually found at FACs of the cell-matrix interface and within the basement membrane (Koch *et al.*, 1999, Salanova *et al.*, 1995, Yan *et al.*, 2007, Yan *et al.*, 2006). Functionally, the apical ES is important for correct positioning of the sperm cell, it influences the elongation process of spermatids and retains the sperm cells until spermiation (Mruk *et al.*, 2004, Yan *et al.*, 2007).

To enable the release of spermatazoa, part of the apical ES has to be exchanged into the apical TBC. The TBC is a cytoplasmic evagination of the spermatid head with tubular and bulbous portions, which are surrounded by a branched actin network and endoplasmic reticulum (ER). Functions of the TBC include elimination of cytoplasm to decrease the volume of the spermatid, endocytosis and recycling of junctional molecules (like nectins or integrins), shaping of the acrosome and transiently anchoring spermatids to the cytoplasmic processes of Sertoli cells before preparing their release into the tubular lumen. By cytoskeletal remodelling and disruption of the apical ES and the TBC, spermiation takes place (Russell, 1979b, Russell, 1979a, Upadhyay *et al.*, 2012).

2.1.3.4 The secretory function of Sertoli cells

Sertoli cells are secretory cells and support germ cell development, growth and movement via various groups of proteins. These include proteases and protease inhibitors, hormones and paracrine factors, growth factors and energy substrates (Mruk *et al.*, 2004).

Proteases and protease inhibitors are involved in many cellular processes, like repair, growth, development and germ cell movement. The protease Cathepsin L for example was described to play a role during spermiogenesis at the apical ES, its expression peaking at the developmental stage of elongated spermatids (Chung *et al.*, 1998). An increase in overall serine protease activity in *in vitro* sperm - Sertoli cell adhesion experiments shows that proteases are also required for junction assembly (Mruk *et al.*, 1997). Proteases and their antagonists, the protease inhibitors, are produced by Sertoli cells, controlling junction assembly and disassembly upon secretion (Wright *et al.*, 1989, Le Magueresse-Battistoni, 2007).

Cytokines, like tumor necrosis factor TNFα, interleukins (IL-1, IL-6, IL-11), interferons (IFN-α), growth factors (NGF, FGF) and transforming growth factors of the TGF-β family are also secreted by Sertoli cells. They can act in an either paracrine or autocrine fashion, supporting Sertoli cell proliferation, sperm cell movement, junction remodelling and differentiation (Xia *et*

al., 2005b). TNFα, for example, can counteract germ cell apoptosis and inhibits TJ formation at the BTB (Pentikainen *et al.*, 2001, Siu *et al.*, 2003).

The glycoprotein-hormones activin and inhibin belong to the TGF-β superfamily and are both expressed in Sertoli cells. They are dimeric proteins formed by two peptide chains, which are linked via a disulfide bond. Activins form homo- or heterodimers using the β-subunits β_A, β_B and β_C. Inhibins contain one of these β subunits and one α-subunit (de Kretser *et al.*, 2001, de Kretser *et al.*, 2004). Like FSH (refer to **2.1.4**) and a big group of growth factors (i.e. FGF, IGF, EGF, TGFα), activins stimulate proliferation and growth of Sertoli cells during development (Boitani *et al.*, 1995, Buzzard *et al.*, 2003, Petersen *et al.*, 2001). Activins, mainly expressed by Sertoli cells, but also found in germ cells, influence germ-cell maturation, i.e. by stimulation of spermatogonial proliferation or by maintaining mitochondrial morphology of germ cells beyond the pre-leptotene stage. Inhibin B (α-β_B dimer) is the major inhibin in testis and is produced by adult Sertoli and Leydig cells (de Kretser *et al.*, 2004, de Kretser *et al.*, 2001). Inhibins are able to antagonize activins directly by binding to the activin type II kinase receptors and blocking type I kinase receptor recruitment, subsequent Smad phosphorylation and its nuclear import and transcriptional activity (Lewis *et al.*, 2000). Additionally, activin activity can be inhibited by another TGF-β family member Follistatin as well as by FSH (Hashimoto *et al.*, 1997). Inhibin B is also thought to inhibit FSH-secretion from the pituitary gland (*Figure 2.5*, after (Borg *et al.*, 2010)).

Nourishing germ cells via their secretory products is another important task of the Sertoli cells. They provide amino acids, carbohydrates, lipids, vitamins and metal ions. Sertoli cells are able to efficiently metabolize glucose to lactate, which is the preferred energy source of germ cells (Robinson *et al.*, 1981). The transport of some nutrients is likely enabled by gap junctions between Sertoli and sperm cells (Mruk *et al.*, 2004).

The seminiferous fluid within the tubular lumen is also produced and secreted by Sertoli cells. It supports spermiation by sheering forces, provides the nutritional and hormonal microenvironment for sperm development and transports released spermatozoa towards the epididymis (Mruk and Cheng, 2004).

2.1.4 Hormonal regulation

Testicular function is not only controlled by intra-testicular paracrine signals, but also by extra-testicular, circulating hormones of the brain. The hypothalamus-pituitary-testis hormone axis regulates spermatogenesis. Gonadotropin releasing hormone (GnRH) is produced by the hypothalamus and is increasing with puberty. It activates the production of the

gonadotropins, follicle stimulating hormone (FSH) and luteinizing hormone (LH), in the pituitary gland (*Figure 2.5*, after (Borg *et al.*, 2010)).

FSH is only regulating one cell population in the testis, the Sertoli cells, which express the correspondent receptor on their surface. It is necessary for Sertoli cell proliferation and it stimulates their aromatase activity and production of inhibin, lactate, transferrin and androgen receptor (AR) (Bicsak *et al.*, 1987, Mita *et al.*, 1982, Skinner *et al.*, 1989). Besides FSH other endocrine factors like TSH (thyroid stimulating hormone) or Prolactin have been implicated in Sertoli cell proliferation and differentiation, TSH being able to interact with the FSH receptor (Scarabelli *et al.*, 2003, Van Haaster *et al.*, 1992). LH on the other hand is stimulating Leydig cells, positioned in the interstitial space of the testis. Upon binding of LH, Leydig cells start to produce testosterone, its synthesis increasing strongly during puberty. The only cell type in the seminiferous epithelium expressing the testosterone-responsive androgen receptor (AR), are the Sertoli cells. The paracrine regulation of Sertoli cells by an adequate level of intra-testicular testosterone is required for BTB function, meiosis and post-meiotic development of sperm cells (Meng *et al.*, 2005, Tan *et al.*, 2005).

Fig. 2.5 Hormonal control of spermatogenesis

Sperm maturation is influenced by the hormonal hypothalamic-pituitary-testis axis. Gonadotropin releasing hormone GnRH is produced by the hypothalamus and activates secretion of the gonadotropins LH and FSH from the pituitary gland. In turn LH is activating Leydig cells to produce testosterone. FSH and testosterone directly influence Sertoli cells, which communicate with sperm cells and ensure sperm cell development. Additionally, two negative regulatory feedback loops are described for the hormonal regulation of the testis. Testosterone, secreted from Leydig cells, and Inhibin B, produced by Sertoli cells, act at the hypothalamus and the pituitary gland, modulating GnRH, LH and FSH secretion. (modified after Borg et al., 2010)

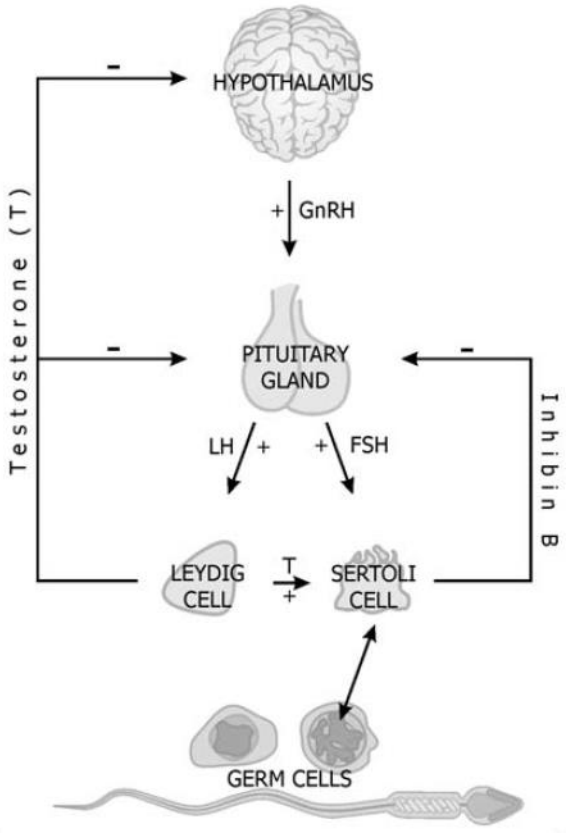

The hormone axis is controlled by negative feedback loops through testosterone from Leydig cells and inhibin B from Sertoli cells, the first one regulating LH levels and the second one

FSH levels (*Figure 2.5*, after (Borg *et al.*, 2010)). Testicular cells are also the source of estrogens and do express estrogen receptors. Immature Sertoli cells are able to produce estrogen via their aromatase activity, the enzyme P450 converting androgens to estrogens. During adulthood Leydig and germ cells take over estrogen production. However, even if male P450 knockout (KO) mice become infertile with age, the direct influence of estrogens on spermatogenesis has not been described yet (Aschim *et al.*, 2004, Carreau *et al.*, 1999, Robertson *et al.*, 1999, Rommerts *et al.*, 1982).

2.1.5 Infertility models

As described in chapter **2.1.1** to **2.1.4,** spermatogenesis is a complex process requiring many steps, signals and cell types. Any mistake or missing action during sperm maturation will subsequently affect the sperm quality and/or quantity. There are many mutant mouse models known, where specific processes during spermatogenesis are impaired, resulting in malfunctioning of sperm cells or infertility. Dependent on the phenotype different types of male infertility are classified.

The loss of all germ cells is referred to as Sertoli cell only syndrome (SCO). As an example, in juvenile spermatogonial depletion (jsd) KO mice one wave of spermatogenesis is completed, but further sperm cycles are impaired since type A spermatogonia fail to differentiate. Adult testes therefore only contain Sertoli cells (Boettger-Tong *et al.*, 2001). A comparable phenotype can be observed for ERM KO mice, which fail to develop new sperm cell layers after 6 weeks of age (also refer to **2.1.3.1**) (Chen *et al.*, 2005).

When sperm cells are missing from the seminiferous epithelium at a certain developmental stage (i.e. meiosis, spermiogenesis), it is defined as germ cell arrest. Examples for meiotic arrest phenotypes are mice depleted of genes encoding for components of the synaptonemal complex or the DNA repair machinery (also refer to **2.1.2**). Dmc1h (disrupted meiotic cDNA1 homologue, involved in strand exchange) KO mice show chromosome synapsis errors during recombination, and spermatocytes with unresolved DNA breaks are eliminated by p53-independent apoptosis (Odorisio *et al.*, 1998, Pittman *et al.*, 1998, Yoshida *et al.*, 1998). The PI_3 kinase ATM (ataxia telangiectasia mutated homologue) is recruited to double strand breaks (DSBs) at the site of meiotic recombination and loss of ATM leads to infertility in mice and man (Barlow *et al.*, 1998). Arrest in spermiogenesis for example is seen in mice deficient of protamines (also refer to **2.1.2**), since DNA compaction cannot be performed and therefore development of spermatids is lost. Sperm cells do not develop beyond the first step of spermiogenesis in Prm1 and Prm2 KO mice as well as in Crem KO mice, which are depleted of the transcriptional regulator “cyclic AMP responsive element modulator” (Crem) that is

involved in regulation of protamine expression (Blendy *et al.*, 1996, Cho *et al.*, 2001, Ha *et al.*, 1997).

In hypospermatogenic testes all sperm stages are present, but at least one type in reduced numbers. Additionally, normal tubules can be located close to tubules missing germ cell populations. Hypospermatogenesis includes the loss of a gene either involved in germ cell development, Sertoli cell function or germ cell colonization. For example, FORKO mice lacking the FSH receptor, usually expressed on Sertoli cells (refer to **2.1.4**), display reduction of Sertoli cells by 50%, accompanied by reduced spermatid numbers and aberrant morphology of sperm. These mice are subfertile (Krishnamurthy *et al.*, 2000). A similar phenotype is described for men harbouring an inactivating mutation of the FSH receptor (Tapanainen *et al.*, 1997).

A defect in Sertoli-sperm cell adhesion can also lead to loss of sperm cells. Apical junction failure may result in abnormal sperm retention in the testis (spermiation failure). In Sox8 KO mice resolution of the apical ES is impaired resulting in increased elongated spermatid retention (O'Bryan *et al.*, 2008). Additionally, premature sloughing of sperm cells is often the reason for adhesion defects. The enzyme α-mannosidase IIx synthesizes a carbohydrate N-glycan, which is necessary for the interaction between germ and Sertoli cells. Loss of this enzyme leads to premature release of sperm cells from the seminiferous epithelium (Akama *et al.*, 2002).

If no defect in testicular development can be observed and sperm morphology as well as sperm count seem to be relatively normal, but mice are nevertheless infertile, changes in post-testicular maturation of sperm cells can be the reason. This can be due to defects in epididymal formation and fluid resorption or because of an impaired sperm function when they enter the female reproductive tract, i.e. impaired acrosome reaction or motility.

The final sperm outcome can be divided into 4 categories: oligoospermia – reduced sperm numbers; azoospermia – no sperm production; teratospermia – sperm with abnormal shape (i.e. globozoospermia: loss of acrosome); asthenospermia – sperm with abnormal motility pattern (Borg *et al.*, 2010, Cooke *et al.*, 2002).

Defects at many different stages of sperm development can lead to infertility. To find the cause of a specific testicular phenotype in mice, a detailed analysis has to be carried out.

2.2 The p53 family

The p53 family of transcription factors includes three family members, p53, p63 and p73. All of them share common features in structure and function, transcriptionally regulating target

genes involved in cell cycle progression, apoptosis and development. They were also intensely studied to show their own specific expression pattern, molecular function and influence on carcinogenesis and development.

2.2.1 Evolution and structure of the p53 family

Evolutionary, the existence of a combined p63/p73-like ancestor gene is first observed in the single cell choanoflagellates and the early metazoan sea anemone. This ancestral gene was duplicated in the early vertebrate lineage of cartilaginous fish, giving rise to the origin of the p53 gene. A second duplication of the ancestor gene with development of bony fish produced separate genes for p63 and p73. With evolution of amphibians, reptiles and mammals, the gene loci of p63 and p73 underwent changes, dramatically increasing the intron size. The p53 gene was not as strongly affected and remained relatively small (Belyi *et al.*, 2010).

p53 was the first family member to be discovered in 1979. In SV40-transformed cells, p53 was found to bind to the SV40 large T-antigen (Lane *et al.*, 1979, Linzer *et al.*, 1979, Melero *et al.*, 1979, Kress *et al.*, 1979). Structurally, three important functional domains can be described for the p53 protein: the transactivation domain TAD (aa 1-42), the DNA-binding domain DBD (aa 102-292) and the oligomerization domain OD (aa 324-355) (*Figure 2.6 B* and *C*, after (Jacobs *et al.*, 2005)). The amino-terminal TA domain is necessary for transcriptional activation or repression of target genes, associating with transcriptional co-factors like the TATA-binding protein and the histone acetyl transferase (HAT) p300/CBP (Chang *et al.*, 1995, Teufel *et al.*, 2007). The hydrophobic amino acids Leucin 22 and Tryptophan 23 are indispensable for the transactivating function of human p53 (Lin *et al.*, 1994). The DBD enables p53-binding to p53 responsive elements (p53RE) in introns or in the promoter region of target genes (Bourdon *et al.*, 1997, el-Deiry *et al.*, 1992). To carry out its function as a transcription factor, p53 has to build a tetramer, which is possible by forming a dimer of two dimers through its carboxy-terminal oligomerization domain (Jeffrey *et al.*, 1995, Kitayner *et al.*, 2006). Until 2005 only one promoter and three splice variants of the p53 gene were described: full length protein (FLp53), C-terminal truncated isoform p53i9 (no transcriptional activity) and N-terminal truncated isoform Δ40p53 (transcriptional activity through a second identified TA domain in aa 43-63), the two latter produced by alternative splicing of intron 9 or 2 (Flaman *et al.*, 1996, Ghosh *et al.*, 2004, Zhu *et al.*, 1998b). In the past years additional information about the expression of new p53 isoforms, arising from a second internal promoter located in intron 4, named Δ133p53, was gained (Bourdon *et al.*, 2005).

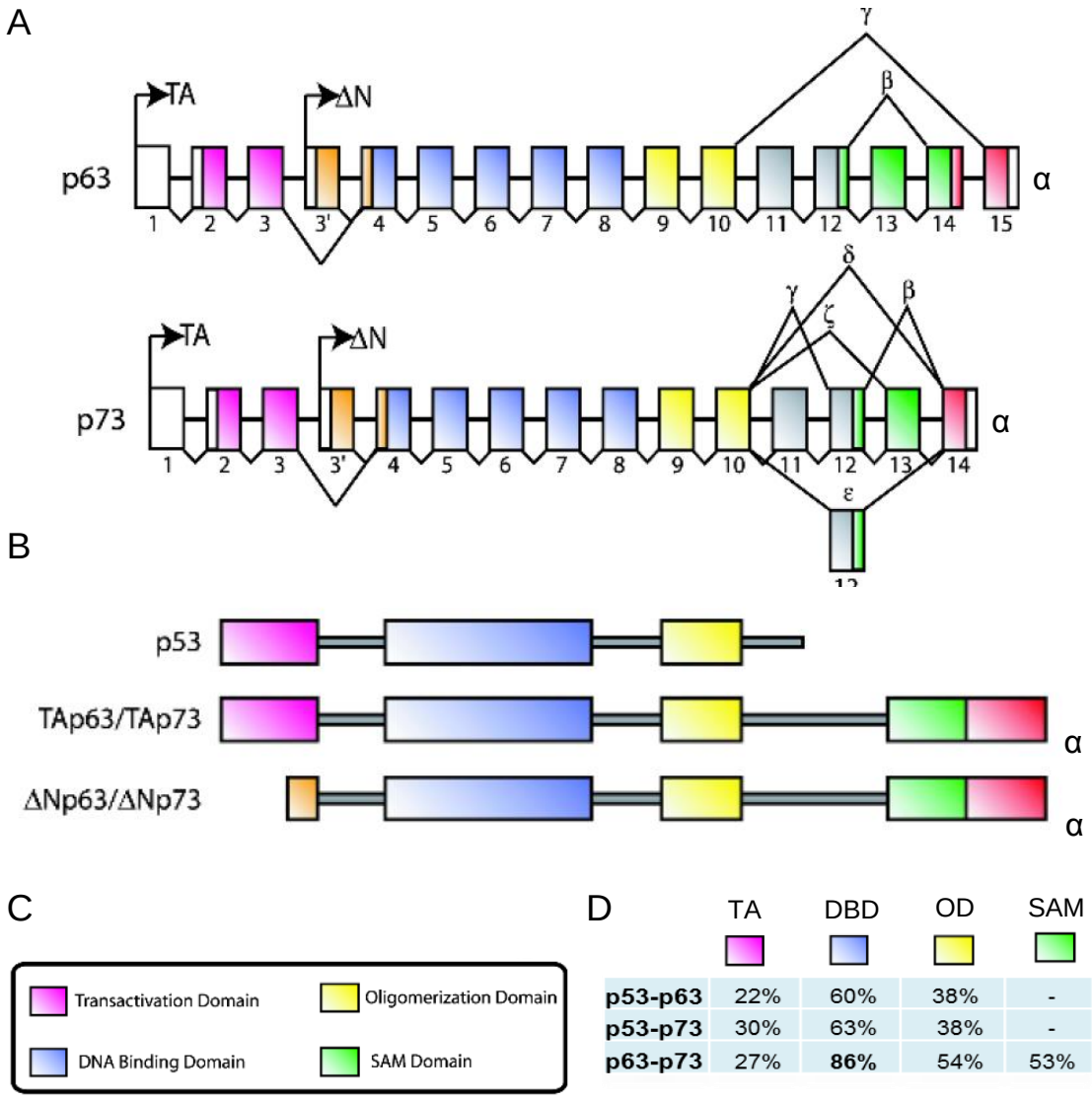

Fig. 2.6 The p53 family: gene loci and domain structure

A) Depicted are the gene loci of the p53 homologues p63 and p73. In both cases two promoters can be used to transcribe two N-terminally differentiating isoforms. Using the promoter upstream of exon 1 the TA-isoforms with the transactivation domain (legend in C) are produced, while ΔN-isoforms, transcribed from the internal promoter in intron 3 and using an alternative 3´exon, lack the TA domain. By differential splicing of the C-terminal exons multiple isoforms are produced. The full length isoform is referred to as TAp63/p73α.
B) Comparison of the domain structure of p53, p63α and p73α. All TA p53 family members possess three highly conserved domains: the transactivation (TA) domain, the DNA binding domain (DBD) and the oligomerization domain (OD). α-isoforms of p63 and p73 additionally harbour the sterile alpha motif domain (SAM) as well as the transcription inhibitory domain (TID, shown in red). ΔN-isoforms lack the N-terminal TA domain. For colour legend refer to C).
C) Colour legend for the protein domains of the p53 family.
D) Alignment of the domains shows highest homology for the DBD between p63 and p73. Evolutionary, p63 and p73 are more closely related to each other than to p53. The ancient p53 family gene locus was thought to be a p63/p73 like gene (Dotsch *et al.*, 2010, Levine *et al.*, 2011). (modified after Jacobs et al., 2004)

A similar dual gene structure was already described for p63 and p73. The two genes were identified in 1997, but it has to be stated that more research was done on the isoforms of p63 and p73 compared to p53 and that the pool of expressed isoforms differs significantly from p53 (Kaghad *et al.*, 1997, Schmale *et al.*, 1997, Trink *et al.*, 1998, Yang *et al.*, 1998). As result of two different promoters within the p63 and p73 gene locus, we can categorize the expressed isoforms into TA- and ΔN-isoforms (*Figure 2.6 A*, after (Jacobs *et al.*, 2004)). The ΔN-isoforms use an internal promoter, lying within intron 3, giving rise to an amino-terminally truncated p63-/p73-protein depleted of the transactivation domain. Through alternative splicing occurring at the C-terminus, TA and ΔN-isoforms of p63 and p73 can further be separated into α, β and γ for p63 and α, β, γ, δ, ε, ζ, η and φ for p73 (De Laurenzi *et al.*, 1998, De Laurenzi *et al.*, 1999, Yang *et al.*, 1998, Zaika *et al.*, 1999) (*Figure 2.6 A*, after (Jacobs *et al.*, 2004)). Even more isoforms are described for p73, since also N-terminal splicing of exons 2 and/or 3 can occur (TA domain). Structurally the γ isoforms are closest to p53. Additionally to the TA, DBD and OD domain, the TAp63/p73α isoforms contain a sterile α motif (SAM), which is a protein interaction domain, and a transcription inhibition domain (TID) (Chi *et al.*, 1999, Thanos *et al.*, 1999) (*Figure 2.6 B* and *C*, after (Jacobs et al., 2004)). Through an intra-molecular interaction between the N-terminal TA domain and the TID, the transcriptional activity of TAp63/p73 can be inhibited by the protein itself (Serber *et al.*, 2002, Straub *et al.*, 2010).

The DNA binding domain of each family member is closely related across species (homologs) (Belyi *et al.*, 2010, Jin *et al.*, 2000). Also between p53, p63 and p73 (paralogs) high homology is observed, especially for the DBD (~60% aa identity). However, the strongest homology can be seen between the domains of p63 and p73 with 86% homology for the DBD, 27% for the TA, 54% for the OD and 53% for the SAM domain (Levine *et al.*, 2011) (*Figure 2.6 D*, after (Jacobs *et al.*, 2004)). This indicates the strong relation of these two family members during evolution and might also explain their functional similarity in contrast to p53 action (refer to **2.2.3**).

2.2.2 The transcription factors p53, p63 and p73

The p53 proteins belong to a family of transcription factors. All members are able to form tetramers and bind to p53REs (canonical sequence: RRRCWWGYYY) in promoters and introns of target genes via their DBD. They activate a common set of target genes, involved in cell cycle (p21WAF1, GADD45, 14-3-3σ) and apoptosis (Igfbp3, Bax, Noxa, Puma), as shown by reporter assays and overexpression experiments (Di Como *et al.*, 1999, Jost *et al.*, 1997, Keyes *et al.*, 2005, Melino *et al.*, 2004, Zhu *et al.*, 1998a). But they also induce

expression of specific genes related to development, tumorigenesis and DNA damage (for functional differences of p53 family members refer to **2.2.3**). p63 for example can bind to p63REs activating p63 specific genes involved in skin, limb and craniofacial development (Osada *et al.*, 2005). While TA-isoforms are the main transcriptional activators, ΔN-isoforms are functioning in a dominant negative manner towards their own family members. By oligomerization p53, TAp63 and TAp73 are able to bind to the DNA and activate gene expression. If heterocomplexes with ΔN-isoforms of p63 or p73 are formed or DNA binding sites are blocked by ΔNp63/p73, the transactivation ability of p53 and the TA-isoforms can be inhibited (Grob *et al.*, 2001, Pozniak *et al.*, 2000, Stiewe *et al.*, 2002b, Yang *et al.*, 1998). ΔNp63 and ΔNp73 were shown not only to inhibit transcription, but also to activate specific target genes, not induced by TA isoforms (Liu *et al.*, 2004, Wu *et al.*, 2003). In sum, the main function of the TA isoforms is to promote cell cycle arrest, cellular senescence and apoptosis, while ΔN isoforms induce proliferation (Murray-Zmijewski *et al.*, 2006). Since homo- and hetero-tetramers between the different family members can be formed, the overall activity of each of the three p53 family members has to be calculated as ratio between their isoforms, also taking expression of TA and ΔN isoforms into account (Levine *et al.*, 2011).

2.2.3 Functions of the p53 family members

The p53 gene is the most frequently mutated gene in human cancer and around 80% of all human tumors are supposed to show a loss of p53 function (Hollstein *et al.*, 1996, Hollstein *et al.*, 1991). Transgenic mice depleted of p53 show no developmental abnormalities, but strongly grow spontaneous tumors (Donehower *et al.*, 1992). The transcription factor p53 harbours an important role as tumor suppressor and is named the “guardian of the genome” (Chen *et al.*, 1990, Finlay *et al.*, 1989). Upon oncogenic signals, stress and DNA-damage it induces apoptosis, cell cycle arrest or senescence to ensure genetic stability of somatic cells by reducing cell growth and inducing DNA repair or cell death (Lane, 1992).

In contrast to p53, the p63 and p73 genes are rarely mutated in human cancer (Han *et al.*, 1999, Kovalev *et al.*, 1998, Sunahara *et al.*, 1998). Nevertheless, it was shown recently that TAp73 can act as a classical tumor suppressor, since isoform specific TAp73KO mice are predisposed to spontaneous and carcinogen-induced tumors (Tomasini *et al.*, 2008). Depletion of p73 from developing lymphomas favors tumor dissemination and extranodal growth in mice and humans (Nemajerova *et al.*, 2010). p63 was also reported to be involved in tumorigenesis. Loss of p63 in squamous cell carcinoma (SCC) cell lines lead to an increase in their metastatic potential (Barbieri *et al.*, 2006). Like p73, p63 cooperates with p53 in tumor suppression, as double heterozygous p53-p63 and p53-p73 mice show a higher

tumor burden and increased metastasis as mice heterozygous only for p53 (Flores *et al.*, 2005). A study on TAp63-specific KO mice furthermore shows that TAp63 enables Ras-induced senescence in a p53 independent manner, thereby antagonizing tumorigenesis (Guo *et al.*, 2009).

However, when p63KO and p73KO mice were analyzed, severe developmental defects could be observed. p63 plays an important role during epithelial development, while p73 is indispensable for the development of the nervous system (Mills *et al.*, 1999, Yang *et al.*, 1999, Yang *et al.*, 2000).

p63 total KO mice (depletion of the DBD) show limb truncations, craniofacial abnormalities, absence of skin as well as adnexa like hair, teeth and glands. Loss of p63 leads to postnatal lethality, since newborn mice die of desiccation due to the absence of skin (Mills et al., 1999; (Mills et al., 1999; Yang et al., 1999). ΔNp63 was shown to be strongly expressed in stem cells of epithelia and is important for maintaining self-renewal of the basal layer. Epithelial stem cells of p63KO mice undergo premature proliferation stop in epidermis and thymus and remaining surface cells display characteristics of differentiating keratinocytes (Senoo *et al.*, 2007). p63 transactivates target genes involved in adhesion (i.e. PERP, Laminin) and differentiation (i.e. CEBP/B, Notch1) of keratinocytes (Pozzi *et al.*, 2009). Since ΔNp63 plays a fundamental role in epithelial development, it is not surprising that overexpression of ΔNp63 is frequently seen in SSCs of the lung, head and neck. In contrast to TAp63, ΔNp63 can function as an oncogene by interacting with Ras and promoting tumor-initiating stem-like proliferation in keratinocytes (Hibi *et al.*, 2000, Keyes *et al.*, 2011, Yamaguchi *et al.*, 2000). TAp63 is stated to contribute to epidermal differentiation of the later stages of keratinocyte maturation and therefore to the onset of the epithelial stratification program (Candi *et al.*, 2006). Furthermore, TAp63KO mice age prematurely and display skin ulcerations, senescence of hair follicle-associated epidermal cells and decreased hair morphogenesis. This indicates an additional role for TAp63 in maintaining stem cell function of the skin and regulating cellular senescence (Su *et al.*, 2009). In humans missense mutations in the p63 DBD sequence lead to the rare autosomal dominant developmental disorder EEC (ectrodactyly, ectodermal dysplasia, facial clefts) (Celli *et al.*, 1999).

p73 total KO mice show severe developmental defects of the central nervous system (CNS), including hippocampal dysgenesis, decrease in cortical layers (cortical hypoplasia) and ex vacuo hydrocephalus. Impaired function of the vomeronasal organ and therefore problems in pheromone detection were stated to lead to abnormal social and reproductive behavior of p73KO mice. 75% of p73KO mice were dying within the first 4 weeks and KO mice were suffering from immunological problems like chronic infections and inflammation (Yang *et al.*,

2000). The high mortality rate could be overcome by nursing the smaller p73KO pups by foster mothers. The ΔNp73 isoform is predominantly expressed in the developing brain, acting as prosurvival factor. NGF-induction (neural growth factor) during nervous system development keeps ΔNp73 levels high and enables it to block TAp73/TAp63/p53-mediated apoptosis in developing neurons. Loss of ΔNp73 in p73KO mice leads to apoptosis of sympathetic neurons in the superior cervical ganglion and the neurons of the developing brain (Pozniak *et al.*, 2000). ΔNp73 is also necessary for long term maintenance of adult neurons, since the number of cortical neurons decreases dramatically in p73KO mice 14 days postnatal (Pozniak *et al.*, 2002). Recently, it was shown that p73 plays an important role in long term maintenance of neural stem cells in embryonic development and adult mice. p73KO mice display proliferative defects for stem and progenitor cells in the SVZ (subventricular zone) of the brain and neurosphere assays show reduced self-renewal potential of p73 depleted stem cells (Agostini *et al.*, 2010, Fujitani *et al.*, 2010, Talos *et al.*, 2010). Like ΔNp63, ΔNp73 has a proliferative, antiapoptotic function and might also act as an oncogene. It was found to be overexpressed in several tumors, including neuroblastoma and ovarial cancer (Casciano *et al.*, 2002, Moll *et al.*, 2004, Zaika *et al.*, 2002).

2.2.4 Mouse models of p73

A lot of information on p73 and its role during development and tumorigenesis was gained by working with mouse models. At present 4 different KO mouse models are known and under investigation. As already described in section **2.2.3,** research on the p73KO mouse could show for the first time that p73 is connected to neural development (Yang *et al.*, 2000). The total p73KO mouse is depleted of all p73 isoforms, TA as well as ΔN. This is achieved by replacing exons 5 and 6, which are part of the DBD, by a Neo cassette (also refer to *Figure 2.6 A*). By depleting the DBD no functional protein can be formed. To shed light on the specific role of transactivating isoforms and inhibiting ΔN isoforms, isoform-specific KO mice have been generated.

In TAp73 KO mice exons 2 and 3, encoding the TA domain, are depleted from the gene locus. Using the second internal promoter ΔNp73 isoforms can still be expressed (also refer to *Figure 2.6 A*). Compared to total p73KO mice, TAp73KO mice show a mild neural phenotype. They only display abnormal hippocampal histology with truncation of the lower blade of the dentate gyrus. In addition they spontaneously develop tumors, mainly lung adenocarcinoma, and are sensitive to carcinogens. This is accompanied by genomic instability associated with enhanced aneuploidy (Tomasini *et al.*, 2008). Also, TAp73KO mice are infertile and show reproductive defects in the female germ line (also refer to **2.3.3**).

Two mouse models of ΔNp73KO mice are currently known. Both use as strategy the depletion of the alternative 3´exon of the ΔNp73 transcript. Tissir et al. investigated the effect of ΔNp73 loss by knocking in a Cre-recombinase-EGFP cassette instead of exon 3´, using its start codon in frame. Via immunofluorescence staining they could monitor cellular localization of ΔNp73 in the brain of heterozygous mice to the thalamic eminence, vomeronasal neurons, Cajal-Retzius cells (CRc) and the choroid plexus, as well as cell death of cortical neurons occurring in ΔNp73KO mice. In contrast to total p73KO mice, ΔNp73KO mice display no overt neural abnormalities. They show an atrophic choroid plexus and increased apoptosis of mature neurons in selected regions, like the preoptic area, the vomeronasal neurons, GnRH positive cells and CRc (Tissir *et al.*, 2009). The second ΔNp73KO mouse model shows similar signs of mild neurodegeneration and apoptosis, but the authors additionally describe a role for ΔNp73 in inhibiting the DNA damage response pathway by interrupting ATM and p53 phosphorylation and subsequent cell cycle arrest and apoptosis. Studies were performed in mouse embryo fibroblasts (MEFs), murine thymocytes and human osteosarcoma cells (U2OS) (Wilhelm *et al.*, 2010).

The description and analysis of isoform-specific p73KO mice has only begun and needs to be investigated further. Mouse models provide a helpful tool to gain information about the protein expression of your GOI (gene of interest) and its function in certain tissues during development and adulthood.

2.3 The p53 family and reproduction

The common p63/p73-like ancestor was first detected in evolution of the modern-day sea anemones (Nematostella vectensis). There, the p53 homologue nvp63 is described to act as protector of the germ line gametes against DNA damage, to ensure genetic stability and production of normal embryos. Upon UV radiation nvp63 can drive damage-induced cell death of early gametes (Pankow *et al.*, 2007). This function is over one billion years old persisting during evolution in the insects (i.e. Drosophila melanogaster), worms (i.e. Caenorhabditis elegans), clams, vertebrates (i.e. Danio rerio) and humans (Belyi *et al.*, 2010). However, with development of vertebrates and mammals the members of the p53-family became diverse in number and function. The next section will summarize today´s knowledge about all three family members in reproduction, concentrating on the murine system.

2.3.1 p53 and the germ line

The role of p53 during maternal reproduction was described recently. First hints towards an influence of p53 on the female germ line were obtained when female p53KO mice were shown to give birth to small litter sizes, while male p53KO mice were breading normally with wildtype (WT) females. Ovulation and fertilization were not changed in p53KO females, but the implantation of fertilized eggs into the uterus was affected (Hu *et al.*, 2007). p53 was shown to regulate the transcription of leukaemia inhibitory factor (LIF). LIF is secreted by the endometrial glands of the uterus and is necessary for decidualization of the uterine tissue and the implantation of the embryo into the uterus 4 days after fertilization. LIF and p53 expression levels correlate in time and location in the glandular cells and the p53KO implantation defect could be rescued by LIF injection into pregnant mice (Hu *et al.*, 2008, Hu *et al.*, 2007). In humans single nucleotide polymorphisms (SNPs) in p53 can have profound effects on the implantation ability of zygotes and female fertility. Women with difficulties in implantation of fertilized eggs more often hold the proline residue at codon 72 of p53 than the arginine (Kang *et al.*, 2009, Kay *et al.*, 2006). In cell culture the proline SNP of p53 was shown to produce decreased LIF levels compared to the arginine SNP, giving an explanation for the implantation problems in women harbouring this polymorphism (Hu et al., 2007).

In addition to the role of p53 for correct implantation, there are hints that p53 might also help to remove DNA-damaged oocytes upon irradiation. In the ovary p53 is expressed mainly on atretic follicles and it regulates expression of the apoptosis-inhibitor bcl-2 and apoptosis activator bax (Herr *et al.*, 2004, Hussein *et al.*, 2006, Miyashita *et al.*, 1994). In response to γ-irradiation and chemotherapy, p53 and p21 expression increases in the nuclei of follicular granulosa cells and mediates apoptosis and follicular degeneration (Gartel *et al.*, 2002, Lee *et al.*, 2008). Moreover, p53 was reported to influence developmental apoptosis during prenatal oogenesis, which is important for oocyte selection during prophase I of meiosis. In p53KO mice a higher proportion of abnormal oocytes and a decrease in apoptotic markers were found (Ghafari *et al.*, 2009).

Prenatal, physiologically occurring apoptosis of sperm cells is partly regulated by p53, since p53KO mice show decreased apoptotic cells in developing testes (Matsui *et al.*, 2000). Upon γ-irradiation and induction of DSBs in adult rat and mice, p53 levels increase mainly in pre-leptotene and pachytene spermatocytes, the maturation stage of sperm cells where DSBs occur during recombination events (Beumer *et al.*, 1998, Sjoblom *et al.*, 1996). Damaged sperm cells are removed dependent on p53, since p53KO mice display abnormal, giant sized sperm cells after irradiation (Beumer *et al.*, 1998). Additionally, human p53 was shown to bind to Rad51, influencing its recombination function, and p53KO mice displayed impaired

DNA repair (Schwartz *et al.*, 1999, Sturzbecher *et al.*, 1996). Some genetic strains of p53KO mice show the giant-cell degenerative syndrome, because primary spermatocytes are unable to complete the meiotic divisions (Rotter *et al.*, 1993). p53 might therefore control meiotic recombination and ensure genetic stability in males and in females.

2.3.2 p63 and the germ line

TAp63 was stated to be the protector of the female germ line. It controls the quality and survival of the oocyte pool during meiotic arrest in prophase I (Suh *et al.*, 2006). Oocytes exist as a limited population and are arrested as primordial follicles at this tetraploid stage of meiosis I. It has to be ensured that only genetically stable primordial follicles will enter the next meiotic steps and maturate to tertiary follicles. TAp63 is expressed in the nuclei of female germ cells during meiotic arrest. Its protein expression is increasing strongly after birth (Livera *et al.*, 2008, Suh *et al.*, 2006). Upon ionizing radiation TAp63 gets phosphorylated and is able to induce apoptosis of DNA-damaged oocytes. TAp63-specific KO mice fail to remove genetic instable oocytes after irradiation, while WT mice reduce the primordial follicle pool by 90% (Suh *et al.*, 2006). Induction of DNA-damage and cell death in oocytes by irradiation or chemotherapeutic treatment with cisplatin seems to be independent of p53, but dependent on activation of TAp63, which is phosphorylated and stabilized by the kinase c-Abl (Suh *et al.*, 2006, Gonfloni *et al.*, 2009). Deutsch et al. furthermore showed that TAp63α is kept in an inactive dimeric state in oocytes and is able to switch to its activated tetramer-form upon DNA damage induced phosphorylation (Deutsch *et al.*, 2011). TAp63 is therefore called “the guardian of the female germ line”.

Kurita et al. showed that the TA isoform of p63 is expressed in ovary as well as in postnatal testis, where nuclei of spermatogonia up to spermatids are positive for p63 staining (Kurita *et al.*, 2005). Additionally to p63 expression in postnatal meiotic and spermiogenic cells, p63 could be detected in the early developing gonocytes from embryonic day E13.5 to E18.5 (Nakamuta *et al.*, 2004, Nakamuta *et al.*, 2003). During embryonic development murine gonocytes pass through three phases: fetal proliferation and apoptosis (13.5 dpc - day post-coitum), quiescent period (14.5-18.5 dpc) and neonatal proliferation and apoptosis (1dpp - day post-partum). p63γ was shown to be strongly expressed in the quiescent period and p63KO mice display increased numbers of gonocytes in this phase as well as in testis organ cultures mimicking neonatal *in vivo* development. These findings accompanied by a decrease in apoptotic cells suggest a function for p63 in regulating prenatal germ cell apoptosis (Petre-Lazar *et al.*, 2007). In addition to developmental apoptosis p63 as well as p53 are involved in germ cell apoptosis of DNA-damage-induced fetal testes, since p63KO and p53KO embryos

display an increased survival of γ-irradiated germ cells compared to WT (Guerquin *et al.*, 2009). Recently, it was shown that a new isoform named GTAp63 is able to protect the adult male germ line against genetic instability upon DNA damage. This isoform is highly and specifically expressed in testis and is driven by an upstream located long terminal repeat (LTR) of the human endogenous retrovirus 9 (ERV9), which is unique to humans and great apes (Hominidae). In response to genotoxic stress, i.e. cisplatin treatment, GTAp63 was able to induce apoptosis and activate expression of apoptotic target genes like puma and noxa in human cancer cell lines (Beyer *et al.*, 2011). TAp63 isoforms therefore seem to protect the female as well as the male germ line upon irradiation and induction of DNA damage.

2.3.3 p73 and the germ line

Like TAp63, TAp73 was also shown to play a role in maternal reproduction. While TAp63 ensures genomic stability upon exogenous DNA damage, TAp73 ensures normal mitosis in the developing blastocyst. TAp73KO mice are infertile and display poor oocyte quality indicative of an increase in spindle abnormalities, like multipolar spindles, spindle relaxation and spindle scattering accompanied by chromosome misalignment (Tomasini *et al.*, 2008). Performing *in vitro* fertilization (IVF) and monitoring preimplantation development it became visible that only 30% of the TAp73KO zygotes were able to become blastocysts, compared to 75% in WT. KO mice gave rise to multinucleated blastomeres and blastocysts with abnormal cell number (Tomasini *et al.*, 2008). The molecular explanation for the failure in preimplantation embryonic development is the observation of TAp73 interaction with components (Bub1, Bub3 and BubR1) of the spindle assembly checkpoint (SAC) (Tomasini *et al.*, 2009). This checkpoint ensures correct attachment of all chromosomes to the spindle before separation in anaphase. Changes in TAp73 expression levels are known to lead to aneuploidy (Tomasini *et al.*, 2008, Vernole *et al.*, 2009). In women of advanced reproductive age (> 38 years), who display increased egg aneuploidy, TAp73 expression was shown to be downregulated in oocytes (Guglielmino *et al.*, 2011). In the female germ line TAp73 therefore seems to ensure genomic stability and euploidy by enabling correct mitosis. TAp73KO oocytes also failed to ovulate into the fallopian tubes upon induction of superovulation. Ovulated oocytes were retained in the ovary and lay trapped under the bursa. TAp73 does not only affect oocyte and blastocyst quality, but also regulates oocyte localization and their ovulation rate through changes in oocyte factor expression (Tomasini *et al.*, 2008).

ΔNp73KO mice were described to be fertile by Wilhelm et al., 2010. However, Tissir et al., 2009 observed impaired fertility for both sexes, “particularly evident for females that

generated only two or three litters". So far, no further data on female or male histology of the germ line of ΔNp73KO mice are available.

In the male germ line p73 was shown to be expressed in spermatogonia, spermatocytes and residual bodies, colocalizing with c-Abl in the cytoplasm of the cells (Hamer *et al.*, 2001). p73-induced activation of apoptotic genes is dependent on c-Abl. Upon ionizing irradiation p73 interacts with c-Abl and in turn gets phosphorylated by the kinase, as shown in human breast cancer cell line (MCF-7) and murine testis (Agami *et al.*, 1999, Hamer *et al.*, 2001). Codelia et al. also observed p73 phosphorylation by c-Abl and induction of apoptosis after etoposide treatment of GC2 spermatocytes and pre-pubertal rats (Codelia *et al.*, 2010). It was stated that the p73 mediated apoptosis could serve as back up of p53 induced apoptosis in p53KO mice exposed to DNA damage (Hamer *et al.*, 2001).

2.4 Scope of the thesis

p73 as well as TAp73KO mice were described to be infertile for both sexes. Originally it was stated that p73 mice fail to mate normally due to behavioral defects and problems in the pheromone sensory system (Yang *et al.*, 2000). However, TAp73 specific KO mice do not show abnormal mating behavior and nevertheless display infertility. Female mice were stated to show severe spindle defects in the developing oocytes and produce aneuploid embryos. Male TAp73KO mice were also described to be infertile, but so far no further data are available to explain this phenotype (Tomasini *et al.*, 2008). Investigations on testis morphology of total p73KO mice only included histologic staining of young mice, still undergoing the first wave of spermatogenesis. No morphological changes could be observed for the developing KO males (Yang et al., 2000: data not shown). Adult mice were not examined so far. In contrast to p73KO mice, p53KO as well as p63KO testes have been analyzed in more detail. Both family members are involved in the regulation of developmental and irradiation-mediated apoptosis in the prenatal testis (Guerquin *et al.*, 2009, Matsui *et al.*, 2000, Petre-Lazar *et al.*, 2007). Furthermore, p53 is implicated in male meiotic recombination and p63 in the protection of genetic stability of sperm cells (Beyer *et al.*, 2011, Sjoblom *et al.*, 1996). Additionally, the role of p53 family members in the female germ line was analyzed extensively. Several studies show that all three family members help maintaining the quality and quantity of the oocyte pool via different mechanisms. TA isoforms regulate implantation (p53), genomic stability (p63 and p73) and ovulation (p73) of oocytes (also refer to **2.3**).

p73 was described to be expressed in spermatogonia and spermatocytes (Hamer *et al.*, 2001), but its physiological function within the male germ line of KO mice deficient for p73 or

its specific isoforms has not been examined so far. While p73 is heavily involved in developmental processes and ensures genetic stability in the female germ line, it still has to be answered, if p73 could take part in regulating the male germ line during development. Therefore, it has to be evaluated, if p73 is necessary for spermatogenesis and the production of viable sperm cells.

This study shall address the question whether p73 loss leads to infertility due to a secondary effect or rather due to direct influence of p73 on sperm cell development. For this approach, histologic analysis of testis sections from total p73KO mice was performed. Additionally, isoform-specific TA and ΔNp73KO mice were analyzed to gain information, which isoform might be necessary for testicular development. Serum levels of hormones, involved in testicular development and produced in the brain, were measured to exclude a secondary effect, originating from the influence of p73 on brain architecture. To determine which cellular processes could be regulated by p73, proliferation, meiosis and apoptosis were studied by applying specific immunological stainings on testis sections. Since defects in spermatogenesis can occur at different developmental steps and sperm maturation is dependent on supporting Sertoli cells, different sperm cell stages as well as Sertoli cells were analyzed in number and morphology. Furthermore, expression analysis on whole testes as well as on primary cell culture was performed to determine testicular target genes of p73 and provide a molecular explanation for the infertility of p73KO and TAp73KO mice. For the first time, the influence of the p53 family member p73 on the male germ line development was examined in detail.

3 MATERIALS

3.1 Technical devices and equipment

Table 3.1: Technical Devices and equipment

Device	Company
Biovortexer MHX (E)	Xenox
Brushes for histology	Neolab
Calliper (digital)	Rettberg
Centrifuge Megafuge 1.0R	Heraeus, Thermo Scientific
Centrifuge MIKRO 22R mikrocentrifuge	Hettich GmbH & Co. KG
Centrifuge Mini Centrifuge MCF-2360	LMS, Tokyo, Japan
Centrifuge Typ GMC-060	LMS Laboratory & Medical Supplies
Centrifuge Typ 5810R	Eppendorf
Chromo4^{TM} Realtime PCR machine	Bio-Rad Laboratories
Cooling centrifuge Typ 5415R	Eppendorf
Cooling plate	Heraeus, Thermo Scientific
DNA gel chamber, slides and combs	Biotech Service Blu, Schauenburg
Embedding chambers	Techno-Med
Forceps and scissors for tissue preparation	Omnilab
Freezer -20° C	Liebherr, Bulle, Switzerland
Freezer -80° C Hera freeze	Heraeus, Thermo Scientific
Gel iX Imager, UV-transilluminator	Intas Science Imaging Instr. GmbH
Glass Hellendahl cuvettes for histology	Omnilab
Glass slide racks with handle for histology	Omnilab
Glass staining dish with cover for histology	Omnilab

Heating Block	Grant Instruments, Hillsborough, US
Heating plate for slides	Heraeus, Thermo Scientific
Humidified chamber histology	Weckert Labortechnik
Ice-machine B100	Ziegra, Isernhagen, Germany
Incubator for cell culture, Hera Cell 150	Heraeus, Thermo Scientific, Waltham, MA, US
Incubator for slides	Memmert GmbH + Co. KG
Laminar flow cabinet Hera Safe	Heraeus, Thermo Scientific
Liquid nitrogen tank LS4800	Labsystems Taylor Wharton
Magnet stirrer MR3001	Heidolph Instruments GmbH & Co.KG
Microm EC350 embedding station	Heraeus, Thermo Scientific
Microscope Axio Scope.A1 with AxioCam MRc and AxioVision 4.8 Software	Carl Zeiss
Microscope Axiovert 40C	Carl Zeiss
Microscope Axiovert 40 CFL with AxioCam ICm1 and AxioVision 4.8 Software	Carl Zeiss
Microscope, confocal Zeiss Confocal LSM 510 meta	Carl Zeiss
Microscope, Leica KL 1500 LCD with DFC 480 camera	Leica
Microscope, transmission electron microscope, Philips CM 120 BioTwin	Philips Inc.Eindhoven, Netherlands
Microslide Box, Cork	Rettberg
Microtome Leica RM2235	Leica
Microwave MW 17705	Cinex, Lippstadt, Germany
NanoDrop® ND-100 spectrophotometer	Peqlab, Erlangen, Germany
Neubauer chamber improved	Brand GmbH & Co. KG
Paraffin oven	Heraeus, Thermo Scientific
PCR Cycler Advanced Primus25	Peqlab Biotechnologie GmbH
PCR machine Thermocycler T personal	Biometra, Göttingen, Germany
Personal Computer	Dell, Round Rock, TX, US

pH-meter WTW-720, InoLab® Serie	WTW GmbH, Weilheim, Germany
Pipet-Aid® portable XP	Drummond, USA
Pipet Multipette	Eppendorf
Pipettes Eppendorf® Research Series 2100 (0.1-2.5µl; 0.5-10µl; 10-100µl; 100-1000µl)	Eppendorf
Power supply unit Powerpack P25T	Biometra
Refrigerator 4°C	Liebherr
Scales Acculab ALC-6100.1	Sartorius, Göttingen, Germany
Scales Expert LE823S	Sartorius, Göttingen, Germany
Scales LE623S	Sartorius, Göttingen, Germany
Shaker	Neolab
Shaker Promax 2020	Heidolph
Shandon Coverplate System	Heraeus, Thermo Scientific
Thermomixer comfort	Eppendorf
Timer	Oregon Scientific, Portland, OR, US
Ultra pure water system Aquintus	membraPure
Vacupack 2 plus sealing machine	Krups GmbH, Lyon, France
Vacusafe Comfort vacuum pump	IBS Integra Biosciences
Vortex Genie 2	Scientific Industries, Bohemia, NY, US
Vortex mixer	VWR
Water bath HIR-3	Kunz Instruments
Water bath TW 20	Julabo Labortechnik, Seelbach, Germany

3.2 Consumables

Table 3.2: Consumables

Product	Company
6-well/12-well cell culture plates	Greiner

8-well microscopy chamber slides	Nunc, Thermo Scientific
96-well plates for qPCR	Sarstedt
Cell culture petri dishes	Greiner
Cell scraper (16 mm/25 mm)	Sarstedt
Cover slips (24x40, 24x60 mm)	Menzel, Thermo Scientific
Filter for histology (Ø185)	Machery-Nagel
Filter tips (0,5-10µl/2-200µl/1000µl)	Sarstedt
Microtome blades Leica 819	Leica
Needles, different sizes	BD Microlance
Parafilm	Brand
PCR reaction tubes 0.2 ml	Sarstedt
PCR tubes, 8er Multiply Strips, 0.2ml	Sarstedt
Pipets, serological (5ml, 10ml, 25ml)	Sarstedt
Pipet tips (0,5-10µl/2-200µl/1000µl)	Sarstedt
PP tubes (15 ml/50 ml)	Greiner
Reaction tubes (0.5ml/1.5ml/2ml)	Eppendorf
Rotilabo® tissue cassettes	Roth
Sealing tape for qPCR plates	Sarstedt
Shandon coverplate system	Heraeus, Thermo Scientific
Slides, 76x26 mm, cut	Knittel Gläser
Sterile filter (0.45µm, 0.2µm)	Sartorius, Göttingen, Germany
Superfrost Plus coated slides	Menzel, Thermo Scientific
Surgical blade, carbon steel, sterile	Swann Morton
Syringes (1ml, 10ml, 20ml)	Henke Sass Wolf
Syringe canula (0.55x25mm, 0.3x12mm)	B.Braun

3.3 Chemicals

Table 3.3: Chemicals

Product	Company
Acetic acid	Carl Roth GmbH + Co. KG
Agar 100	ordered by AG Riedel, MPI-bpc
Agarose	Carl Roth GmbH + Co. KG
Ammonium sulfate ($(NH_4)_2SO_4$)	Carl Roth GmbH + Co. KG
Avertin (2-2-2 tribromoethanol)	Sigma-Aldrich GmbH
Bromphenol blue	Sigma-Aldrich GmbH
Calcium chloride ($CaCl_2$)	Carl Roth GmbH + Co. KG
Citric acid monohydrate	Carl Roth GmbH + Co. KG
Chloroform	Carl Roth GmbH + Co. KG
4',6-diamidino-2-phenylindole (DAPI)	Sigma-Aldrich GmbH
3,3`-Diaminobenzidin-tetrahydrochloride (DAB)	Carl Roth GmbH + Co. KG
Di-sodium hydrogenphosphate di-hydrate (Na_2HPO_4 x 2 H_2O)	Carl Roth GmbH + Co. KG
DNA-standard 1kb ladder mix	Fermentas, Thermo Scientific
Eiweiß-Glycerin for histology	Carl Roth GmbH + Co. KG
Eosin G	Carl Roth GmbH + Co. KG
Ethanol >99,8%	Carl Roth GmbH + Co. KG
Ethanol >99,9% p.a. (EtOH)	Merck
Ethidium bromide (EthBr)	Sigma-Aldrich GmbH
Ethylenediamine-tetraacetate (EDTA)	Carl Roth GmbH + Co. KG
EZ Link Sulfo-NHS-LC-Biotin	Thermo Scientific, Rockland, IL
Fluorescent Mounting Medium	DakoCytomation

Formaldehyde, 37% solution	Carl Roth GmbH + Co. KG
Glutaraldehyde, 25% EM Grade Aqueous	Electron microscopy sciences
Glycerol	Carl Roth GmbH + Co. KG
Glycogen Glyco blue	Ambion, Life Technologies
H_2O, RNase-free	Ambion, Life Technologies
Histofix, Roti-Histokitt II	Carl Roth GmbH + Co. KG
Hydrochloride acid (HCl)	Carl Roth GmbH + Co. KG
Hydrogen peroxide solution (H_2O_2), 30%	Carl Roth GmbH + Co. KG
Immersion oil	Carl Zeiss
Isoamylalcohol	Carl Roth GmbH + Co. KG
Isopropanol	Th. Geyer, Renningen, Germany
Lead citrate	ordered by AG Riedel, MPI-bpc
Magnesium chloride hexahydrate ($MgCl_2$ x $6H_2O$)	Carl Roth GmbH + Co. KG
Mayer`s haematoxylin solution	Merck
Nailpolish, optically clear	Essence
Osmium tetroxide	ordered by AG Riedel, MPI-bpc
Paraffin Rotiplast	Carl Roth GmbH + Co. KG
Paraformaldehyde	Carl Roth GmbH + Co. KG
pH solution 4.01	Carl Roth GmbH + Co. KG
pH solution 7.01	Carl Roth GmbH + Co. KG
pH solution 10.01	Carl Roth GmbH + Co. KG
Potassium chloride (KCl)	Carl Roth GmbH + Co. KG
Potassium di-hydrogenphosphate (KH_2PO_4)	Carl Roth GmbH + Co. KG
RNase inhibitor	Fermentas, Thermo Scientific
Sodium cacodylate buffer, 0.2M	Electron microscopy sciences

Sodium chloride (NaCl)	Carl Roth GmbH + Co. KG
Sodium hydrogenphosphate ($NaHPO_4$)	Carl Roth GmbH + Co. KG
Sodium hydroxide (NaOH)	Sigma-Aldrich GmbH
Sucrose	Sigma-Aldrich GmbH
SYBR Green	Invitrogen, Life Technologies
Tert-amyl alcohol (2-methyl-2-butanol)	Fisher Scientific
Trehalose, α, α -Trehalose, dihydrate	USB Corporation
Tris base (tris(hydroxymethyl)aminomethane)	Carl Roth GmbH + Co. KG
Triton X-100	Applichem
Trizol	Invitrogen, Life Technologies
Tween-20	Applichem
Uranyl acetate	ordered by AG Riedel, MPI-bpc
Xylol, >98%	Carl Roth GmbH + Co. KG

3.4 Buffers and solutions

Anesthesia working solution:

2% Avertin (stock solution dissolved in tert-amyl alcohol)
98% PBS
sterile filtered

Antigen retrieval solution, IHC:

10mM citric acid pH 6.0 (equilibrate with NaOH)
dissolved in H_2O

Antigen retrieval solution, TUNEL:

100mM citric acid pH 6.0 (equilibrate with NaOH)
dissolved in H_2O

Biotin stock solution:

9mM EZ Link Sulfo-NHS-LC-Biotin
1mM $CaCl_2$
dissolved in sterile PBS, pH 7

Blocking solution, IF and IHC:

5-10% FCS dissolved in PBS

Developing solution, IHC:

0.01% H_2O_2
2mM DAB
dissolved in PBS

Differentiation solution, HE:

1% HCl
70% Isopropanol
fill up with H_2O

DNA loading buffer, 6x:

0.25% Bromphenol blue
40% Sucrose
10% Glycerin
dissolved in H_2O

Eosin staining solution, HE:

0.1% Eosin G
dissolved in H_2O, with 3-4 drops of acetic acid

Fixation buffer, 4%, IF and IHC:

37% Formalin solution, diluted to 4% in PBS

Fixation buffer, EM:

2.5% Glutaraldehyde
0.1M Cacodylate buffer
fill up with H_2O

Phosphate buffered saline (PBS), pH 7.5:

24mM NaCl
0.27mM KCl
0.81mM Na_2HPO_4 x $2H_2O$
0.15mM KH_2PO_4
dissolved in H_2O

qPCR reaction buffer, 10x:

750mM Tris, pH 8.8 (equilibrate with HCl)
200mM $(NH_4)_2SO_4$
0.1% Tween 20
dissolved in H_2O, sterile filtered

qPCR reaction mix, 25x:

1x 10x qPCR reaction buffer
1:80.000 SybrGreen, dissolved in DMSO
3mM $MgCl_2$
300mM Trehalose, dissolved in 10mM Tris, pH 8.5, sterile filtered
0.2mM dNTPs
0.25% Triton X-100
20 U/ml Taq polymerase
dissolved in H_2O

Permeabilization buffer, IF:

0.5% Triton X-100
dissolved in PBS

Peroxidase blocking buffer, IHC:

3% H_2O_2
dissolved in PBS

TAE buffer:

40mM Tris
20mM acetic acid
2mM EDTA, pH 8
dissolved in H_2O

3.5 Enzymes and PCR solutions

Table 3.4: Enzymes and PCR solutions

Product	Order number	Company
25 mM $MgCl_2$	R0971	Fermentas, Thermo Scientific
dNTP-Mix, 25 µM each dNTP	U1420	Promega/ Bio-Budget, Krefeld
dNTPs (ATP, TTP, CTP, GTP) 100mM for qPCR Mix	1202.4 - 1205.4	Primetech
M-MuLV reverse transcriptase	M0253	NEB
NEBuffer for M-MuLV, 10x	B0253	NEB
Primer mix for RT-PCR (random nonamer and $dT_{23}VN$)	/	Metabion
RNase inhibitor, recombinant	M0307	NEB
Taq DNA polymerase for qPCR Mix	1800	Primetech
Taq DNA polymerase	EP0402	Fermentas, Thermo Scientific
Taq buffer with KCl, 10x	B38	Fermentas, Thermo Scientific

3.6 Kits

Table 3.5: Kits

Product	Order number	Company
Invisorb Spin Tissue Mini Kit (250)	10321003	Stratec (former Invitek)
In situ cell death detection kit, POD (TUNEL)	11684817910	Roche
TUNEL Enzyme from calf thymus (single component, TUNEL kit)	11767305001	Roche
TUNEL Label Mix (single component, TUNEL kit)	11767291910	Roche

3.7 Cell culture solutions

3.7.1 Cell culture components

Table 3.6: Cell culture components

Product	Company
Ciprofloxacin (Ciprobay)	Bayer
Collagenase/Hyaluronidase, 10x	Stem Cell Technologies
DMEM, High Glucose Phenol-Red Free	GIBCO, Invitrogen
DNase I (1mg/ml)	Stem Cell Technologies
F-12 Nutrient Mixture (Ham), liquid	GIBCO, Invitrogen
Fetal calf serum (FCS)	GIBCO, Invitrogen
Geltrex, reduced growth factor basement membrane matrix	GIBCO, Invitrogen
Hanks' Balanced Salt Solution (HBSS) (1X), liquid	GIBCO, Invitrogen
L-glutamine	GIBCO, Invitrogen
Penicillin/Streptomycin	GIBCO, Invitrogen
Trypsin/EDTA	GIBCO, Invitrogen

Trypsin from porcine pancreas	Sigma Aldrich GmbH

3.7.2 Solutions for Sertoli cell preparation

Collagenase/Hyaluronidase and DNase digestion:

1x Collagenase/Hyaluronidase and 1µg/ml DNase I diluted in 1xHBSS

Trypsin digestion:

50mg/ml stock (sterile filtrated) diluted 1:100 in 1xHBSS

Hypotonic shock:

20mM Tris-HCl, pH 7.2

3.7.3 Sertoli cell culture media

10 µg/ml Ciprobay

50 U/ml Penicillin

50 µg/ml Streptomycin

200 µM L-glutamine

5% FCS

dissolved in 1:1 DMEM (High Glucose)/ F-12

PBS buffer:

PBS for cell culture was prepared using PBS tablets (GIBCO, Invitrogen) according to manufacturer's instructions and then autoclaved.

3.8 Antibodies

Table 3.7: Primary antibodies

Antibody	Dilution	Species	Company
anti Apg1 (N-96)	1:200	polyclonal rabbit	Santa Cruz, sc-6242
anti DDX4/VASA	1:1000	polyclonal rabbit	Abcam, ab13840
anti GCNA1 (10D9611)	1:400	polyclonal rat	provided by Prof. Dr. Adham (University Göttingen)
anti Espin (clone 31)	1:400	monoclonal mouse	BD Biosciences,611656
anti Ki67 (clone TEC-3)	1:25	monoclonal rat	Dako, M7249
anti phospho H3 (Ser10), Alexa Fluor 488 conjugate	1:100	polyclonal rabbit	Cell Signaling, #9708
anti Timp1	1:10	polyclonal goat	R&D systems, AF980
anti Vimentin	1:100	polyclonal rabbit	Santa Cruz, sc-7557-R
anti WT1	1:300	polyclonal rabbit	Abcam, ab15249

Table 3.8: Secondary antibodies and streptavidin conjugates

Antibody	Dilution	Company
AlexaFluor488 goat anti-mouse IgG	1:500	Molecular Probes
AlexaFluor488 goat anti-rabbit IgG	1:500	Molecular Probes
AlexaFluor594 donkey anti-goat IgG	1:500	Molecular Probes
donkey anti-rabbit IgG (F_{ab}-fragment), biotinylated	1:500	GE Healthcare
goat anti-rat IgG (F_{ab}-fragment), biotinylated	1:500	GE Healthcare
ExtrAvidin®−Peroxidase	1:1000	Sigma-Aldrich GmbH
Streptavidin, Texas Red Conjugate	1:100	Calbiochem, Merck

3.9 Oligonucleotides

All primers were ordered from Metabion, Martinsried. Lyophilized oligonucleotides were dissolved in sterile water to obtain stock solutions with a concentration of 100 µM.

3.9.1 Oligonucleotides for mouse genotyping PCR

Table 3.9: Primers for PCR

Primer name	Sequence: 5´- 3´
p73_common_forward	GGGCCATGCCTGTCTACAAAGAA
p73_WT_reverse	CCTTCTACACGGATGAGGTG
p73_KO_reverse	GAAAGCGAAGGAGCAAAGCTG
TAp73_common_forward	CTGGCCCTCTCAGCTTGTGCCACTTC
TAp73_WT_reverse	CTGGTCCAGGAGGTGAGACTGAGGC
TAp73_KO_reverse	GTGGGGGTGGGATTAGATAAATGCCTG

3.9.2 Oligonucleotides for quantitative PCR

Table 3.10: Oligonucleotides for quantitative PCR

Primer name	Sequence: 5´- 3´
Adam23_forward	TGTCCTTGGGGGCACAGGCT
Adam23_reverse	TCCGGCAGCATGGCTGAAAACA
FSH_beta_forward	CAGTAGAGAAGGAAGAGTGCCG
FSH_beta_reverse	CGGTCTCGTATACCAGCTCC
GnRH_forward_1	GGGTTGCGCCCTGGGGGAAA
GnRH_reverse_1	CTGAGGGGTGAACGGGGCCAG

GnRH_forward_2	CCCCGTTCACCCCTCAGGGAT
GnRH_reverse_2	CCACCTGGGCCAGTGCATCTAC
Itgax_forward	GGCAGCTGTCTCCAAGTTGCTCA
Itgax_reverse	TGGTGCTCCAACCACCACCCA
Itga5_forward	GCGTGCCCAAGGGGAACCTC
Itga5_reverse	AGCAGGGGTGCCCCTACCAG
LH_beta_forward	GCCGGCCTGTCAACGCAACT
LH_beta_reverse	TGGGGTCTACACCCGGTGGG
p73_pan_forward	GGGCCATGCCTGTCTACAAGAA
p73_pan_reverse	GATGGTGGTAAATTCTGTTCC
TAp73_forward	GAGCACCTGTGGAGTTCTCTAGAG
TAp73_reverse	GGTATTGGAAGGGATGACAGGCG
ΔNp73_forward	GTGTGCAGACCCCCACGAGC
ΔNp73_reverse	GGTATTGGAAGGGATGACAGGCG
Serpina3n_forward	CAGCAGCCTCGTCAGGCCAA
Serpina3n_reverse	GCCTCCTCTTGCCCGCGTAG
Serpin6b_forward	TGCTGACAGCCTGAACCTGGGG
Serpin6b_reverse	GCCAGGGCTGAGGAGACGCT
Serping1_forward	GGAGCCGCTTGCTCAGTGCTC
Serping1_reverse	GCTCTTGGTGCTGTCTCCAGCC
Timp1_forward	CACCAGAGCAGATACCATGATGGC
Timp1_reverse	TATCTGCGGCATTTCCCACAGC
Tnfrsf12a_1var_forward	TTCTTGCCTCGGGACCGGCA
Tnfrsf12a_1var_reverse	TTGTCGAGGTCCGCGCTCCA

Vimentin_forward	AGGAGCTGCAGGCCCAGATTCA
Vimentin_reverse	GCAGGGCATCGTTGTTCCGGT
36B4_forward	GCAGATCGGGTACCCAACTGTTG
36B4_reverse	CAGCAGCCGCAAATGCAGATG

3.10 Mouse strains

TAp73KO, p73KO and corresponding WT strains were bred at the animal facility of the ENI (European Neuroscience Institute) in Göttingen. Mice were held in accordance to the restrictions of the German law regarding animal experiments. TAp73KO founder animals were kindly provided by Prof. Dr. Tak Mak from the Campbell Family Institute for Breast Cancer Research Ontario in Toronto, Canada. p73KO founder animals were a gift by Prof. Dr. Xin Lu from the Ludwig Institute for Cancer Research in Oxford, UK. ΔNp73KO and corresponding WT tissue samples were kindly provided by André Goffinet from the Developmental Neurobiology lab of the University of Louvain in Brussels, Belgium.

Table 3.11: Mouse strains

KO	Background	Generation
p73 total	129/Sv	N7
TAp73 specific	C57BL/6J	N6
ΔNp73 specific	Mixed 129/Sv and C57BL/6	--

3.11 Software

Table 3.12: Software

Name	Company
Adobe Photoshop CS5	Adobe Systems, San Jose, CA, US
AxioVision 4.8	Carl Zeiss

CFX Manager Software for qPCR cycler	Bio Rad
Excel	Microsoft, Redmond, WA, US
Nanodrop Software	Peqlab
R (version 2.14.0)	The R foundation for statistical computing
UV Imager Software	Intas Science Imaging Instruments

4 METHODS

4.1 Mouse histology

4.1.1 Tissue preparation

TAp73, p73 and ΔNp73 KO and WT mice between 3 to 18 weeks of age were euthanized with carbon dioxide. Preparation was done by fixing the mice on the preparation table, cleaning them with ethanol and performing a Y-cut. Testes and epididymes were taken out and all connected fat tissue was removed. Before further processing testes size was measured using a caliper and testis weight was determined with a special accuracy balance. At this step also images of whole testes were taken for some samples, using the stereomicroscope Leica KL 1500 LCD and the DFC 480 camera. As other organs (brain, thymus and liver), one testis was frozen in liquid nitrogen and used for later RNA isolation (refer to **4.3.4**). The other testis and epididymis was either fixed for subsequent histologic staining or the testis was used for electron microscopy (EM) analysis.

4.1.1.1 Fixation and processing for histologic staining

For subsequent immunohistologic stainings each prepped testis was enclosed in a labeled plastic grid and fixed in 4% Formalin/PBS fixation buffer at room temperature on a shaker overnight for at least 20 hours. After 3 times washing with PBS for 1 hour, tissue was dehydrated using an ascending alcohol series (*Table 4.1*). Dehydrated samples were transferred to liquid paraffin in a 60°C oven and paraffin was changed 3 times, once per day, to allow paraffin infiltration of the whole tissue. Tissue samples were embedded in paraffin using the Microm EC350 embedding station and left on a cooling plate for hardening. Precooled paraffin blocks could then be sectioned at the rotation microtome Leica RM2235. Transversal and longitudinal sections were transferred to a 40°C warm water bath to smooth the tissue and remove wrinkles. Sections were either shifted to "*Eiweiß*"-glycerin-coated slides for subsequent H&E staining or to superfrost plus coated slides for all other staining procedures. Charged superfrost slides can hold the tissue even under harsh conditions like boiling. To ensure sticking of the tissue to the slides, slides were left in an incubator at 60°C overnight. For all staining procedures 3µm thick sections were used.

Table 4.1: Ascending alcohol series prior to embedding

	Alcohol	Incubation time
2x	50% ethanol	15 minutes
1x	70% ethanol	30 minutes
1x	70% ethanol	overnight
2x	80% ethanol	30 minutes
2x	90% ethanol	45 minutes
2x	96% ethanol	60 minutes
2x	100% ethanol	45 minutes
1x	100% isopropanol	overnight
1x	75% isopropanol/25% xylol	30 minutes
1x	50% isopropanol/50% xylol	30 minutes
1x	25% isopropanol/75% xylol	30 minutes
2x	100% xylol	60 minutes
1x	100% xylol	overnight

4.1.1.2 Fixation and processing for electron microscopy (EM)

After dissection of the testis, the tissues were fixed by immersion using the 2.5 % glutaraldehyde/cacodylate fixation buffer for EM. Fixation of the testes were performed for 10 min at room temperature, before they were cut into small pieces and fixed overnight in the fixative at room temperature. The subsequent steps were performed by the research group of Dietmar Riedel in the facility for transmission electron microscopy at the Max Planck Institute for Biophysical Chemistry in Göttingen. After postfixation in 1% osmium tetroxide and preembedding staining with 1% uranyl acetate, tissue samples were dehydrated in a series of ethanol and embedded in Agar 100. Thin sections (30-60 nm) were counterstained with methanolic uranyl acetate and lead citrate and examined using a Philips CM 120 BioTwin transmission electron microscope (Philips Inc.Eindhoven, The Netherlands). Images were taken with a 1K slow scan CCD camera (Olympus SIS, Münster). 9 to 10 mice per genotype were analyzed.

4.1.2 Haematoxylin and Eosin (H&E) staining

H&E staining is a classical histologic method to visualize all cells within the tissue and get information about the morphology and different structures of the analyzed organs. Thereby, Haemalaun stains the basophilic nuclei, while Eosin reacts with the acidophilic cytoplasma. For H&E staining testis sections were rehydrated using a descending alcohol series (*Table 4.2*). The tissue has to be rehydrated to enable staining in hydrophilic staining solutions. Furthermore, the remaining paraffin is removed during this procedure. After washing the

slides in distilled water, sections were stained in Haemalaun solution for 5 minutes and excess Haemalaun was removed by short incubation in differentiation solution. To enable the final staining reaction by increasing the pH, slides had to be incubated in running tab water containing ions for 10 minutes.

Table 4.2: Descending alcohol series – H&E

	Alcohol	Incubation time
4x	100% xylol	5 minutes
1x	100% isopropanol	4 minutes
1x	96% isopropanol	4 minutes
1x	90% isopropanol	3 minutes
1x	80% isopropanol	3 minutes
1x	70% isopropanol	3 minutes
1x	50% isopropanol	3 minutes
1x	aqua bidest	rinse

The following Eosin staining was done for 1 to 5 minutes dependent on the strength of the solution. After washing in distilled water slides had to be dehydrated in an ascending alcohol series (*Table 4.3*). Embedding of tissue sections was performed using the hydrophobic embedding solution Roti-Histokit II. Images were taken at the Zeiss Axio Scope. A1, using the AxioCam MRc and the AxioVision 4.8 Software.

Table 4.3: Ascending alcohol series – H&E

	Alcohol	Incubation time
1x	aqua bidest	rinse
1x	50% ethanol	rinse
1x	70% ethanol	rinse
1x	90% ethanol	rinse
2x	100% ethanol	4 minutes
1x	50% isopropanol/50% xylol	rinse
4x	100% xylol	5 minutes

4.1.3 Immunohistochemistry staining (IHC)

To obtain information about the expression and localization of specific proteins, IHC staining with protein specific antibodies can be applied to tissue sections. A primary antibody directed against the protein of interest (POI) is produced by immunizing a certain species (i.e. mouse, rabbit, rat, donkey) with a small peptide of your POI. It will specifically detect the POI. To

amplify the signal and visualize the protein within the tissue a secondary antibody directed against the species, where the first antibody was produced in, is used. This antibody is coupled to biotin. By introducing a third step, addition of the extravidin-coupled peroxidase, extravidin will cross-link different biotin molecules further amplifying the signal. The enzyme peroxidase will finally visualize the protein by producing a precipitate, when converting its substrate 3,3`-Diaminobenzidin-tetrahydrochloride (DAB).

For IHC staining sections had to be rehydrated as described for H&E (*Table 4.2*). To permeabilize the tissue, sections were boiled in antigen retrieval solution 3 times for 5 minutes. After washing in distilled water sections were incubated in peroxidase blocking buffer for 10 minutes. This step blocks the endogenous peroxidase to ensure specific staining of the POI. Sections were transferred into the Shandon Coverplate System and washed 2 times with PBS. For all following steps 120µl solution per slide were taken. Saturation of unspecific binding sites was achieved by blocking the sections with 10% FCS blocking solution for 45 minutes at room temperature. Incubation with the primary antibody was done overnight at 4°C. After washing with PBS slides were incubated with the biotinylated secondary antibody for 45 minutes at room temperature. For used primary and secondary antibodies refer to **3.8**. Incubation with the extravidin-peroxidase was done for 1 hour at room temperature after another washing step with PBS. Slides were removed from the Shandon Coverplate System and transferred into PBS. The enzyme reaction was enabled by adding the DAB containing developing solution to the slides. Dependent on the antibody, sections were developed for 1 to 10 minutes until a strong brown precipitate could be seen. The reaction was stopped with water. Cell nuclei were counterstained with Haemalaun as described in chapter **4.1.2**. After dehydrating the slides in an ascending alcohol series (*Table 4.4*), they were embedded in Roti-Histokitt II. Images were taken at the Zeiss Axio Scope. A1, using the AxioCam MRc and the AxioVision 4.8 Software. For analysis and quantitation of stainings refer to **4.1.7**.

Table 4.4: Ascending alcohol series – IHC

	Alcohol	Incubation time
1x	aqua bidest	rinse
1x	50% isopropanol	rinse
1x	70% isopropanol	rinse
1x	90% isopropanol	rinse
2x	100% isopropanol	4 minutes
1x	50% isopropanol/50% xylol	rinse
4x	100% xylol	5 minutes

4.1.4 Immunofluorescence staining (IF)

Similar to IHC staining IF staining is performed to detect specific proteins within the tissue. However, visualization of the protein is not enabled by an enzymatic reaction, but through fluorescence-labeled secondary antibodies. The advantage of this method is the possibility to detect several proteins at once in one sample, using different primary antibodies produced in different species as well as corresponding secondary antibodies with fluorescence-labels of different wavelength. Additionally, the signal might be stronger in IF staining, but it will fade faster and has to be protected against light. Each fluorophore has to be stimulated with a specific excitation wavelength to emit and detect light of a specific higher wavelength, which can be achieved with fluorescence microscopes. Commonly used excitation wavelengths are: 358nm (blue light, i.e. 4`,6-diamidino-2-phenylindole (DAPI)), 488 nm (green light, i.e. AlexaFluor 488) and 594 nm (red light, i.e. AlexaFluor 594).

For IF staining sections had to be rehydrated in a descending alcohol series (*Table 4.2*). Antigen retrieval was done as described for IHC staining. After washing with PBS slides were transferred into the Shandon Coverplate System and unspecific binding of antibodies was blocked by incubation with 10% FCS blocking solution for 45 minutes at room temperature. Primary antibody staining was performed overnight at 4°C. The next day the secondary antibody was applied for 45 minutes at room temperature, after washing the slides with PBS. For used primary and secondary antibodies refer to **3.8**. Nuclei were counterstained by incubating the sections with DAPI (0.5µg/ml in PBS) for 5 minutes. After 3 additional washing steps with PBS, slides were mounted with fluorescence mounting medium. Images were either taken at the Zeiss Axio Scope. A1 using the AxioCam MRc and the AxioVision 4.8 Software or at the Zeiss confocal microscope LSM 510 meta (high resolution of DAPI stained testis sections to distinguish sperm cell types). For analysis and quantitation of stainings refer to **4.1.7**.

4.1.5 TUNEL assay

The TUNEL assay, **T**dT-mediated d**U**TP-X **n**ick **e**nd **l**abeling, is a method for detecting apoptotic cells. During apoptosis DNA of dying cells gets fragmented and these oligonucleotide fragments can be labeled by an enzymatic reaction. The enzyme terminal deoxynucleotidyl transferase (TdT) is able to catalyze a template-independent polymerization of deoxyribonucleotides to the 3´-end of single- and double-stranded DNA. Thereby, modified nucleotids, like fluorescin-dUTPs, are used as source for the TdT to label the fragmented DNA.

Comparable to IF staining, sections had to be rehydrated up to water and permeabilized using the TUNEL antigen retrieval solution. After 3 times washing in PBS, slides were transferred to a humidified chamber and sections were incubated with the enzyme reaction mix (Roche in situ cell death detection kit) for 1 hour at 37°C. Slides were washed with PBS and counterstained with DAPI (0.5µg/ml in PBS) for 5 minutes. After additional washing in PBS, sections were mounted using the fluorescence mounting medium. Images were taken at the Zeiss Axio Scope. A1 using the AxioCam MRc and the AxioVision 4.8 Software. Fluorescin-labeled cells could be detected in the green channel (488nm excitation).

4.1.6 *In vivo* Biotin assay

The *in vivo* Biotin assay was already described by Nalam et al., 2009. It is performed on living, anaesthetized mice to measure the integrity of the BTB in the testis. Thereby the water soluble reagent EZLink Sulfo-NHS-LC-Biotin is used. Upon application it will bind unspecifically to all primary amines of proteins, forming permanent, irreversible amide bonds. Injection in the testis of WT mice will lead to labeling of the basal cell layer in the testis. Further layers are not stained, since the BTB prevents diffusion of the reagent into the special microenvironment of developing sperm cells. A defect in the BTB would lead to staining of further layers in the seminiferous epithelium.

8 to 9 months old animals were anesthetized using 0.5 to 1ml of the anesthesia working solution and testes were exposed. 50µl of 5mg/ml EZLink Sulfo-NHS-LC-Biotin that had been freshly prepared in PBS-$CaCl_2$ were injected into the testicular interstitium. The contralateral testis was injected with PBS-$CaCl_2$ solution only and served as a negative control. After 30 min had elapsed, the animals were euthanized, and the testes were harvested and fixed in 4% Formalin/PBS fixation buffer. Embedding and sectioning was done as described in chapter **4.1.1.1**. Testis sections were subsequently stained for immunofluorescence (refer to **4.1.4**). Slides were probed sequentially with streptavidin-Texas Red, to detect the infiltrated biotin, and anti-espin antibody followed by AlexaFluor 488 donkey anti-mouse secondary antibody. Images of mounted sections were taken at the Zeiss Axio Scope. A1 using the AxioCam MRc and the AxioVision 4.8 Software. Texas Red labeled tissue could be detected in the red channel (594nm excitation).

4.1.7 Quantitation of histologic stainings

All quantitation were done with the help of the AxioVision 4.8 Software.

4.1.7.1 H&E staining – sperm cell mass

The relative sperm cell mass per testicular tubule was determined using H&E staining of testis sections. Therefore, the total tubule area as well as the cell area within the tubule was measured. The relative sperm cell mass was calculated in percent as ratio between cell area and tubule area. Per mouse 8 tubules were analyzed. The mean value and the standard deviation of the mean (SDM) were calculated for 4 to 5 mice per genotype.

Furthermore, tubules were classified into three categories, according to their sperm amount: low (only 1 to 3 layers remain of the seminiferous epithelium), middle (4 to 5 layers are visible in the seminiferous epithelium) and high (at least 6 layers are visible). All tubules of 3 areas per section were counted and the relative amount of tubules with low, middle and high sperm amount was calculated in percent. The mean value and the SDM were calculated for 5 mice per genotype.

4.1.7.2 GCNA1 staining – number of spermatogonia

The relative number of spermatogonia was determined by analyzing GCNA1 IHC-stained testis sections. The number of basal, GCNA1 positive cells per 120µm was counted. 10 distances were analyzed per mouse. The mean value and the SDM were calculated for 3 to 5 mice per genotype.

4.1.7.3 Ki67 staining – quantitation of proliferation

To gain information about the proliferation rate in testicular tubules, Ki67 stained testis sections were analyzed. Ki67 positive tubules, relative to the total tubule amount within the section, were calculated in percent. 3 sections were analyzed per mouse. The mean value and the SDM were calculated for 2 to 5 mice per genotype.

4.1.7.4 H3Ser10 staining – quantitation of meiotic rate

To determine the meiotic rate within the seminiferous epithelium, H3Ser10 stained testis sections were analyzed. Therefore, all H3Ser10 positive cells were counted per testis section. 3 sections were analyzed per mouse. The mean value and the SDM were calculated for 2 to 5 mice per genotype.

4.1.7.5 WT1 staining – Sertoli cell number

The relative number of Sertoli cells was determined by analyzing WT1 IF-stained testis sections. Therefore, the number of WT1 positive cells per tubular circumference was counted

and scaled up to the correspondent length in mm. 20 to 25 tubules were analyzed per mouse. The mean value and the SDM were calculated for 2 to 5 mice per genotype.

4.1.7.6 Vimentin – Sertoli cell arms

To analyze the morphology of Sertoli cells, the length of Sertoli cell arms was calculated using Vimentin stained testis sections. Therefore, all cytoplasmic arms, reaching from the basal layer towards the tubular lumen, were measured in length (µm) within one view (200x magnification). The sum of all measurements per area was taken and determined as the "total length" of Vimentin Sertoli cell arms. 5 to 10 areas were analyzed per mouse. The mean value and the SDM were calculated for 3 mice per genotype.

4.1.7.7 Timp1 staining – intensity

The intensity of Timp1 stained testis sections was analyzed in Adobe Photoshop CS5. Therefore, images were taken at the Zeiss Axio Scope. A1 using the AxioCam MRc and the AxioVision 4.8 Software. Same exposure times were applied to all sections. The mean gray value within an area of fixed size embedded in the seminiferous epithelium was determined. 3 to 5 images were analyzed per mouse. The mean value and the SDM were calculated for 5 to 7 mice per genotype.

4.1.7.8 Biotin staining – infiltration

The intensity of Texas Red stained, Biotin-infiltrated tissue was analyzed in Adobe Photoshop CS5. Therefore, images were taken at the Zeiss Axio Scope. A1 using the AxioCam MRc and the AxioVision 4.8 Software. Same exposure times were applied to all sections. The seminiferous epithelium of TAp73KO mice was classified into high germ epithelium (more than 3 cell layers) and low germ epithelium (1 to 3 cell layers). The mean gray value within an area of fixed size embedded in the seminiferous epithelium was determined for WT sections and the two categories of TAp73KO epithelium. The mean value and the SDM were calculated for 4 to 5 mice per genotype.

4.2 Primary cell culture of Sertoli cells

4.2.1 Preparation and culturing of Sertoli cells

To analyze Sertoli cell structure and function of TAp73 mice of different genotypes *in vitro*, preparation of primary Sertoli cells was done. For each isolation procedure both testes were

taken to increase the Sertoli cell amount. Sectioned testes were transferred into PBS and decapsulated in 5ml Hanks' Balanced Salt Solution (HBSS) in a small cell culture dish. Together with the HBSS, testicular tubules were transferred into 15ml Falcons. Tubules were washed two times in 5ml PBS by sedimentation. The tissue was dispersed by adding 3-4ml of Collagenase/Hyaluronidase/DNase-HBSS solution and incubating the samples for 20 minutes at 37°C on a shaker. After two washing steps with 5ml PBS and sedimentation of the tubules, another digestion step was performed. Therefore, 3-4ml of Trypsin-HBSS solution were added and samples were incubated for 15 minutes at 37°C on a shaker. The tubules were washed two times with 5ml PBS and 2ml DMEM/F12 were added to the sedimented pellet. To fragment the tissue and free the Sertoli cells from the seminiferous epithelium tubules were resuspended several times. Cells were pelleted by centrifugation at 300g for 3 minutes. The supernatant, enriched for Sertoli cells, was transferred to a new falcon. Again 2ml DMEM/F12 were added to the cell pellet and cells were resuspended strongly. After centrifugation the supernatant was pooled with the first obtained supernatant. Sertoli cells were equally distributed onto four wells of 12-well plates. Cells were cultured at 34°C (testicular temperature) with 5% CO_2 in DMEM/F12, containing 5% FCS. The remaining sperm pellet was kept for RNA isolation (refer to **4.3.4**).

After two days, when Sertoli cells were attached to the cell culture plate, media was changed. To obtain a clean Sertoli cell culture without contaminating sperm cells, sperm was removed by hypotonic shock. Sertoli cells could be expanded to 6-well plates (2ml media per well) after 2 to 3 weeks. Therefore, Sertoli cells were washed with PBS and transferred to new wells by trypsination and addition of new media. Sertoli cells grew very slowly and could be transferred or expanded to new plates every 1 to 2 weeks. To ensure viability of the cells, they should only be splitted, if they reach a density of at least 90%. Media change was performed every 2 to 4 days.

For growth and trypsination control, Sertoli cells were examined under the Zeiss microscope Axiovert 40C. Images of different passages of Sertoli cells were taken at the Zeiss microscope Axiovert 40 CFL, using the AxioCam ICm1 and the AxioVision 4.8 Software.

4.2.2 Immunofluorescence staining

To test the purity of the primary Sertoli cell culture, immunofluorescence (IF) staining using the Sertoli cell marker Vimentin was performed. Applying IF staining to fixed cells, to detect a specific antigen, works in the same way as IF staining on paraffin tissue sections (refer to **4.1.4**).

Sertoli cells were seeded on Geltrex-coated 8 well chamber slides. When they had reached around 80% confluence, they were washed two times with PBS and fixed in 4% Formalin-PBS fixation buffer for 20 minutes at room temperature. After two washing steps with PBS cells were permeabilized by incubation with the Triton-based permeabilization buffer for 10 minutes. Sertoli cells were rinsed in PBS two times and unspecific binding sites were blocked by incubating the cells in 5% FCS blocking solution for 30 minutes at room temperature. The primary antibody (Vimentin) was diluted in blocking solution and applied to the cells. After incubation for 1 hour at room temperature, cells were washed three times in PBS and incubated with the secondary antibody for 45 minutes at room temperature. For used primary and secondary antibodies refer to **3.8**. Counterstaining of nuclei with DAPI was performed for 5 minutes, after another two washing steps with PBS. Sertoli cells were rinsed in PBS for 3 times and mounted in fluorescence mounting medium. Images were taken at the Zeiss Axio Scope. A1 using the AxioCam MRc and the AxioVision 4.8 Software.

4.3 Molecular biology

4.3.1 Isolation of genomic DNA from murine tails

For genotyping of the different mouse strains genomic DNA has to be gained from murine biopsies, in this case mouse tails. For DNA isolation the Invisorb Spin Tissue Mini Kit from Stratec was used. Lysis of the tails and isolation of DNA via a column-based purification was done after the manufacture's protocol. All steps were performed at room temperature. In short, tails were lysed in the provided lysis buffer combined with proteinase K. After digestion at 52°C on a shaker for 4 up to 20 hours, the lysate was mixed with the binding buffer and applied to the column. The samples were shortly incubated to allow binding of the DNA and the flow through after centrifugation was discarded. All centrifugation steps were done for 1 to 2 minutes at 13.000 rpm. After 2 washing steps with the ethanol-based washing buffer, 200µl elution buffer were applied per column and the samples were incubated for 3 minutes. The eluat contained the purified genomic DNA that was used for the subsequent genotyping-PCR (refer to **4.3.2**).

4.3.2 Polymerase chain reaction (PCR)

Genotyping of running p73 and TAp73 mouse strains was done by amplifying genotype specific sequences by polymerase chain reaction (PCR). Using gene specific primers the PCR allows to amplify specific sequences in a DNA template in a rapid 3 step process. The

denaturation step at high temperature results in melting of the double-stranded DNA into single-stranded DNA. Now specific primers are able to bind to the target sequence during the annealing step. The applied temperature is dependent on the length and nucleotide composition of the primers. Finally a thermo-stable DNA polymerase will extend the annealed primers, amplifying the sequence of interest. By repetition of these steps for 30 to 40 times the target sequence will be amplified in a near-exponential manner.

For the p73 and TAp73 genotyping PCRs a basic PCR reaction mix was used (*Table 4.5*). To distinguish between WT and KO allele three primers were used in one PCR reaction. One of these primers was able to bind to the WT as well as to the KO allele (common primer). The other two primers were either specific for the WT (gene sequence) or for the KO (Neo cassette). By choosing different sizes for the two amplified PCR products, WT, Het and KO could be determined in one reaction. For primer sequences refer to **3.9.1**. The PCR program of the PCR thermocycler is displayed in *Table 4.6*. Annealing temperatures were adjusted to lie below the melting temperatures of the used primers. Elongation time was adjusted dependent on the PCR product length.

Table 4.5: PCR reaction mix

	Final concentration	Per reaction [µl]
10x Taq buffer KCl^+	1x	2.5
dNTPs (20 mM)	0.13 mM	0.16
Primer common (100 µM)	1 µM	0.25
Primer WT (100 µM)	1 µM	0.25
Primer KO (100 µM)	1 µM	0.25
$MgCl_2$ (25mM)	2.5 mM	2.5
Taq polymerase (5 U/µl)	1 U/reaction	0.2
H_2O		ad 25.0
+ DNA template		1.0 - 2.0

Table 4.6: PCR program (p73/TAp73)

Step	Temperature	Time	
Enzyme activation	95°C	3 min	
Denaturation	95°C	60/45 sec	30-35x
Annealing	60/70°C	90/30 sec	
Elongation	72°C	90/120 sec	
Final elongation	72°C	10 min	
	12°C	pause	

4.3.3 DNA gel electrophoresis

DNA gel electrophoresis is a method to separate the different PCR products of the genotyping PCR on an agarose gel. Since the phosphate backbone of the DNA is negatively charged DNA will run from the anode to the cathode. Fragments can be separated according to their size, small fragments running faster and bigger fragments running slower. Visualization of the PCR products is enabled by adding ethidium bromide to the gel, which will intercalate into double-stranded DNA and can be visualized by UV light.

To analyze the genotyping PCR, the PCR products were loaded to a 2% agarose gel. Beforehand the appropriate amount of 6x loading buffer was added to the samples. Bromphenol blue within the dye enables visualization of the fragments while they are separated and sucrose/glycerin will increase the density of the samples preventing that they float away from the loading pockets. A DNA ladder yielding bands of defined size was also loaded to facilitate size determination of the sample fragments. Samples were run at 120V for 30 to 45 minutes. Analysis was performed at the UV-transilluminator using the UV Imager Software.

4.3.4 Isolation of total RNA

RNA isolation was performed on harvested Sertoli cells and sperm pellet (refer to **4.2.1**) or on prepped murine tissue (refer to **4.1.1**). After washing with PBS, Sertoli cells were either directly lysed in Trizol reagent or scraped in PBS, centrifuged at 5000 rpm for 10 minutes at 4°C and the cell pellet lysed in Trizol. The remaining sperm pellet during Sertoli cell preparation was washed in PBS, lysed in Trizol and stored at -80°C. Tissue samples were fragmented and disrupted in Trizol using a biovortexer. Lysed Sertoli and sperm cells as well as tissue samples were incubated for 5 minutes at room temperature. The following steps apply to all sample types and steps were done on ice, if not indicated otherwise.

For RNA separation chloroform was added to the samples, taking 20% of the used Trizol amount. After vortexing the samples for 15 seconds and incubation at room temperature for 2 minutes, they were centrifuged at 13.000 rpm for 15 minutes at 4°C. The aqueous phase, containing the separated RNA, was transferred into a new eppendorf tube. The RNA extraction step with chloroform could be repeated to obtain a higher amount of RNA. 100% pure ethanol, 3 times the amount of the aqueous phase, was added to the aqueous phase and precipitation was performed over night at -20°C. The next day, residual Trizol was removed from the samples by pelleting the RNA at 13.000 rpm at 4°C and washing it with 70% ethanol. The dry RNA pellet was dissolved in nuclease-free water. A further clean up

step could be performed to remove possible protein contamination and ensure purity of the RNA. Therefore, another ethanol precipitation step with shock freezing of the samples in liquid nitrogen followed by a washing step was performed. After determining the concentration of water-resolved RNA (refer to **4.3.5**), samples could be used for RT-PCR (refer to **4.3.6.1**).

4.3.5 Determination of RNA concentrations

RNA concentrations were measured with the NanoDrop Spectrophotometer. The absorption at a wavelength of 260 nm was determined using 1.5µl of each RNA sample. To calculate the corresponding RNA concentration in the sample, the resulting absorption coefficient was used. This was automatically done by the Nanodrop Software.

4.3.6 Quantification of messenger RNA (mRNA) by PCR

To quantify the amount of a certain RNA transcript (gene of interest, GOI) from a cell line or tissue sample, quantitative PCR (qPCR) is performed. Therefore, the isolated total RNA pool (refer to **4.3.4**) has to be reverse transcribed into complementary DNA (cDNA), which is done by RT-PCR (**4.3.6.1**). The cDNA pool can now be used for qPCR to amplify the GOI using sequence-specific primers, while measuring the amount of the polymerized PCR product in real time (**4.3.6.2**).

4.3.6.1 Reverse transcriptase PCR (RT-PCR)

RT-PCR allows the unspecific reverse transcription of the total RNA pool into cDNA. This is accomplished by using a viral enzyme, the reverse transcriptase (RT), which is able to polymerize cDNA using mRNA as target sequence. The total RNA pool is reverse transcribed by adding oligo-dT primers as well as random nonamer primers to the reaction. Oligo-dT primers can bin to the poly-A tails of RNAs, enabling polymerization of the cDNA from the 3`end. Dependent on their random nonamer sequence, nonamer primer can bind to the complementary sequence in any RNA and enable polymerization independent of a poly-A tail.

After measurement of RNA concentration (refer to **4.3.5**), 1µg sample RNA was added to the RT-PCR reaction tube and filled with nuclease-free water up to 10µl. Two tubes were prepared for each sample to also run a negative control in parallel to ensure purity of the RNA. 6µl of mix 1 were added to each sample and probes were heated up at 70°C for 5 minutes to open RNA and resolve secondary structures. Mix 2 contained the RT and 4µl

were added to one prepared sample to obtain cDNA transcription. Mix 3 contained the same reagents as mix 2, but without the RT, to serve as negative control (DNA contamination). Preparation of master-mix 1 to 3 is displayed in *Table 4.7*. Reverse transcription was enabled by incubating the 20µl samples at 42°C for 1 hour. Enzyme reaction was stopped at 95°C. Samples were diluted to 50µl with water. Reaction size could also be scaled down to 0.5µg or up to 2µg RNA. cDNA samples were subsequently used for qPCR analysis.

Table 4.7: RT-PCR mix 1-3

	Per reaction [µl]
Mix 1	**6.0**
mixed Primer (100µM) (nonamer and $dT_{23}VN$)	2.0
dNTP mix (2.5 mM)	4.0
Mix 2	**4.0**
10x reaction buffer	2.0
RNase Inhibitor (10U)	0.25
M-MuLV reverse transcriptase (RT) (25U)	0.125
DEPC water	1.625
Mix 3: Mix 2, without RT	**4.0**

4.3.6.2 Quantitative real-time PCR (qPCR)

Quantitative real-time PCR (qPCR) enables real-time measurement of a (c)DNA sequence of interest during amplification via PCR. Therefore, the amount of a specific cDNA within the total cDNA pool can be determined by using sequence specific primers. Here, qPCR was used to quantify mRNA levels. For primers refer to **3.9.2**. Sequence-specific primers were designed in this way that a short fragment (100 to 300 bp) of the cDNA template was amplified. To exclude unspecific amplification of intron-containing genomic DNA, only primers were used that were spanning exon-junctions or that were located in different exons. Real-time measurement of the PCR product was possible by adding the intercalator SybrGreen to the PCR-mix. SybrGreen is a fluorescent dye and can only bind to double-stranded DNA. It can be detected by excitation with a certain wavelength and read out was performed at every amplification cycle of the PCR reaction directly after the elongation step (*Table 4.10*). Quantitation of the cDNA amplification is displayed in a logarithmic graph. After passing the threshold of detection, the amount of PCR product will increase in a linear manner with every cycle until saturation is reached. Ideally, the sequence of interest will be doubled every cycle (100% amplification efficiency). Calculation of the DNA amount can be done within the linear range of the graph. The obtained data point is referred to as Ct-value, cycle over threshold. A

high Ct-value correlates to a low amount of DNA, a low Ct-value to a higher amount. For normalization the Ct-value of the cDNA of interest is calculated against the Ct-value of a housekeeping gene (reference gene), which shows stable expression levels independent of the sample.

Here, a ribosomal subunit was used as reference gene for all qPCR reactions (36B4). Relative quantitation of the PCR product of KO and WT samples was performed by applying the ΔΔCt method. The executed calculation for the relative mRNA expression is the following:

$$2^{\textbf{(ΔCt (reference gene KO/target gene KO)) – (ΔCt (reference gene WT/target gene WT))}}$$

For all samples the qPCR reaction master mix was used (*Table 4.8*). A two-step PCR program was applied to all reactions. Annealing and elongation were performed at 60°C. Purity of the qPCR product was controlled by measuring the melting curve after the PCR reaction. It should yield a single melting point for a specific product (*Table 4.9*). cDNA resulting from RT reactions without reverse transcriptase and qPCR samples without cDNA template served as negative controls. All samples were analyzed in triplicates.

Table 4.8: Master mix for qPCR reaction

	Volume [µL]
25x qPCR reaction mix	14.0
Forward primer (100 pmol/µL)	0.15
Reverse primer (100 pmol/µL)	0.15
H_2O	9.7
+ cDNA	1.0
Total volume	25.0

Table 4.9: Cycler program for qPCR

Temperature	Time	
95°C	2 min	
95°C	15 sec	
60°C	1 min - read	40x
Melting curve		

4.3.7 Whole genome microarray

To compare the total mRNA expression pool of TAp73KO and WT testis, a whole genome microarray was performed. For each genotype 3 adult mice (10 weeks old) were objected to the analysis. Total RNA was isolated from testis tissue as described in **4.3.4**. The additional clean up step ensured purity of the RNA. RNA was handed to the transcriptome analysis laboratory (TAL) in Göttingen, where the samples were objected to microarray analysis. In short, RNA quality was controlled, RNA concentration was determined and 200ng of samples were reverse transcribed into cDNA. The labeling reaction was performed by adding Cyanine 3-CTP (Cy3-CTP) to the transcription master mix including the sample cDNA, dNTPs and the T7 RNA polymerase. This enzyme is able to transcribe cDNA into aRNA. The Cy3-labeled, purified and amplified aRNA was hybridized to the microarray slide, where it binds to the complementary sequences printed on the array. Printed probes contained the 3´ sequences of the corresponding mRNAs. Fluorescence detection and intensity measurement was enabled by readout of the array plates with a laser, exciting the fluorescence dye Cy3. Strong emission at a certain RNA spot resembles high expression of this specific gene in the sample. Data analysis was done by Lennart Opitz. Combined TAp73KO data were analyzed relative to combined WT samples. The threshold of deregulated mRNA expression in TAp73KO testis compared to WT was set to 2, resulting in 160 hits. Induction was calculated as log2 values. Positive numbers indicate upregulation, negative numbers downregulation of gene expression in TAp73KO mice, compared to WT mice. The table of all TAp73-regulated genes can be found in the appendix.

4.4 Measurement of serum hormone levels

To measure the amount of different hormone levels within the serum, blood was taken from freshly euthanized mice. The thorax was opened and the still pumping heart was punctured with a syringe. Collected blood was incubated overnight at 4°C to enable agglutination of blood cells. The next day samples were centrifuged at 4000 rpm at 4°C for 20 minutes. The supernatant, containing the serum, was transferred into a new eppendorf tube and subsequently used for measurement of hormone levels of FSH, LH and testosterone. All hormone levels were determined performing ELISA-assays. The **E**nzyme-**l**inked **i**mmuno**s**orbent **a**ssay, or short ELISA, is an antibody-based method to specifically detect surface or bead-attached antigens (hormones) and quantify their amount in the sample with help of an antibody-coupled enzyme. After addition of the substrate, the converted product can be measured by spectrophotometry.

Testosterone levels were kindly measured by Wagnerstibbe in Göttingen, using the testosterone II RIA kit from Roche (cobas, #05200067). FSH as well as LH levels were determined by Andrew Wolfe from the division of Pediatric Endocrinology at the Johns Hopkins University School of Medicine in Baltimore, USA. The bead-based Luminex ELISA from Millipore was used.

4.5 Statistical analysis

Statistical calculations were done with Microsoft Excel. Statistical significance was determined using the unpaired, one-tailed student's t-test. Significance was assumed for p-values below 0.05. Asterisks indicate resulting p-values as follows: * $p < 0.05$, ** $p < 0.01$, *** $p < 0.005$. n.s. = not significant. The *n* in figure legends indicates the number of animals analyzed.

5 RESULTS

5.1 TAp73 depletion leads to sperm cell loss in testis

5.1.1 With completion of the first wave of spermatogenesis, p73KO mice show a strong loss of sperm cells throughout the seminiferous epithelium

Members of the p53 family were described to play various functions during germ cell development, protection of genetic stability and maintenance of fertility (Hu *et al.*, 2011, Levine *et al.*, 2011). While p53 and p63 are known to regulate the male germ line, p73 function was only evaluated in the female germ line (Tomasini *et al.*, 2008). p73KO mice previously were described to show normal histology of the testis. Infertility was stated as a result of the developmental defect of the vomeronasal organ and the accompanied change in mating behaviour (Yang *et al.*, 2000). p73 was shown to play an important role in the female germ line, but its function in the male germ line was not analyzed in detail so far. Thus, we asked whether the loss of p73 might have an impact on testicular development.

Therefore, p73KO mice of different age were applied to histologic analysis. Testes of p73KO mice and WT littermates were removed, fixed in Formalin, dehydrated in an ascending alcohol series and embedded in Paraffin. Haematoxylin and Eosin (H&E) staining was performed on transverse sections of the testis. 3 weeks old mice (P20) have not yet completed the first wave of spermatogenesis. The sperm cell pool mainly consists of spermatogonia and spermatocytes, going through the meiotic divisions. Spermiogenesis is not finished at this stage and rarely round spermatids can be seen (Bellve *et al.*, 1977, Borg *et al.*, 2010). When we compared H&E stainings of testes from 3 weeks old p73KO mice with WT testis we observed no difference in testicular histology and the stage-specific germ cell pool (*Figure 5.1 A*). Analysis of testis size and weight revealed slightly smaller and lighter testes for p73KO mice (*Figure 5.1 A and Table 5.1*).

	young mice (P20)		adult mice (P42-70)	
	WT	**p73KO**	**WT**	**p73KO**
Size in mm x mm	5.6 +/-0.5 **x** 4 +/-0.3	5.1 +/-0.7 **x** 3.8 +/-0.6	7.8 +/-0.7 **x** 5 +/-0.5	7.9 +/-0.7 **x** 5.2 +/-0.5
Weight in mg	47 +/- 12.3	31.4 +/- 3.6 *	130 +/- 23.7	122 +/- 34.5

Table 5.1: No difference in testis size and weight of adult p73KO and WT mice.

Quantitation of testis size and weight of young (P20, n=5-6) and adult (P42-P70, n=7-13) mice. Adult p73KO testes display similar numbers for size and weight. Testes of developing p73KO mice (P20) are slightly smaller and significantly lighter. * = $p < 0.05$ (Student´s t-test).

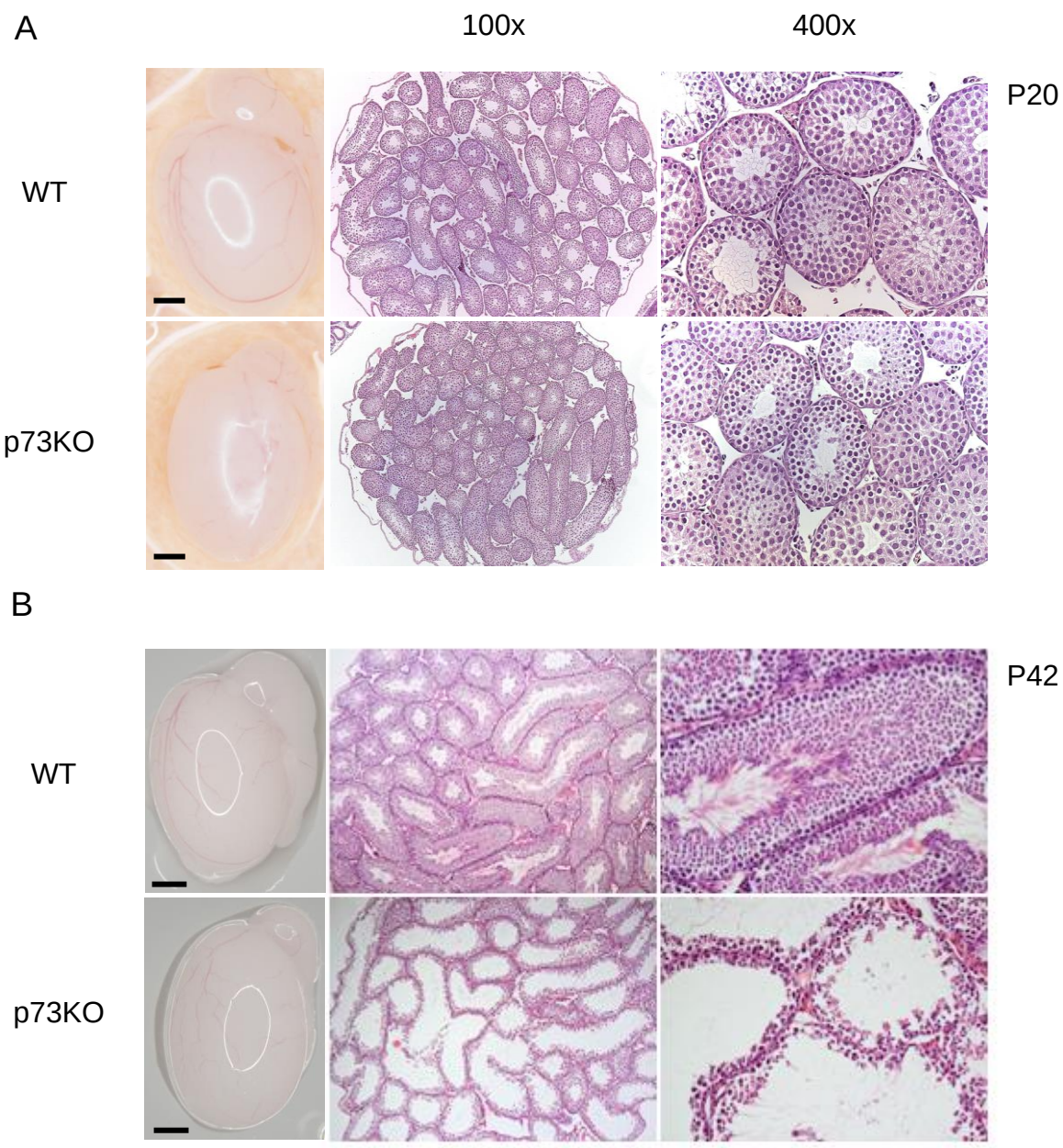

Fig. 5.1 Testes of developing p73KO mice show normal morphology. Only with adulthood a strong sperm cell loss is visible in p73KO mice compared to WT.

A+B) Stereomicroscopy of whole testis with epididymis and transverse sections of the testis from p73KO and WT littermate mice at stage P20 (A) and P42 (B). Mayer's haematoxylin and eosin (H&E) staining. 6 weeks old p73KO mice show highly decreased numbers of developing sperm cells as well as mature spermatozoa. Scale bar = 1mm

This observation can be explained by comparing testis size with body size. Newborn p73KO mice are known to be smaller and weaker when competing with their WT littermates (Yang *et al.*, 2000). By separating p73KO mice from WT littermates after the difference of weight and

size becomes visible, p73KO mice survive and grow to adult mice of comparable size. While adult p73KO mice did not show noticeable differences in testis size and weight, we observed a striking phenotype for testicular histology (*Figure 5.1 B* and *Table 5.1*). In comparison to WT testis, 6 weeks old p73KO testis showed a strong sperm cell loss throughout the seminiferous epithelium of the tubules. H&E staining of testis sections visualized the reduced number of developing sperm cells resulting in a decreased height of the germ epithelium (*Figure 5.1 B*). In contrast to previous studies, these observations indicate for the first time that p73 affects the development of the male germ line.

5.1.2 TAp73 but not ΔNp73 is necessary for sperm development

Dependent on its isoforms p73 can have certain effects on different cells and tissues. For example the transactivating TAp73 isoform and the N-terminal truncated ΔNp73 isoform are both known to be expressed in the CNS. TAp73 was lately described to be of importance in maintaining the stem cell pool of neural cells (Fujitani *et al.*, 2010, Talos *et al.*, 2010). ΔNp73 was stated to be an important prosurvival factor of mature neurons of the adult brain (Lee *et al.*, 2004a, Tissir *et al.*, 2009). To gain information about the relevance of specific p73 isoforms for testicular development we subjected TAp73- and ΔNp73-isoform-specific KO mice to histologic analysis. When we performed H&E staining on longitudinal sections of adult TAp73KO and WT testes we could observe a strong loss of sperm cells in the tubules of TAp73KO testis. This reduction of the seminiferous epithelium was comparable to the phenotype observed for p73KO mice (*Figure 5.2 A*). However, when we analyzed adult ΔNp73KO testes no difference in testis morphology compared to WT mice could be found in H&E stained sections (*Figure 5.2 B*). Quantitation of a number of p73KO, TAp73KO and ΔNp73KO testes revealed 86-100% penetrance of the sperm-loss phenotype for p73 and TAp73KO mice. ΔNp73KO testis did not show any morphological changes for all analyzed mice (*Table 5.2*). To look for the mRNA expression levels of p73 and its isoforms, we performed qPCR analysis on RNA samples isolated from WT testis, comparing it to murine brain, thymus and liver. Expression levels of total p73 in testis were comparable to thymus, but significantly lower compared to brain (*Figure 5.3*). p73 was already described to play a role in the immune response and T cell development (Ichimiya *et al.*, 2002, Nemajerova *et al.*, 2009, Yang *et al.*, 2000). Therefore, low p73 mRNA level in thymus and testis nevertheless have a strong effect on the development of these tissues. When we additionally compared the expression levels of TAp73 and ΔNp73 in testis using isoform-specific primers, we observed significantly higher mRNA levels for the TAp73 specific isoform of p73 (*Figure 5.3*).

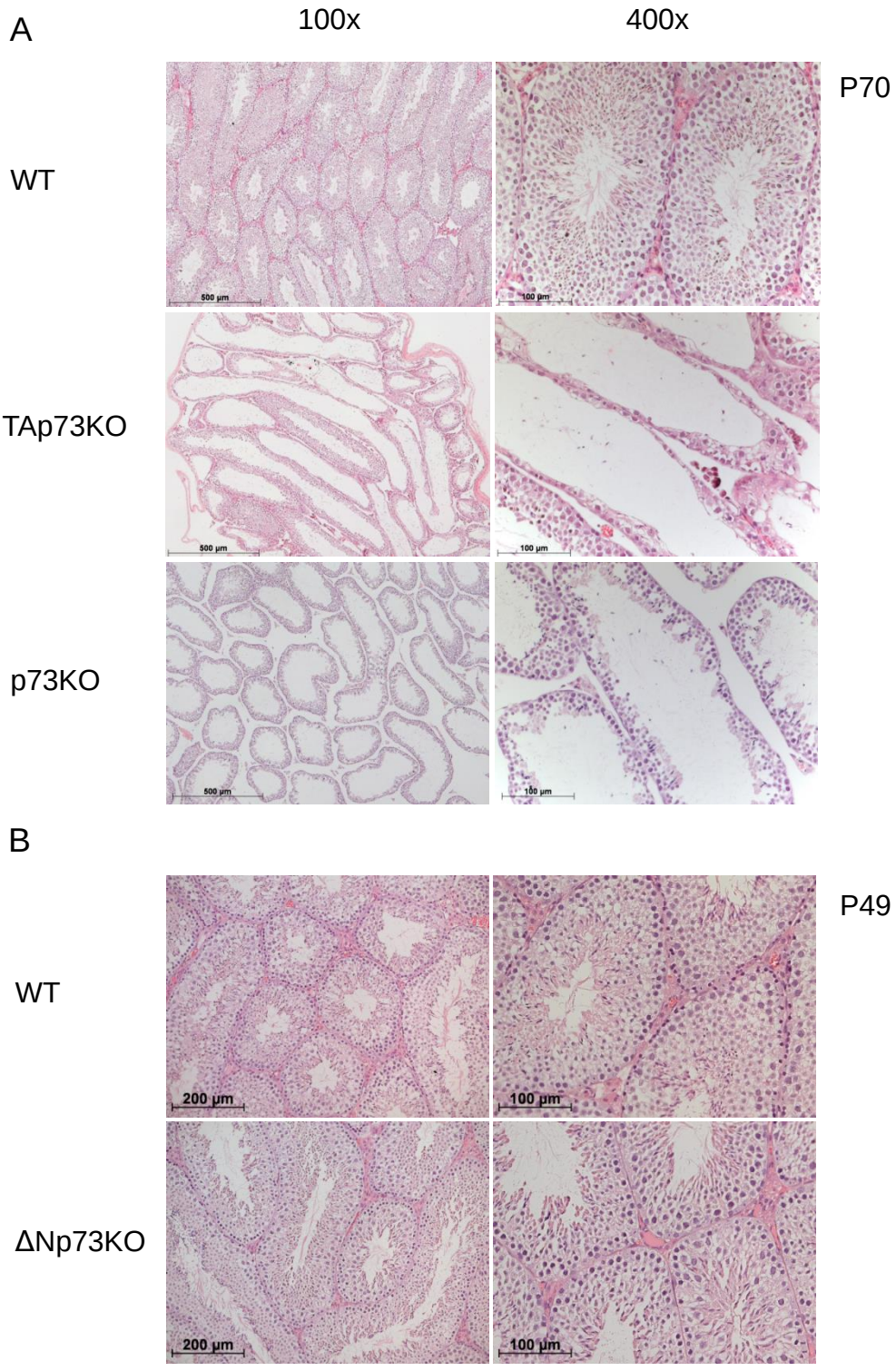

Fig. 5.2 TAp73KO mice resemble the observed phenotype for p73KO mice, while ΔNp73 mice show normal testicular morphology.

A) Longitudinal sections of the testis from TAp73KO, p73KO and WT mice at stage P70. H&E staining. TAp73KO mice show a strong decrease of the seminiferous epithelium, as observed for p73KO mice.
B) Longitudinal sections of the testis from ΔNp73KO and WT mice at stage P49. H&E staining. No sperm cell loss can be observed in isoform specific ΔNp73KO mice. They show normal testicular morphology as their WT littermates.

TAp73 therefore can be stated to be the major isoform expressed in testis, its loss leading to a defect in sperm development.

phenotype	p73KO	ΔNp73KO	TAp73KO
strong	60%	0%	75%
middle	26%	0%	25%
weak	7%	0%	0%
no	7% *	100%	0%
n =	15	6	20

Table 5.2: Summary of analyzed p73KO, ΔNp73KO and TAp73KO mice, examining H&E stained testis sections.

86% of p73KO and 100% of TAp73KO mice show a middle to strong loss of sperm cells in the seminiferous epithelium. Loss of sperm cells was categorized as “strong”, if only 1 to 3 germ cell layers were retained in the seminiferous epithelium. If 4 to 5 cell layers were present, the phenotype was stated as “middle”. The phenotype was classified as “weak”, if only some tubules showed decreased layers. “No” phenotype resembles the WT and Heterozygous (Het) situation. All ΔNp73KO mice display normal morphology of the testis. All animals were beyond 5 weeks of age. ***** Compared to its littermates, this 6 week old animal displayed a rather small testis, indicating a slow development.

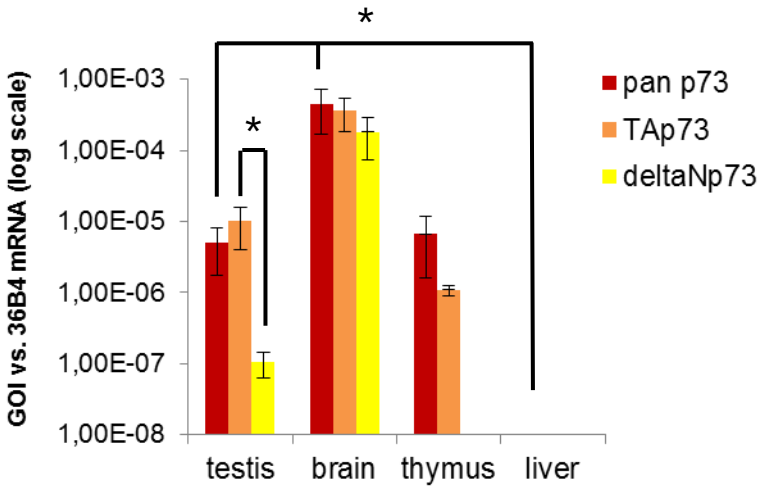

Fig. 5.3 TAp73 is the major isoform of p73 expressed in testis.

Quantitation of mRNA isolated from whole organs, performing qPCR with murine primers for p73 as wells as isoform-specific primers amplifying TAp73 or ΔNp73. log scale of absolute values is depicted. Comparing testis and thymus p73 is expressed in a similar extent in both organs. Brain levels are significantly higher. Comparing TAp73 and ΔNp73 expression in testis, TAp73 is the predominant isoform. n=2-3 mice were analyzed per tissue. Error bars represent the SDM. * = $p < 0.05$ (Student´s t-test).

5.1.3 During spermatogenesis, the late developing stages of sperm cells are lost in p73KO and TAp73KO mice

TAp73 as well as total p73KO mice show a strong decrease in sperm cell numbers for male mice. To look in more detail which type of developing sperm cells is lost in these mice we applied immunofluorescence (IF) staining to testis sections of KO and WT mice. To visualize meiotic cells and round spermatids, tissue sections were analyzed by using the marker VASA (also called DEAD box helicase protein DDX4 or MVH) (Castrillon *et al.*, 2000). TAp73KO mice showed a decrease in the VASA positive layer of testicular tubules (*Figure 5.4 A*). Also a strong reduction in spermatid numbers could be observed when TAp73KO testes were stained for APG1 (member of the heat shock protein family HSP110), a marker for round and elongated spermatids and mature spermatozoa (Held *et al.*, 2006). Additionally we could observe a loose, disorganized structure of the seminiferous epithelium, with some developing sperm cells detaching from the sperm layers into the lumen (*Figure 5.4 A*). Confocal microscopy on DAPI stained sections confirmed these results. Pachytene spermatocytes (*Figure 5.4 B; star*) could be observed in normal numbers, while round and elongated spermatids (*Figure 5.4 B; arrow, dashed arrow*) were strongly reduced in p73KO mice. Again, the disturbed layer structure of developing sperm cells was visible. To quantify the described sperm-loss phenotype of p73KO mice, we calculated the ratio of cell mass per tubule and additionally classified the tubules concerning their sperm amount (*Figure 5.4 C and D*). For quantitation H&E stained sections were chosen and analyzed using the Axio Vision Software (also refer to **4.1.7.1**). The analysis confirmed a significantly lower amount of sperm cells within the tubule epithelium of p73KO mice. The germ cell mass of the seminiferous epithelium of p73KO mice was reduced by 20-30% (*Figure 5.4 C*). Most of the tubules analyzed contained only a small amount of sperm cells, while tubules with a high amount of sperm cells were rarely seen in p73KO testes (*Figure 5.4 D*). To exclude a change in number of immature, pre-meiotic cells, KO testes were analyzed for the amount of spermatogonia. Immunohistochemistry (IHC) was applied to testis sections of adult KO and WT mice, using an antibody directed against the germ cell nuclear antigen 1 (GCNA1), a marker for immature germ cells (Enders *et al.*, 1994). While the total amount of sperm cells was highly reduced in p73KO and TAp73KO mice, the number of basal spermatogonia did not change (*Figure 5.5 A*). The quantitation of GCNA1 positive cells per distance, using the Axio Vision Software, confirmed the observed result (*Figure 5.5 B*). For detailed description of the quantitation refer to **4.1.7.2**. Taken together, p73KO and TAp73KO mice display a strong decrease of developing sperm cells in the seminiferous epithelium. Early stages of sperm development

like spermatogonia do not seem to be affected, but numbers of round and elongated spermatids are significantly reduced in KO mice.

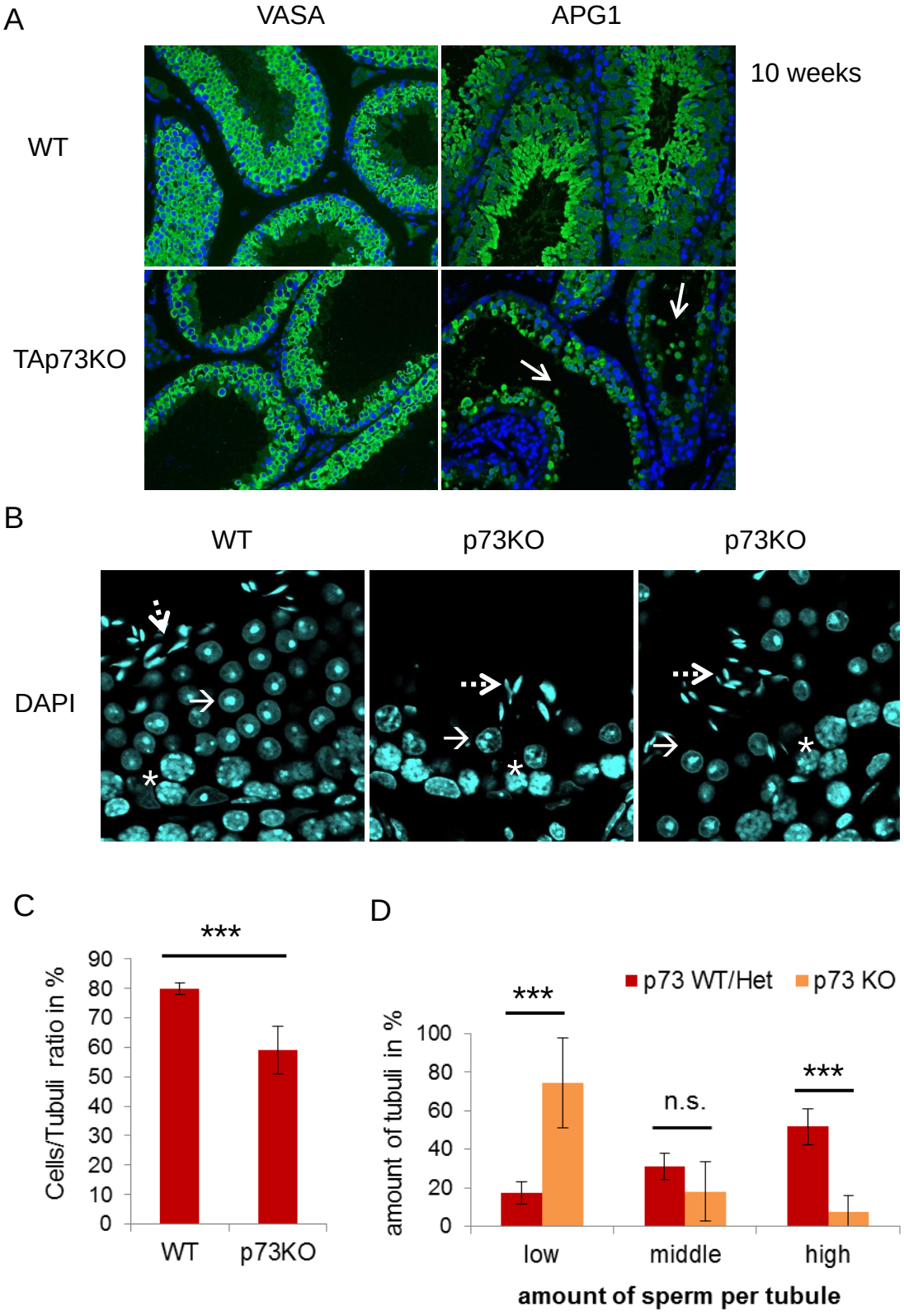

Fig. 5.4 Testes of TAp73KO mice show reduced numbers of developing sperm cells, especially round and elongated spermatids.

A) Immunofluorescence staining of testis sections from adult TAp73KO and WT mice (10 weeks old). Antibodies against VASA (spermatocytes and round spermatids) and APG1 (spermatids and spermatozoa) were applied. TAp73KO mice reveal a decrease of developing sperm cells, including round and elongated spermatids. Magnification: 400x
B) DAPI staining of testis sections from adult p73KO and WT mice. Numbers of round (arrow) and elongated spermatids (dashed arrow) are highly reduced in p73KO mice. * = pachytene spermatocyte; Magnification: 630x
C) Quantitation of total sperm cell number per tubule comparing p73KO and WT mice. p73KO mice display 20-30% reduction of sperm cells within the seminiferous epithelium. n=4-5 mice were analyzed per genotype. Error bars represent the SDM. *** = $p < 0.005$ (Student´s t-test).
D) Quantitation of tubule distribution in p73KO versus WT/Heterozygous (Het) mice. p73KO mice show a significantly higher number of tubules with low sperm amount. n=5 mice were analyzed per genotype. Error bars represent the SDM. *** = $p < 0.005$; n.s. = not significant (Student´s t-test).

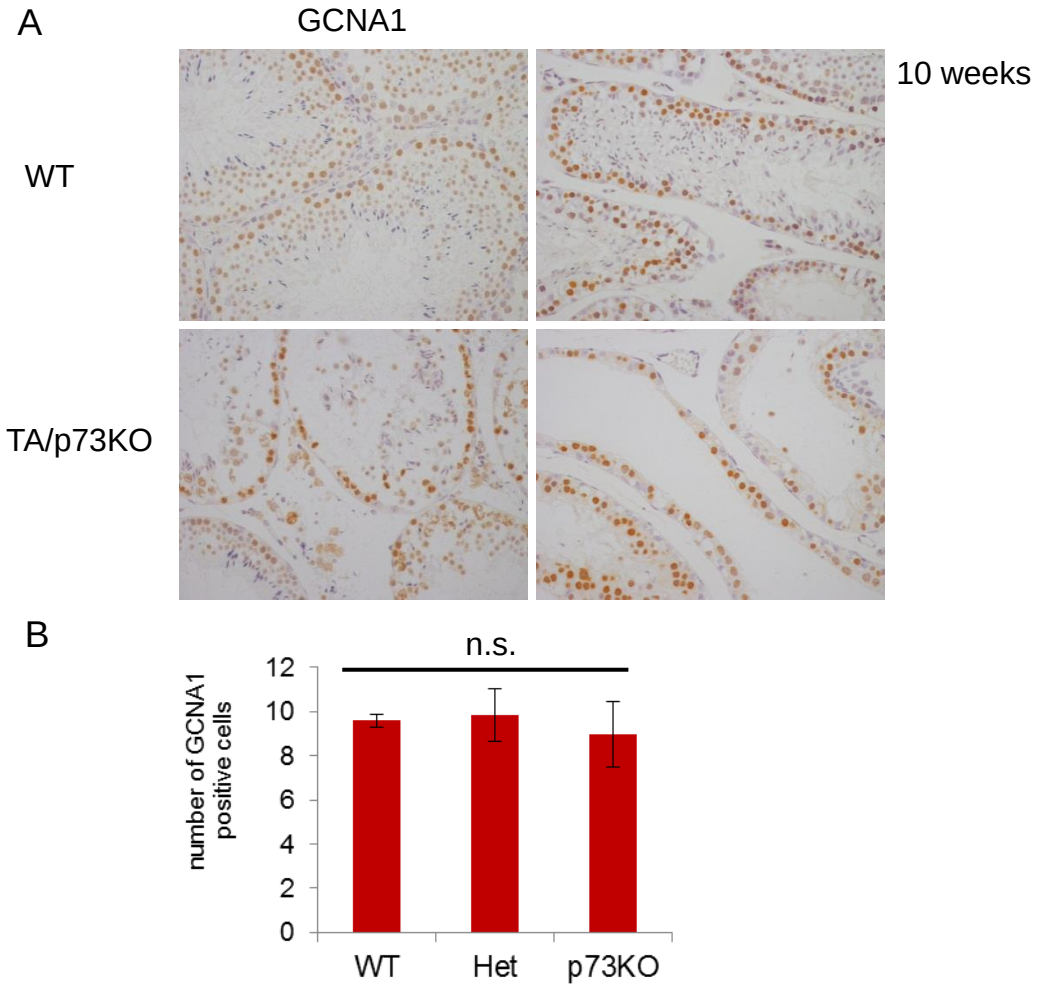

Fig. 5.5: Number of spermatogonia in KO mice is unchanged

A) Immunohistochemistry staining of testis sections from adult TAp73KO and WT mice. Antibody used is directed against GCNA1 (spermatogonia). TA and p73KO mice show no difference in staining of basal spermatogonia. Magnification: 400x
B) Quantitation of basal spermatogonia in p73KO versus WT and Het mice, 6 weeks of age. Number of GCNA1 positive cells within a distance of 120µm was determined. No significant difference in cell number could be detected. n=3-5 mice were analyzed per genotype. Error bars represent the SDM.
$p > 0.05$; n.s. = not significant (Student´s t-test).

5.2 Basal proliferation, meiosis and hormonal regulation are not affected in p73KO and TAp73KO testis

5.2.1 Basal spermatogonia of p73KO mice retain mitotic ability

To enable constant production of meiotic sperm cells, a certain pool of basal spermatogonia has to go through asymmetric mitotic divisions. This process ensures creation of two types of spermatogonia. Type A spermatogonia will stay in the proliferation status, intermediate spermatogonia will differentiate into type B spermatogonia, which will progress into meiosis to produce haploid sperm cells (Borg *et al.*, 2010, Hermo *et al.*, 2010). We therefore wanted to check whether the decrease of post-meiotic sperm cells in p73KO testis could be due to spermatogonia, losing their ability to proliferate. To gain information about the amount of mitotic cells within p73KO testis we applied IHC to testis sections, using the proliferation marker Ki67 (Gerdes *et al.*, 1984). Comparing KO with WT mice, we could not find any differences in the proliferation ability of basal cells (*Figure 5.6 A*). Quantitation of Ki67 positive tubules per testis section did show comparable levels of proliferating tubules for p73KO, heterozygous (Het) and WT mice. This observation was independent of age (*Figure 5.6 C*). The loss of sperm cells within the seminiferous epithelium of p73KO mice cannot be explained by a reduction or loss of the basal mitotic rate.

5.2.2 The meiotic rate is not changed in p73KO testis

Haploid sperm cells derive from diploid spermatogonia by going through meiosis. To permanently produce mature sperm cells for reproduction, constantly a number of basal spermatogonia have to pass through two meiotic divisions (Borg *et al.*, 2010, Hermo *et al.*, 2010). Loss of sperm cells in p73KO mice could be a result of a decreased meiotic rate within the seminiferous epithelium. To test this hypothesis, testis sections of p73KO and WT mice were stained for phosphorylated Histone 3 (H3-phosphoSer10) performing IF. H3 is only phosphorylated at Serine 10 during chromosome condensation, which occurs during mitosis as well as meiosis (Hendzel *et al.*, 1997, Wei *et al.*, 1999). H3Ser10 positive cells within the seminiferous epithelium, excluding basal mitotic cells (also refer to **5.2.1**), can therefore be counted as meiotic spermatocytes. Comparing p73KO and WT mice we could observe no difference in H3Ser10 staining pattern of positively stained tubules (*Figure 5.6 B*). Quantitation of H3Ser10 positive cells per testis section revealed comparable numbers for p73KO, Het and WT mice, independent of age (*Figure 5.6 D*). Therefore the meiotic rate seems to be normal in p73KO testis.

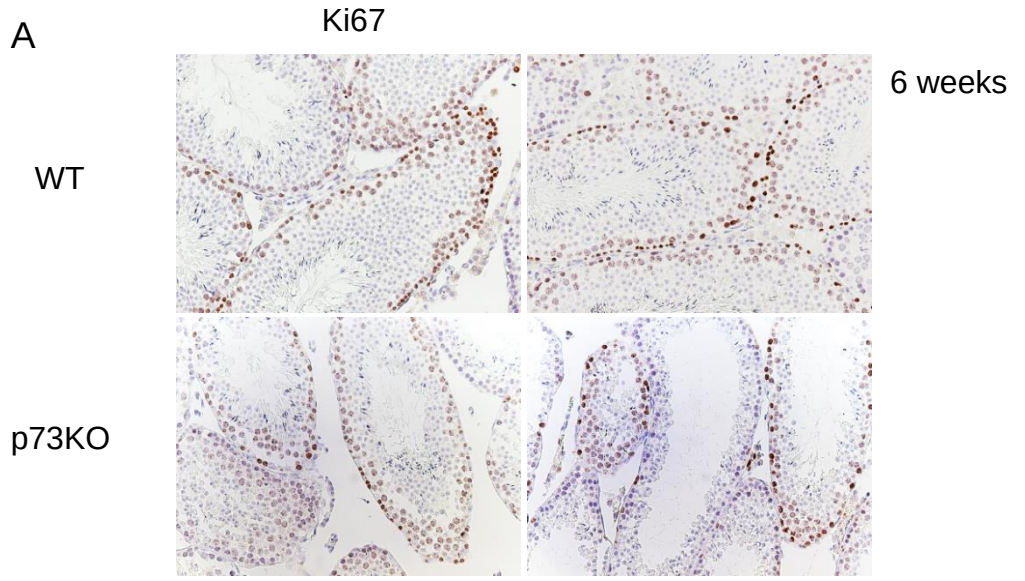
A
Ki67
WT
p73KO
6 weeks

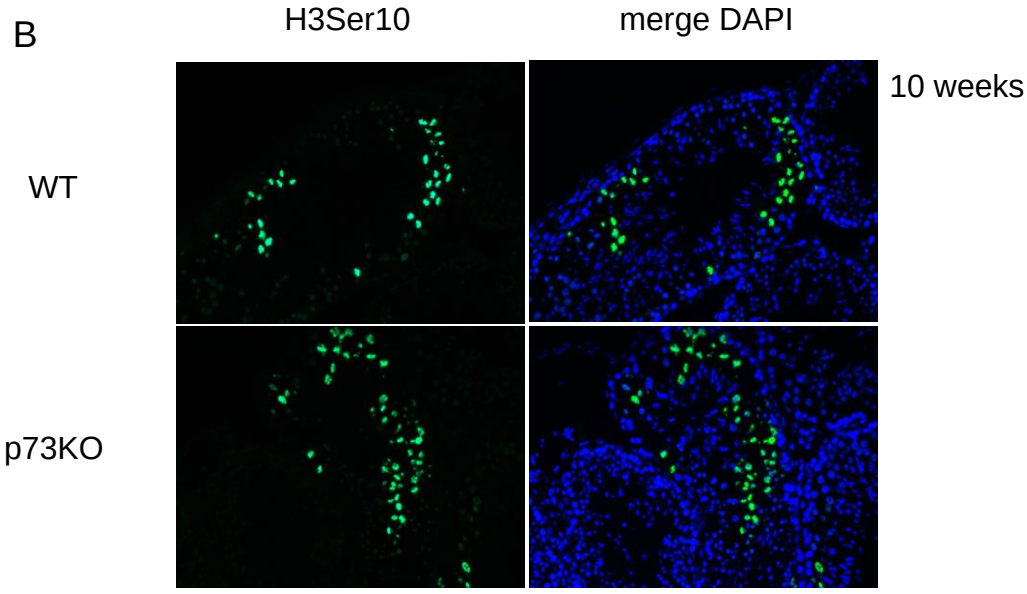
B
H3Ser10
merge DAPI
WT
p73KO
10 weeks

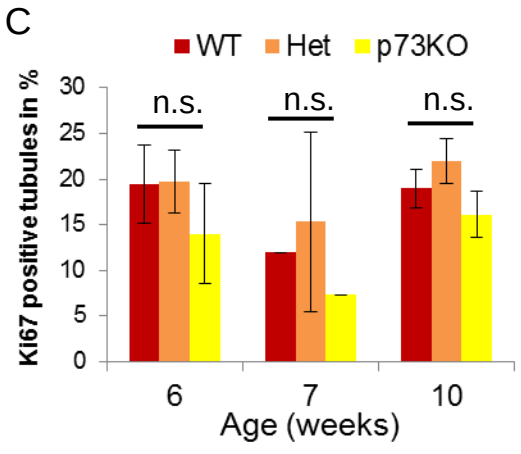
C
WT
Het
p73KO
Ki67 positive tubules in %
30
25
20
15
10
5
0
n.s.
n.s.
n.s.
6
7
10
Age (weeks)

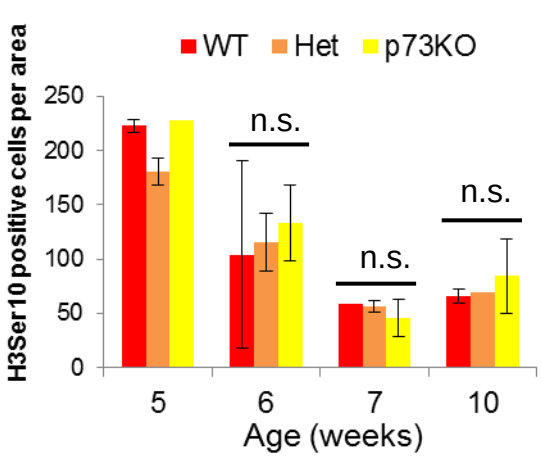
D
WT
Het
p73KO
H3Ser10 positive cells per area
250
200
150
100
50
0
n.s.
n.s.
n.s.
5
6
7
10
Age (weeks)

Fig. 5.6 Loss of sperm cells in KO mice is not a result of decreased proliferation or impaired meiosis.

A) Immunohistochemistry staining of testis sections from adult p73KO and WT mice. Antibody against Ki67 (mitotic cells) was applied to sections. Basal proliferation is also observed in p73KO mice. Magnification: 400x
B) Immunofluorescence staining of testis sections from adult p73KO and WT mice. Antibody directed against phosphorylated H3 (mitotic and meiotic cells) was applied to sections. Meiosis is not impaired in p73KO mice. Magnification: 400x
C) Quantitation of proliferating cells in p73KO versus WT and Het mice of different age. No significant difference in number of Ki67 positive tubules could be detected. n=2-5 mice were analyzed per genotype and age. Error bars represent the SDM. $p > 0.05$; n.s. = not significant (Student´s t-test). Conducted with Sona Pirkuliyeva.
D) Quantitation of meiotic cells in p73KO versus WT and Het mice of different age. No significant difference in number of H3Ser10 positive cells could be detected. n=2-5 mice were analyzed per genotype and age. Error bars represent the SDM. $p > 0.05$; n.s. = not significant (Student´s t-test). Conducted with Sona Pirkuliyeva.

5.2.3 No impairment of the hormonal axis of p73 and TAp73KO mice

Germ cell development is tightly regulated by a complex hierarchic hormone system. Gonadotropin releasing hormone (GnRH) is produced in the hypothalamic neurons and its secretion will activate the release of follicle-stimulating hormone (FSH) and luteinizing hormone (LH) from the pituitary gland. Both gonadotropins will travel through the blood stream and stimulate testicular cells (also refer to **2.1.4**). FSH is influencing spermatogenesis by activating Sertoli cells, while LH is binding to its receptor on intertubular Leydig cells, which will subsequently produce testosterone. Testosterone itself is also important for activation of spermatogenesis (Borg *et al.*, 2010). As already described, p73KO mice are known to show severe neural defects in the brain (refer to **2.2.3**). To exclude a secondary effect for the observed testicular phenotype by deregulation of the hormonal axis starting in the brain, we wanted to measure mRNA expression and serum levels of these hormones. Quantitation of the expression levels of GnRH mRNA, isolated from brain, by performing qPCR revealed no difference for WT and p73KO mice (*Figure 5.7 A*). The same was true for FSH and LH mRNA, isolated from the pituitary gland of TAp73KO, Het and WT mice (*Figure 5.7 B*). To affirm physiological levels of the secreted hormones in KO mice, serum levels of FSH and LH were determined by antigen-specific ELISA assays. Results for FSH as well as LH showed comparable levels of both hormones in the blood stream of TAp73KO and WT mice (*Figure 5.7 C* and *D*). Additionally, serum testosterone levels of p73KO, TAp73KO and WT mice were determined by ELISA. Independent of the genotype the measurements displayed high variance for the data points of each group, but a similar distribution comparing WT and KO mice. No significant difference in testosterone levels could be observed (*Figure*

5.7 E and F). In sum, the described hormonal axis important for germ cell development seems to function normally in p73 and TAp73KO mice.

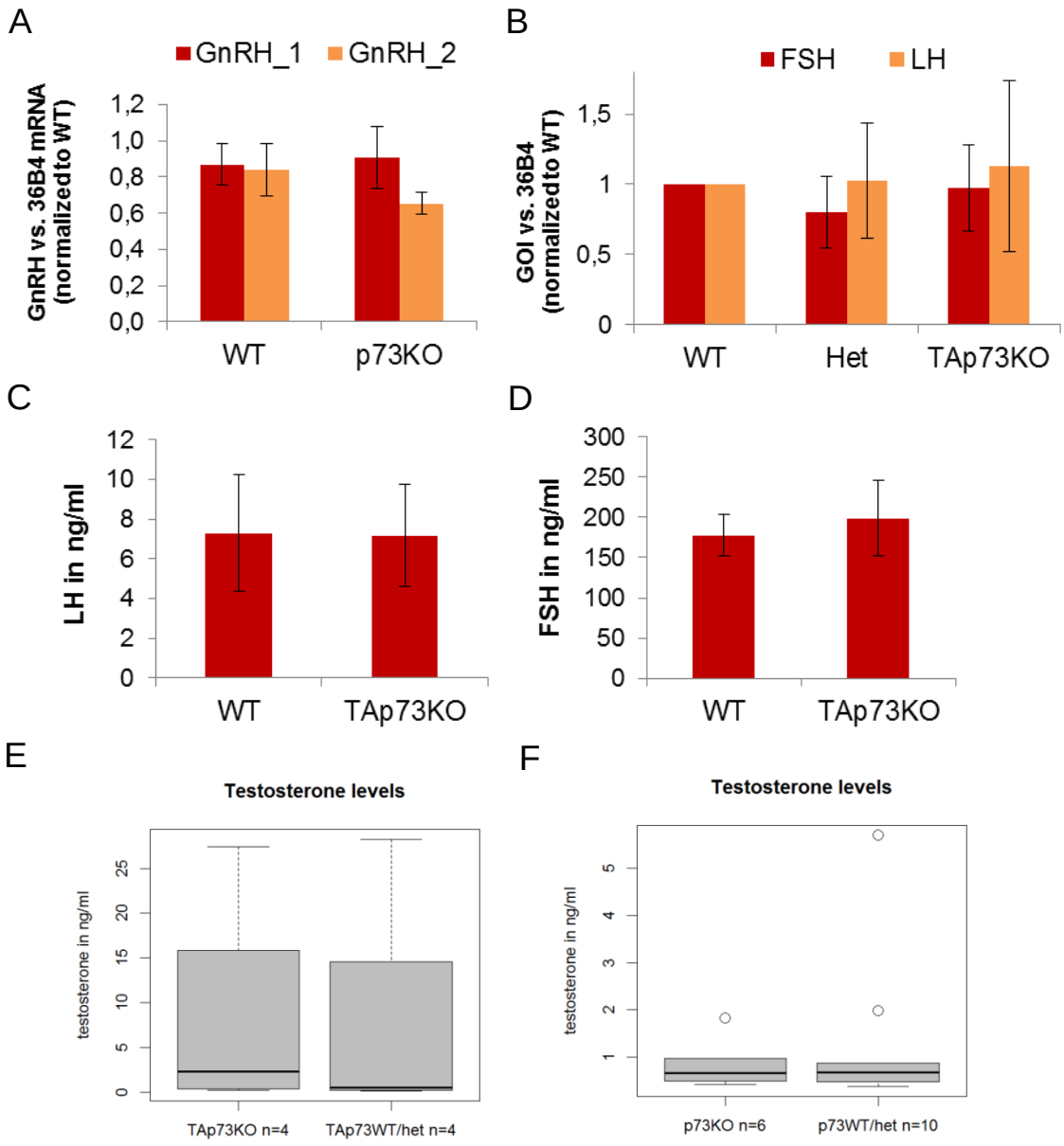

Fig. 5.7 The hormonal axis is not affected in p73 and TAp73KO mice.

A+B) Quantitation of mRNA isolated from brain (GnRH, n=3) or pituitary gland (FSH and LH, n=5-10) of adult KO and WT mice, performing qPCR. Expression levels of all three hormones are physiologically normal in p73 and TAp73KO mice. GOI = gene of interest
C+D) Measurement of LH and FSH levels applying ELISA assay. n=4-5 adult mice were analyzed per genotype. In KO mice serum levels of both hormones are comparable to WT.
E+F) Measurement of testosterone levels via ELISA assay. No change in testosterone serum levels can be observed for adult p73WT/Het and TAp73 KO mice. The indicated numbers of mice were analyzed per genotype. To all quantitations the student´s t-test was applied. $p > 0.05$

5.3 Premature sloughing of sperm cells and detachment from the Sertoli-sperm cell cluster

5.3.1 Mature sperm cells are depleted from p73KO and TAp73KO epididymis whereas immature sperm cells are present

Sperm cells have to go through many differentiation and maturation steps before they are released from the seminiferous epithelium into the lumen of the tubule, which is called the spermiation process. Subsequently, sperm cells travel from the rete testis into the efferent ducts that lead to the epididymis. They travel through its caput and corpus, thereby undergoing further epididymal maturation steps. The cauda of the epididymis mainly functions as storage for the mature spermatozoa before they are released in the ejaculation process via the vas deferens (Borg *et al.*, 2010). Since TAp73KO mice show a strongly reduced number of sperm cells in the testis, we asked whether mature sperm cells would still be present in the cauda epididymidis. Therefore, we applied H&E staining to epididymal sections of TAp73KO and WT mice. Looking at the storage region of the epididymis, the cauda epididymidis, we found empty tubules or little amount of spermatozoa in 50% of all analyzed KO mice (*Figure 5.8 A and Table 5.3*).

	Testis	Epididymis	Epididymis	Epididymis	Epididymis
Applied H&E or IF staining	*TUNEL+ (Lumen)*	*TUNEL + (Lumen)*	*Reduced/no sperm amount (H&E)*	*Reduced APG1 staining*	*Increased VASA staining*
Detection of	apoptosis	apoptosis	sperm number	mature sperm	immature sperm
KO mice, showing positive staining	10 of 17	3 of 8	9 of 20	4 of 9	4 of 9

Table 5.3: Summary of stainings applied to p73KO and TAp73KO testis and epididymis of adult mice.

Various observations can be made throughout p73KO and TAp73KO mice: Around 50% of all analyzed KO mice show an increase of apoptotic cells in lumina of testis and epididymis (TUNEL positivity). Additionally, in nearly 50% of the KO mice the number of mature sperm is decreased (H&E, APG1) and immature cells are increased (VASA) within the epididymis.

WT mice always displayed tubules full of mature spermatozoa within this region (*Figure 5.8 A*). IF staining for APG1, a marker for mature sperm cells (also refer to **5.1.3**), confirmed the reduced amount of spermatozoa in the lumen of TAp73KO epididymis (*Figure 5.8 B and Table 5.3*). Additionally, a higher amount of immature sperm cells could be observed in the epididymis of KO mice. Immature spermatocytes and round spermatids can be visualized by IF staining using the antibody directed against VASA (*Figure 5.8 B*, also refer to **5.1.3**).

Quantitation of the described IF staining revealed abnormal distribution of mature (APG1) and immature (VASA) sperm cells in around 50% of the analyzed KO mice (*Table 5.3*). These two observations were made in parallel or individually.

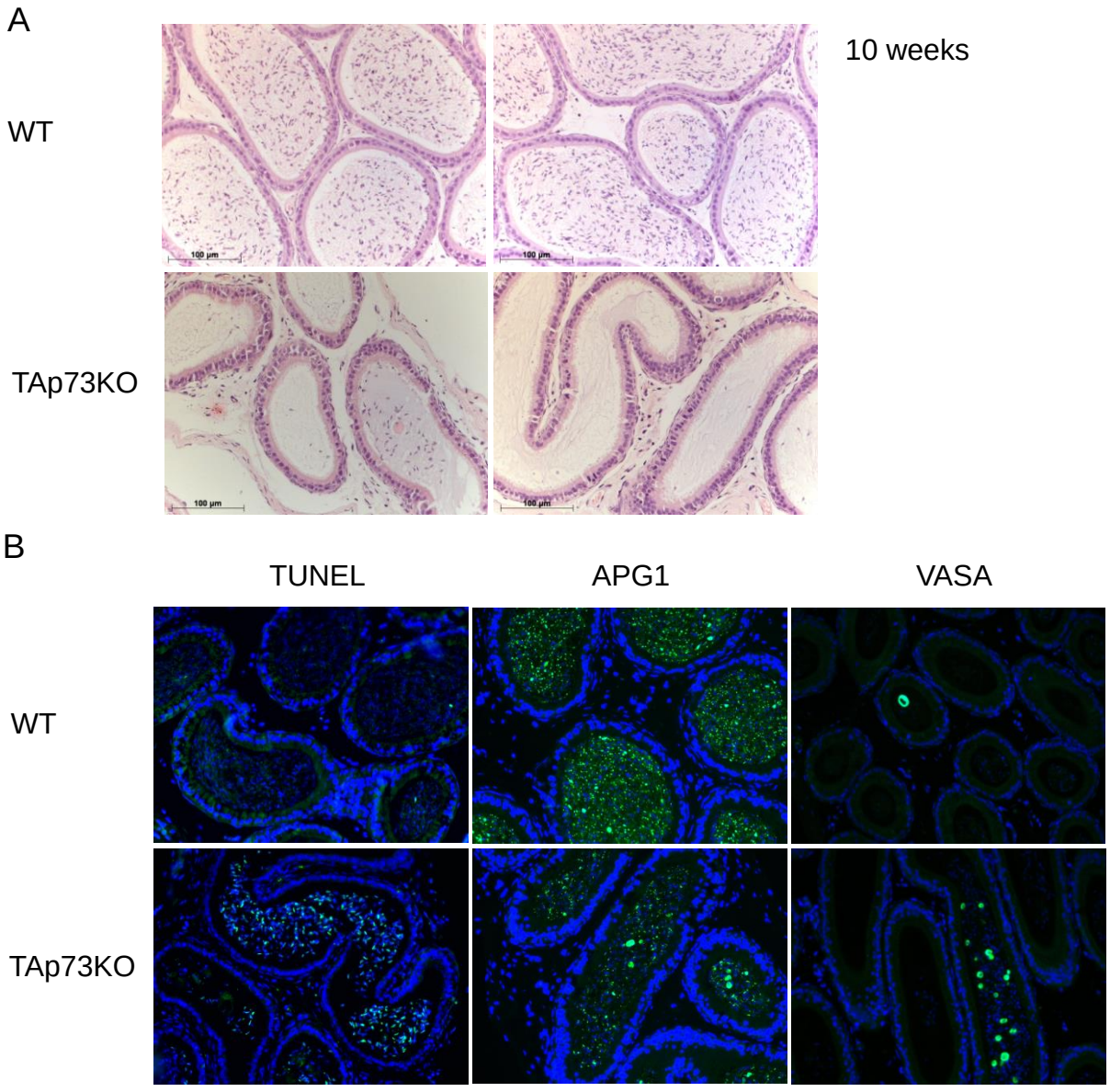

Fig. 5.8 Epididymes of TAp73KO mice display reduced numbers of mature sperm as well as increased numbers of apoptotic and immature sperm.

A) Longitudinal sections of the epididymis. Caudal part of adult TAp73KO and WT littermates is shown. H&E staining. 50% of adult TAp73KO mice show reduced numbers or no sperm cells within the lumina of the epididymis. Magnification: 400x
B) Immunofluorescence staining of the cauda epididymidis. TUNEL staining and antibodies against VASA (spermatocytes and round spermatids) and APG1 (spermatids and spermatozoa) were applied to longitudinal sections. TAp73KO mice reveal loss of sperm cells visualized by increased apoptosis and decreased staining for mature sperm. Additionally, increased numbers of immature sperm are observed in TAp73KO epididymis. Magnification: 400x

Finally, we used an immunofluorescence TUNEL assay on testicular and epididymal sections to check for apoptotic cells (*Figure 5.8 B*). 50% of the analyzed tissue of p73KO and TAp73KO mice showed increased apoptosis in the lumen of the tubules (*Table 5.3*). These results indicate that sperm cells are prematurely released from the seminiferous epithelium of the testis. Therefore, they cannot survive and die by apoptosis. This subsequently seems to result in a loss of mature spermatozoa from the epididymis of TAp73KO mice.

5.3.2 Sertoli cell number is unchanged in p73KO and TAp73KO testis

Besides the different developmental stages of germ cells the Sertoli cells are also part of the seminiferous epithelium in the testis. Since we observed a disorganized structure of the tubule layers as well as a strong sperm cell loss in testis and epididymis we asked whether the loss or reduction of Sertoli cells could be the reason for this phenotype. Sertoli cells hold an important role during sperm cell development, functioning as supporter, nutrition provider and protector of the sperm cells (Griswold, 1998). To gain information about the number of Sertoli cells in p73KO and TAp73KO mice compared to WT, we applied IF staining to testis sections. The transcription factor Wilms tumor protein 1 (WT1) is known to be a nuclear marker for Sertoli cells (Gao *et al.*, 2006, Rao *et al.*, 2006, Sharpe *et al.*, 2003). Using a WT1-specific antibody we could not observe any difference in the staining pattern when we looked at KO and WT testis. Sertoli cell nuclei were found at the basal site of the tubules and followed each other in a similar regular distance (*Figure 5.9 A*). Quantitation of WT1 positive cells per unit length with help of the Axio Vision Software showed comparable numbers of Sertoli cells for 6 to 7 weeks old KO, Het and WT mice. 10 weeks old p73KO mice displayed slightly decreased numbers of WT1 positive cells (*Figure 5.9 B*). In contrast to strongly reduced numbers of sperm cells, the Sertoli cell amount in testis does not seem to be reduced in p73KO and TAp73KO mice.

5.3.3 Sertoli cell morphology of TAp73KO mice is impaired

When we were looking at Sertoli cell numbers we did not find a striking difference in KO testis compared to WT. Since the structure of Sertoli cells is very important to enable positioning and movement of sperm cells from basal to apical through the different layers of development, we additionally wanted to check for Sertoli cell morphology. For this approach we carried out IHC staining on testis sections.

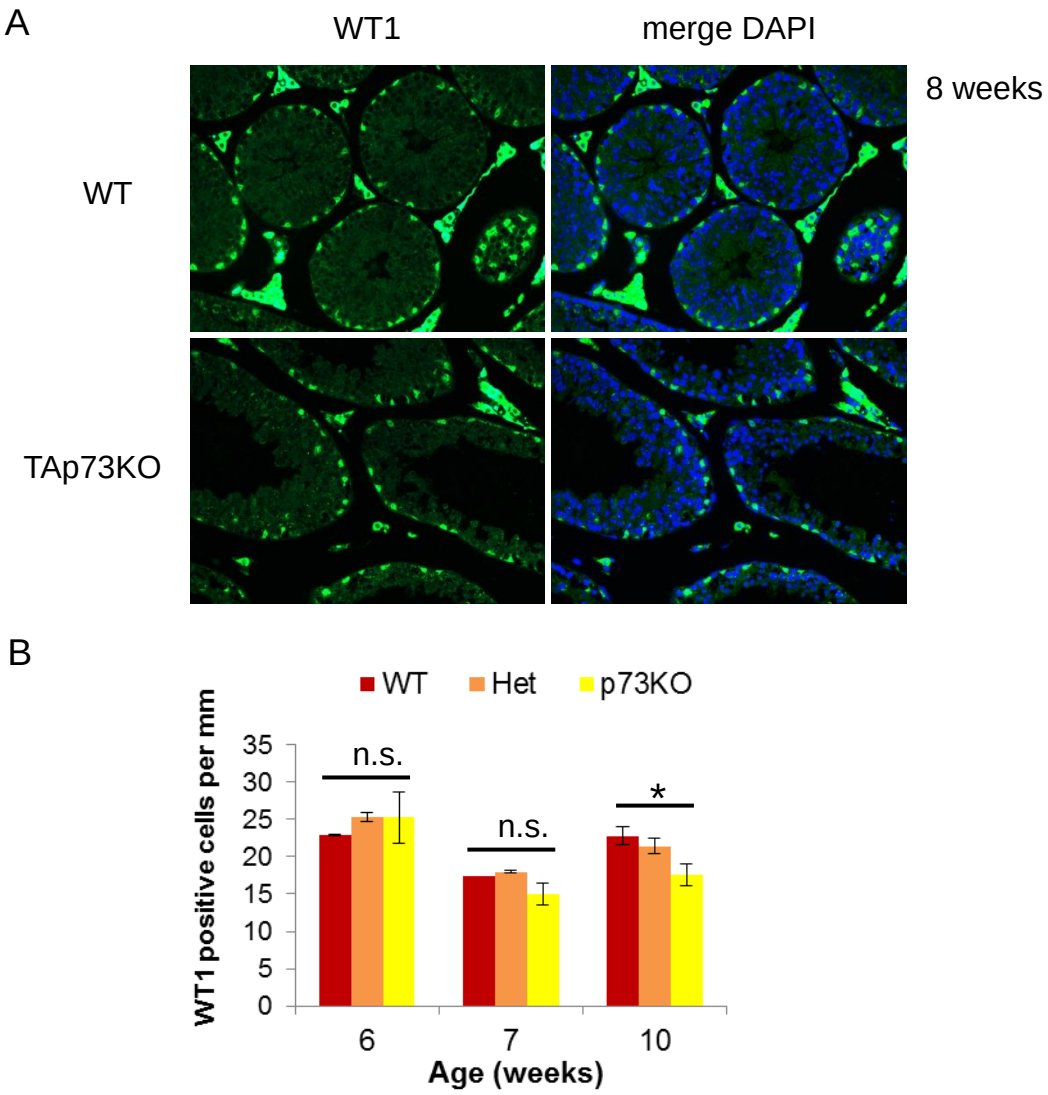

Fig. 5.9 TAp73KO mice display no change in Sertoli cell numbers.

A) Immunofluorescence staining of testis sections from adult TAp73KO and WT mice. The antibody used is directed against WT1 (nuclear Sertoli marker). Number of Sertoli cells is not changed in KO mice. Magnification: 400x
B) Quantitation of WT1 positive cells (=Sertoli cells) in p73KO versus WT and Het mice of different age. No significant difference in Sertoli cell number could be detected. n=2-5 mice were analyzed per genotype. Error bars represent the SDM. $p > 0.05$; n.s. = not significant; * = $p < 0.05$ (Student´s t-test). Conducted with Sona Pirkuliyeva.

Using an antibody against the intermediate filament Vimentin, we could visualize the long arms of Sertoli cells reaching through all layers of the seminiferous epithelium and building pockets for the sperm cells to sit in (Aumuller *et al.*, 1988, Paranko *et al.*, 1986). Comparing IHC staining of TAp73KO and WT mice, we found shortened Sertoli cell arms accompanied by a thin and disorganized structure in the KO tubules (*Figure 5.10 A*). When we quantified

the total length of Vimentin-stained Sertoli cytoskeleton per area, using the Axio Vision Software, a highly significant reduction could be shown for TAp73KO mice (*Figure 5.10 B*). For analysis of Vimentin quantitation refer to **4.1.7.6**.

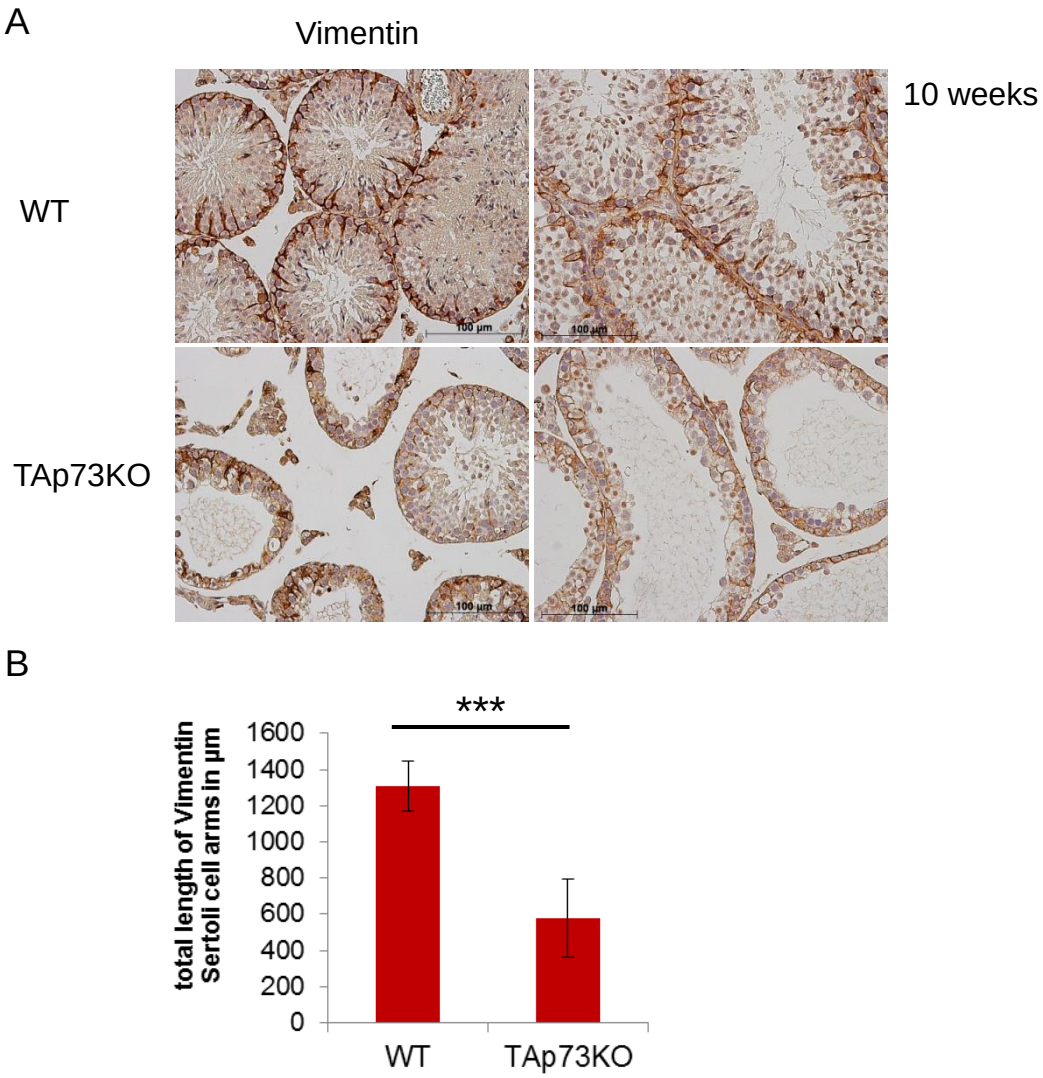

Fig. 5.10 Sertoli cell morphology is impaired in TAp73KO mice.

A) Immunohistochemistry staining of testis sections from adult TAp73KO and WT mice. The antibody used is directed against Vimentin (intermediate filament, Sertoli marker). Sertoli cells display shortened cytoplasmic arms within the seminiferous epithelium. Magnification: 400x

B) Quantitation of Sertoli cell arms in adult TAp73KO versus WT mice. All cytoplasmic arms, reaching from the basal layer towards the tubular lumen, were measured in length within one view. The sum of all measurements per area was taken and determined as the “total length” of Vimentin Sertoli cell arms. Length of Sertoli cell arms reaching from the basal layer through the seminiferous epithelium is significantly decreased in TAp73KO mice. n=3 mice were analyzed per genotype. Error bars represent the SDM. *** = $p < 0.005$ (Student´s t-test).

Fig. 5.11 Sperm cells are not retained properly by KO Sertoli cells

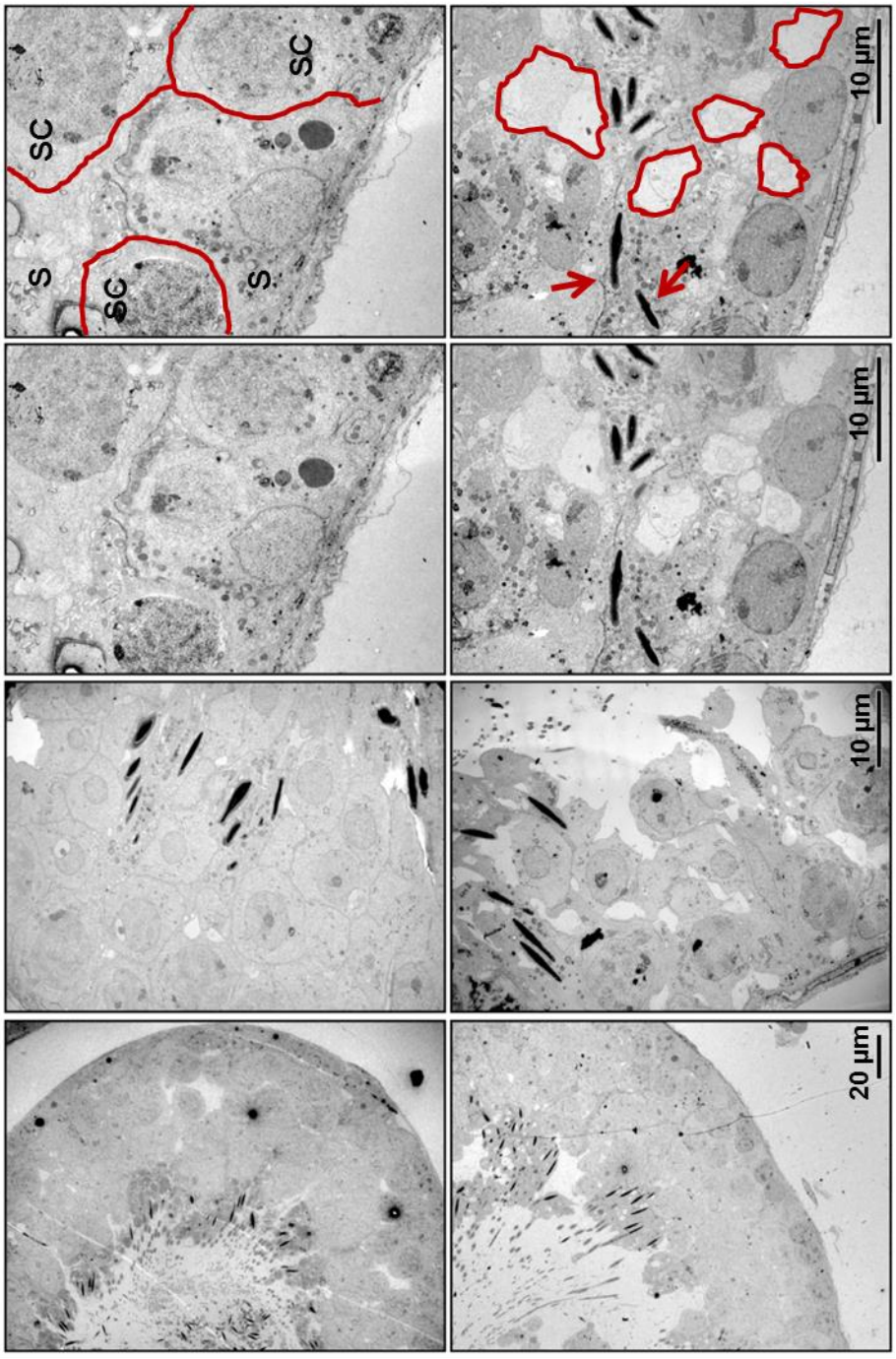

Electron microscopy of ultra thin testis sections from adult TAp73KO and WT mice. Sperm cells of the seminiferous epithelium are not packed tightly in KO testis and Sertoli cells fail to retain the developing sperm cells. The right picture shows a modified image of the highest magnification. Gaps and holes within the KO tissue are marked with red. The arrows indicate elongated spermatids close to the basement membrane of KO testis. In contrast, WT mice display a tightly packed seminiferous epithelium with sperm cells (SC) attaching close to a Sertoli cell (S). n=9-10 mice were analyzed per genotype.

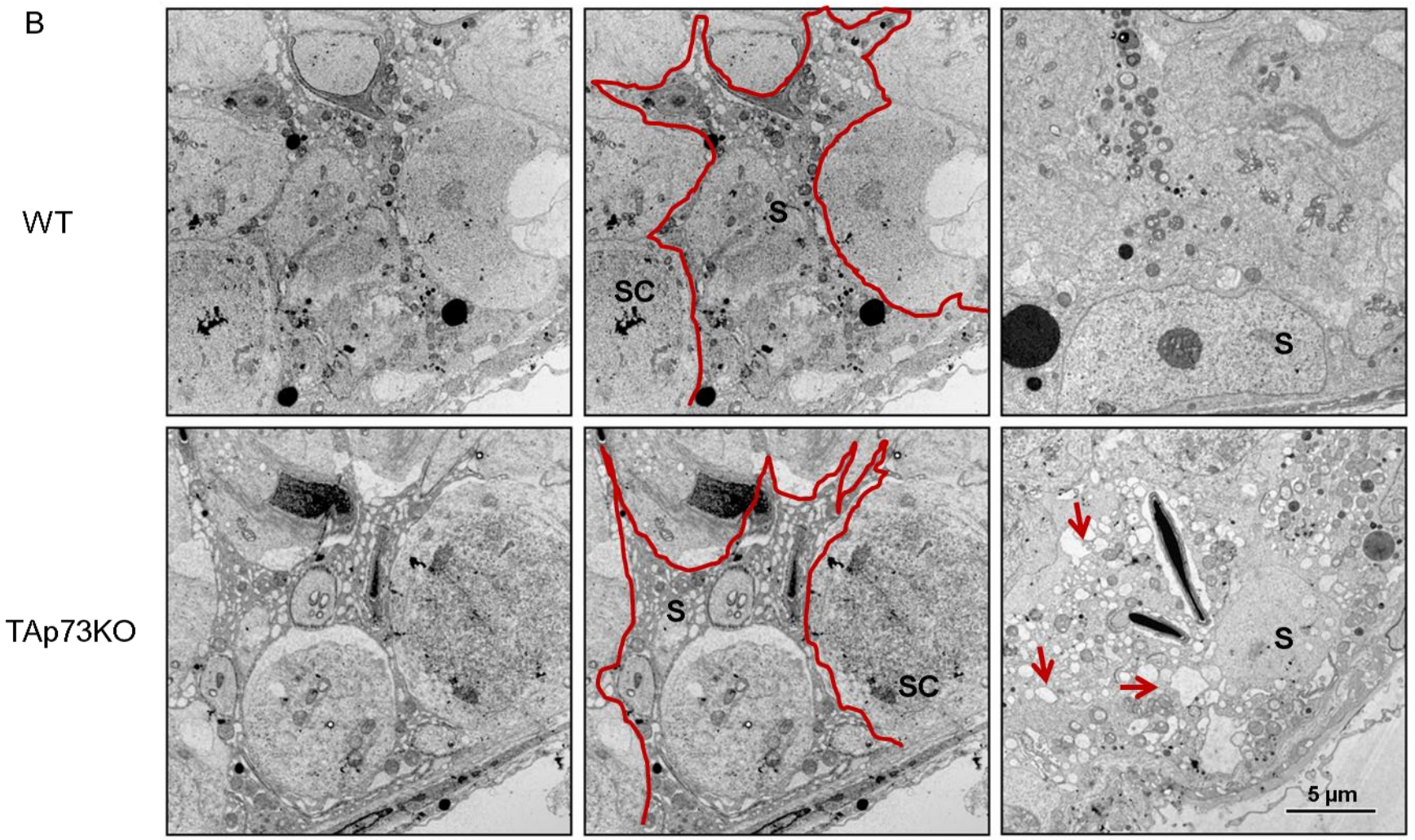

Sertoli cells (S) of KO mice display thin cytoplasmic arms and increased vesicular morphology. The sketch shows the outline of the Sertoli cells in red. Its arms branch in many directions. Cytoplasmic arms are tightly wrapped around sperm cells (SC) in WT testis. KO Sertoli cells show a degenerated shape. Arrows indicate high vacuolization in KO Sertoli cells. n=9-10 mice were analyzed per genotype.

To analyze the germ epithelium and Sertoli cell structure in more detail we fixed testis samples in 2.5% glutaraldehyde, stained them in 1% osmiumtetroxide and 1% uranyl acetate and embedded the samples in Agar 100 for electron microscopy. Ultrathin sections of tubules confirmed the reduction of developing germ cells in TAp73KO testis (*Figure 5.11 A*). Electron microscopy furthermore showed nicely packed layers of spermatocytes and spermatids in WT sections, while the seminiferous epithelium of KO mice displayed a loose structure and sperm cells seemed to float away from the cell compound. Closed cell-cell attachments were often missing in KO tubules and the seminiferous epithelium exhibited many cavities. Elongated spermatids were already found close to the basement membrane, not in the upper layers of the germ epithelium (*Figure 5.11 A*). Sertoli cells wrap their cytoplasmic arms tightly around sperm cells in WT testis. When we looked at KO Sertoli cells we found thin arms that seemed degenerated and could not hold sperm cells anymore. The contact between Sertoli and sperm cell was loosened and often displayed big gaps. Additionally, KO Sertoli cells showed increased vacuolisation (*Figure 5.11 B*). The change in morphology of Sertoli cells points towards a defect in their functions important for sperm attachment and development.

5.4 Adhesion- and migration-related genes are upregulated in TAp73KO mice, thereby interfering with Sertoli-sperm cell interaction

5.4.1 TAp73 functions as transcriptional inhibitor in the male germ line

To gain more insight in the molecular regulation of germ cell development by the transcription factor TAp73 we performed a whole transcriptome microarray. TAp73KO and WT testes (n = 3) from 10 weeks old mice were prepped out, RNA was isolated and 6 samples were objected to microarray analysis in the transcriptome analysis lab (TAL) of the university of Göttingen. For quantitation of the obtained data a threshold of 2 times regulation was set. Surprisingly, 148 out of 160 regulated genes showed an upregulation upon KO of TAp73. The heatmap of the top 50 genes deregulated in TAp73KO mice features this distribution. A positive value of the Z-Score mirrors a high expression rate of the analyzed gene (green colour code), a negative value a low expression rate (blue colour code) (*Figure 5.12*). If the loss of TAp73 leads to an upregulation of gene expression in testis, it can be stated that TAp73 must in some way act as transcriptional inhibitor within this tissue.

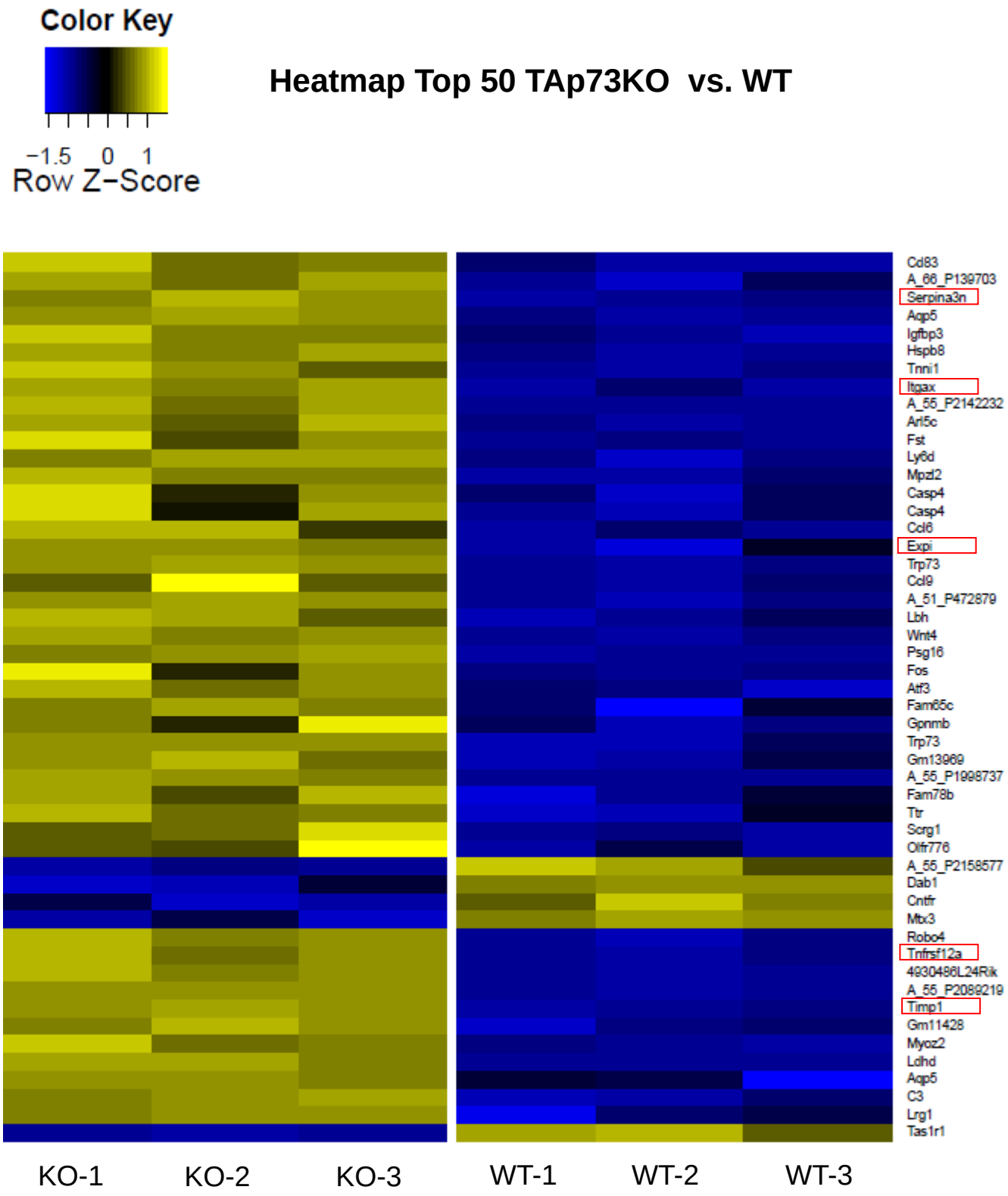

Fig. 5.12 TAp73 exhibits inhibitory functions within the male germ line.

Microarray analysis was performed on 10 weeks old TAp73KO mice, comparing their testicular mRNA pool with WT littermates. n=3 mice were analyzed per genotype. The heatmap features the top 50 regulated genes in TAp73KO mice. By applying a threshold of 2 times induction/repression, 160 genes were found to be regulated in TAp73KO mice. 92% of these genes were upregulated indicating a repressor function for TAp73 in the male germ line. Highlighted genes in red are associated with adhesion and migration.

5.4.2 TAp73KO leads to upregulation of proteinase inhibitors and adhesion-related molecules in the testis

When we looked more closely at the genes regulated in TAp73KO testis, we found several genes strongly related to adhesion and migration. The first hit with the strongest induction in the microarray, tissue inhibitor of metalloproteinases (Timp1), is described to be expressed in testis and plays a role during sperm migration in the seminiferous epithelium (Guyot *et al.*, 2003, Le Magueresse-Battistoni, 2007, Siu *et al.*, 2003). Interestingly a big group of genes upregulated in TAp73KO testis harbour proteinase or peptidase inhibitor function like Timp1 does. Several genes of the Serpin family (serine peptidase inhibitors) as well as the extracellular proteinase inhibitor Expi were found to be induced in KO mice (*Table 5.4*).

Candidate	Symbol	Description	Gene	Uniprot	logFC KO - WT	P.Value KO - WT	Validated via qPCR
3	**Timp1**	tissue inhibitor of metalloproteinase 1	21857	1729	**3,82**	1,44E-07	yes
16	**Serpina3n**	serine (or cysteine) peptidase inhibitor, clade A, member 3N	20716	NA	**3,01**	1,73E-06	yes
19	**Expi**	extracellular proteinase inhibitor	14038	4722	**2,87**	4,13E-04	no
27	**Tnfrsf12a**	tumor necrosis factor receptor superfamily, member 12a	27279	14202	**2,44**	7,02E-06	yes
37	**Itgax**	integrin alpha X	16411	15777	**1,86**	1,01E-05	yes
67	**Serpinb6b**	serine (or cysteine) peptidase inhibitor, clade B, member 6b	20708	2876	**1,45**	1,40E-04	yes
90	**Serping1**	serine (or cysteine) peptidase inhibitor, clade G, member 1	12258	961	**1,25**	5,80E-06	yes
93	**Adam23**	a disintegrin and metallopeptidase domain 23	23792	8390	**1,24**	1,89E-06	yes
98	**Itga5**	integrin alpha 5 (fibronectin receptor alpha)	16402	10360	**1,23**	5,32E-06	yes
108	**Serping1**	serine (or cysteine) peptidase inhibitor, clade G, member 1	12258	961	**1,19**	3,31E-06	yes
113	**Tnfrsf1b**	tumor necrosis factor receptor superfamily, member 1b	21938	3907	**1,18**	2,48E-04	not done
130	**Cldn10**	claudin 10	58187	14323	**-1,11**	1,19E-03	not done
143	**Spink8**	serine peptidase inhibitor, Kazal type 8	78709	5340	**1,05**	3,00E-04	not done
148	**Mmp23**	matrix metallopeptidase 23	26561	294	**1,04**	9,40E-04	not done

Table 5.4: Adhesion- and migration-associated genes are deregulated in TAp73KO testis.

Several genes associated with adhesion and migration are strongly upregulated in TAp73KO testis. Many of the regulated proteins have proteinase inhibitory function, some possess peptidase activity and others are part of intercellular junctions. The table includes the name of the upregulated gene, as well as its NCBI gene and Uniprot number. Induction is depicted as log2, since the threshold is set at 2. Therefore a positive number indicates upregulation in TAp73KO mice, as compared to WT mice. The fold induction can be calculated by 2^x.

Besides Timp1, Serpins are also discussed to enable migration of developing germ cells from the basement membrane to the apical luminal part of the tubules (Le Magueresse-Battistoni,

2007). Additionally, some peptidases regulated by this kind of peptidase inhibitors, like the matrix metallopeptidases Adam23 and Mmp23, were deregulated (*Table 5.4*).

With focus on the strongly upregulated proteinase inhibitors Timp1 and Serpina3n we next wanted to validate the obtained microarray results and compare upregulation of these genes in p73KO, TAp73KO and WT mice of different age. To quantify mRNA expression we carried out qPCR analysis on testicular RNA, using gene specific primers for Timp1 and Serpina3n. Looking at different stages the variance of Timp1 expression within one group was very high, but all KO mice showed stronger expression compared to WT levels (*Figure 5.13 A*).

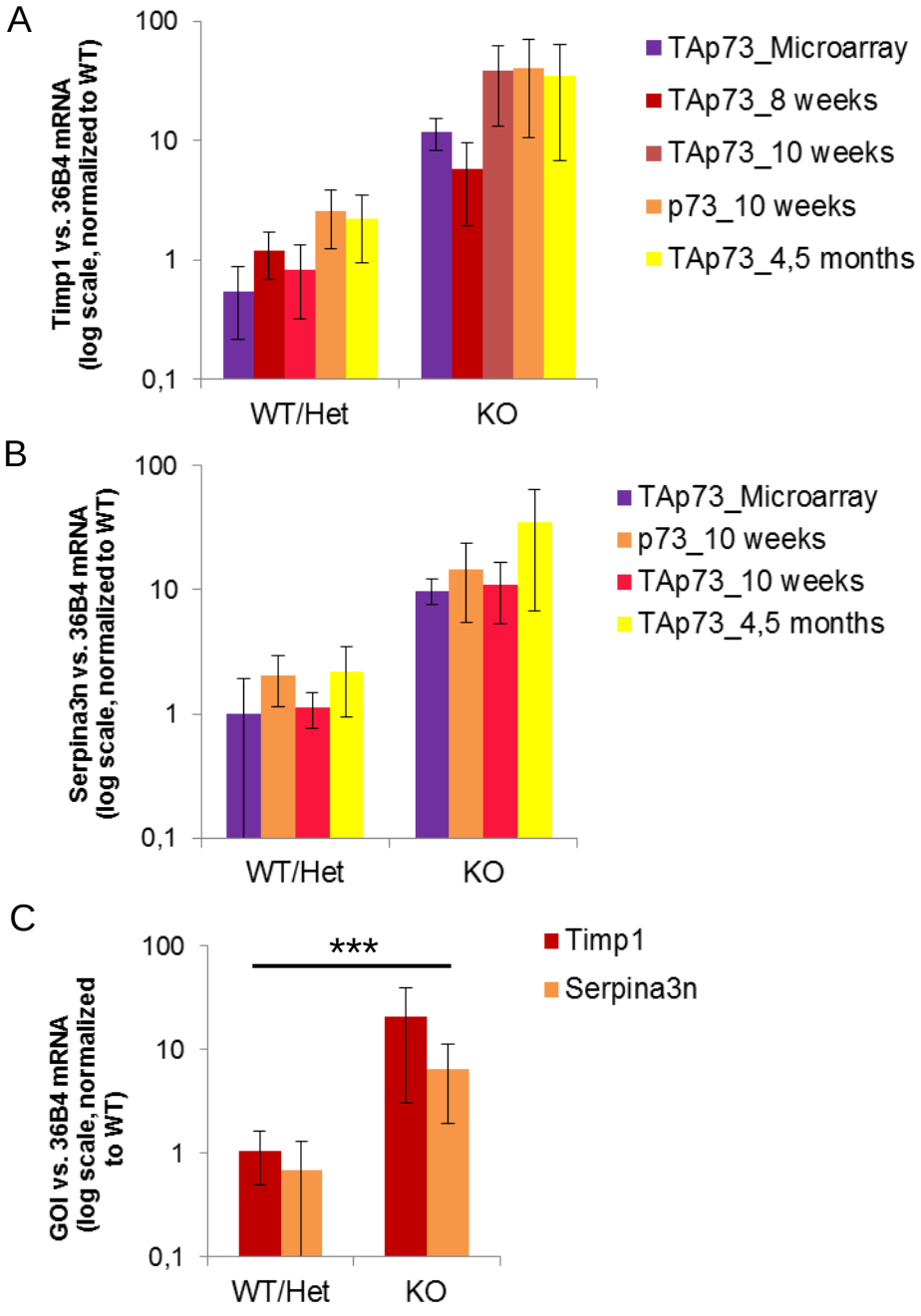

Fig. 5.13 The tissue inhibitor of metalloproteinases Timp1 and the serine peptidase inhibitor Serpina3n are strongly upregulated in p73KO and TAp73KO testis.

A+B) Quantitation of Timp1 (A) and Serpina3n (B) mRNA isolated from p73KO, TAp73KO and WT/Het testis, performing qPCR. Testes from adult mice objected to microarray analysis as well as testes from mice of different age were analyzed. Timp1 (A) as well as Serpina3n (B) are highly upregulated in all populations of adult p73KO and TAp73KO mice independent of age. n=3-6 mice were analyzed per genotype and age.
C) Summary of Timp1 (A) and Serpina3n (B) expression in adult mice: Expression of both genes is significantly higher in KO testes compared to WT/Het littermates. n=16-22 mice were analyzed per genotype. Error bars represent the SDM. *** = $p < 0.005$ (Student´s t-test). Conducted with Kristina Gamper.

Induction was independent of age with 8 weeks old TAp73KO mice having slightly lower expression levels compared to 10 weeks and 4.5 months old mice. Timp1 was upregulated in total p73KO mice as well as TAp73 isoform-specific KO mice (*Figure 5.13 A*). Taking all analyzed mice together, Timp1 expression was 10-60 times higher in KO testis and was therefore significantly increased compared to WT mice (*Figure 5.13 C*). Similar results could be obtained for the peptidase inhibitor Serpina3n. Expression levels were significantly increased and around 10 times higher in KO testes (*Figure 5.13 C*). Induction was largely independent of age, with slightly higher Serpina3n expression levels in 4.5 months old TAp73KO mice. Again, upregulation of the peptidase inhibitor could be shown for total p73KO as well as TAp73 isoform-specific KO mice (*Figure 5.13 B*).

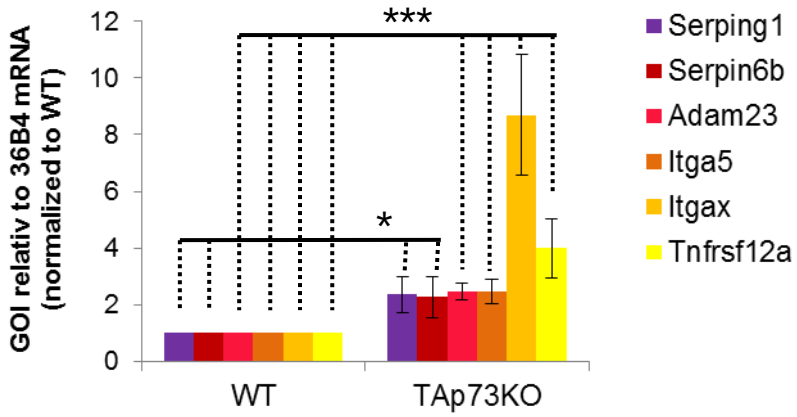

Fig. 5.14 Adhesion- and migration related genes are upregulated in TAp73KO mice.

Quantitation of mRNA isolated from adult TAp73KO and WT testis, performing qPCR. Adhesion- and migration-associated genes like the serine peptidase inhibitors Serping1 and Serpin6b, the metallopeptidase Adam23, the integrins Itga5 and Itgax as well as the Tnf-receptor Tnfrsf12a are significantly upregulated in adult TAp73KO mice. n=3 mice were analyzed per genotype. Error bars represent the SDM. * = $p < 0.05$ and *** = $p < 0.005$ (Student´s t-test).

We next wanted to validate further proteinase inhibitors upregulated in the microarray as well as additional adhesion-related genes (*Table 5.4*). Quantitation of mRNA expression levels in testis was gained by performing qPCR with gene specific primers. In contrast to Serpina3n, the peptidase inhibitors Serping1 and Serpin6b were only induced 2 times in TAp73KO mice, but this induction was significant (*Figure 5.14*). Upregulation in TAp73KO testis could also be validated for mRNA of matrix metallopeptidase Adam23, the integrins Itga5 and Itgax and the tumor necrosis factor receptor Tnfrsf12a. The induction of these genes in TAp73KO mice was highly significant (*Figure 5.14*).

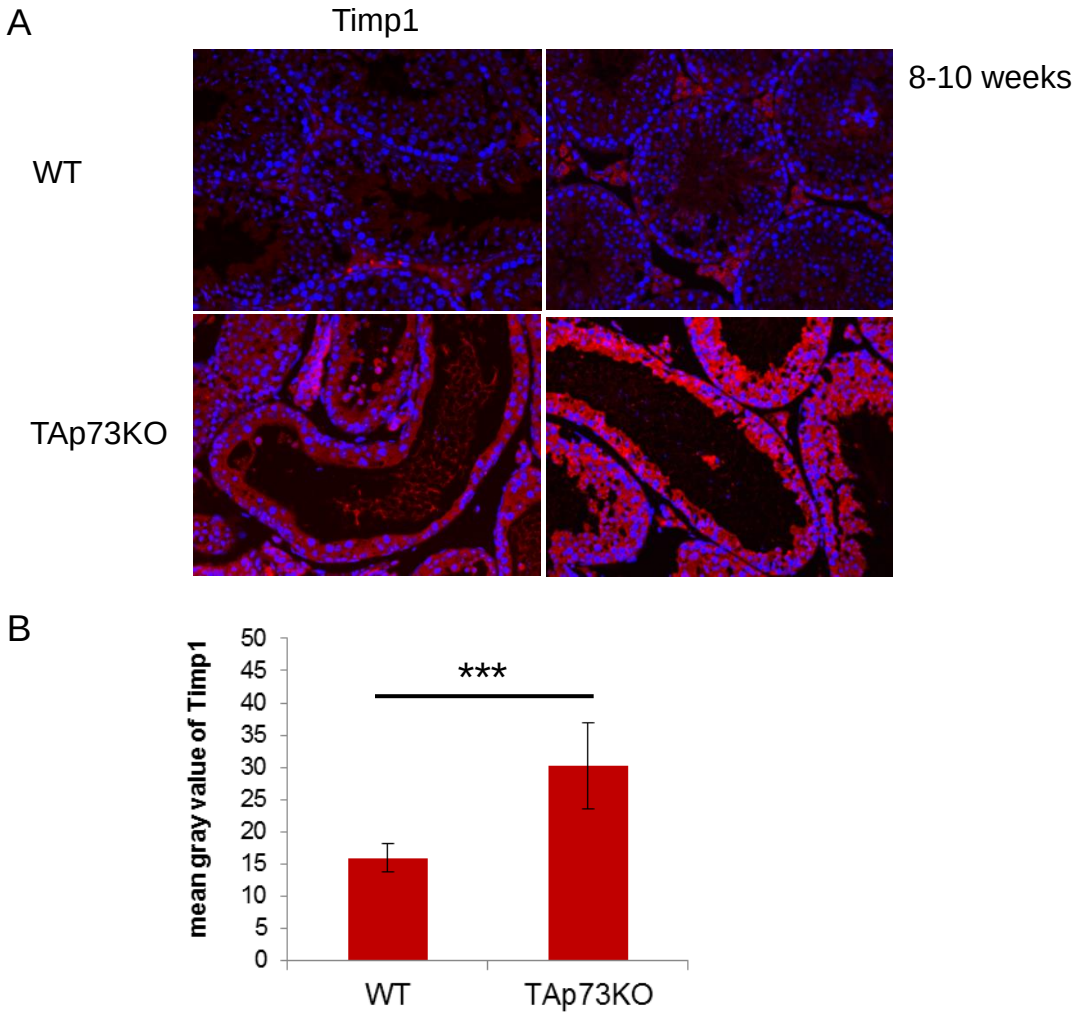

Fig. 5.15 Adhesion- and migration related genes are upregulated in TAp73KO mice.

A) Immunofluorescence staining of testis sections from adult TAp73KO and WT mice. Protein levels of Timp1 were detected by usage of an antigen-specific antibody. Timp1 is found in the cytoplasm of all cells of the seminiferous epithelium as well as extracellular. TAp73KO mice show high expression levels for Timp1 in the testis. Magnification: 400x
B) Quantitation of Timp1 staining (A) in TAp73KO versus WT mice. The mean gray value shows a significant higher expression for Timp1 in testicular TAp73KO sections. n=5-7 mice were analyzed per genotype. Error bars represent the SDM. *** = $p < 0.005$ (Student´s t-test).

To additionally analyze the protein expression levels of the strongly induced candidate Timp1, we performed IF staining on testis sections. To detect Timp1 an antigen-specific antibody was applied to TAp73KO and WT samples. Protein levels of Timp1 were very low in WT testis and only a faint staining was visible. Hormone producing Leydig cells were stained non-specifically. In TAp73KO testis, we found a strong staining for Timp1. The metalloproteinase inhibitor was located to the cytoplasm throughout all layers of the seminiferous epithelium. It was also found extracellular and in the lumen of the tubules (*Figure 5.15 A*). For quantitation of Timp1 protein expression we calculated the mean gray value of the stained area using Adobe Photoshop CS5. 3 to 5 photos per mouse were taken and 5 to 7 mice were analyzed per genotype (also refer to **4.1.7.7**). Comparing TAp73KO and WT tubules, we found a significantly increased expression of Timp1 in the seminiferous epithelium of KO mice (*Figure 5.15 B*).

Peptidase inhibitors like Timp1 and the Serpin family are strongly upregulated in TAp73KO mice. In parallel also peptidases themselves as well as other adhesion associated molecules are induced. TAp73 therefore seems to influence adhesion and migration processes within the testis. It might be important for sperm adhesion and be part of the sperm cell migration through the seminiferous epithelium.

5.4.3 The structure of the apical ectoplasmic specialization (ES) is impaired in TAp73KO mice

Since we found that regulation of adhesion and migration seemed to be affected on mRNA level in TAp73KO testis, we wondered whether this might have an impact on cell-cell adhesion on histologic level. Spermatids on the apical site of the seminiferous epithelium are attached to Sertoli cells by the apical ectoplasmic spezialisation (ES), an adherens junction-like structure (Mruk *et al.*, 2004, Lee *et al.*, 2004b) (also refer to **2.1.3.3**). It can be visualized by staining for the ES-specific protein Espin, which is an important microfilament binding protein within these junctions (Bartles *et al.*, 1996). We performed IF staining using an antigen-specific antibody against Espin, comparing TAp73KO testis sections with WT. Looking at WT sections we found a strong staining of Espin at the luminal site of the tubules. The structure of the apical ES displayed an organized pattern of parallel junctions (*Figure 5.16, WT, arrows*). When we looked at TAp73KO testis we either found an unstructured staining of Espin reaching through all sperm layers or in case of thin tubules only sporadic staining of junctions (*Figure 5.16, TAp73KO, arrows*). These data indicate that loss of TAp73KO affects normal adhesion of sperm cells to Sertoli cells. A deregulation of the

complex adhesion machinery in the testis might lead to the premature release of sperm cells from the seminiferous epithelium.

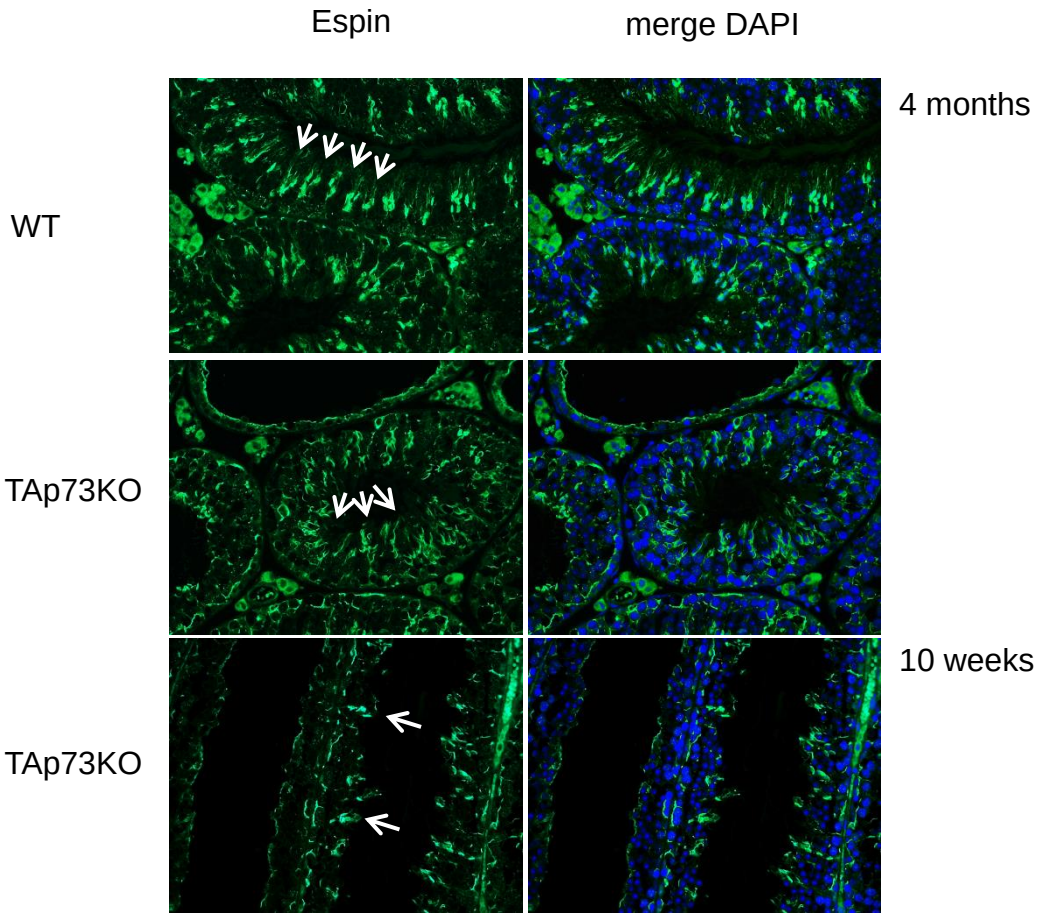

Fig. 5.16 The structure of the apical ectoplasmic specialization (ES) is impaired in TAp73KO mice.

Immunofluorescence staining of testis sections from adult TAp73KO and WT mice. The ectoplasmic specialization (ES) between Sertoli and germ cells was visualized using an antibody directed against Espin. TAp73KO mice show reduced interaction points between the two cell types as well as a strongly disorganized structure of the apical ES (white arrows). n=5 mice were analyzed per genotype. Magnification: 400x

5.5 Adhesion- and migration-related genes are differentially expressed in sperm and Sertoli cells, and p73 affects gene expression in both cell types

5.5.1 Timp1 and Serpina3n expression in sperm and primary Sertoli cells

Analyzing TAp73KO testis, we found an impaired morphology of Sertoli cells as well as strongly upregulated expression levels of proteinase inhibitors in whole testis (refer to **5.3.3** and **5.4.2**). We next asked, whether the expression of these proteinase inhibitors could be correlated to Sertoli cell morphology and function and whether expression of Timp1 and Serpina3n would be restricted to Sertoli or sperm cells only. To get an idea if deregulation of Sertoli cells could be the reason for the observed phenotype, we performed primary Sertoli cell culture. Whole testes were isolated from adult mice, the tunica albuginea was removed and the cell structure was mechanically disrupted. After additional enzymatic digestion and washing steps samples were centrifuged. The supernatant contained the germ cell fraction enriched for Sertoli cells. Cells of the supernatant were plated on 12 well plates and while Sertoli cells were able to attach germ cells underwent apoptosis. A clean Sertoli cell culture could be obtained after 3 weeks culturing and further passaging to 6 well plates. IF staining using the Sertoli cell marker Vimentin confirmed the pureness of the primary cell culture. No difference in morphology of TAp73KO and WT cells could be observed in these *in vitro* experiments (*Figure 5.17*).

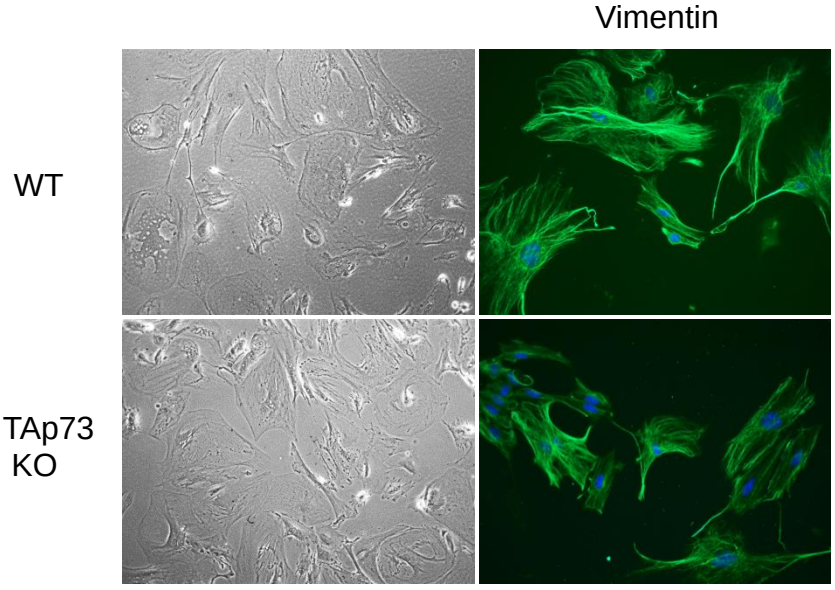

Fig. 5.17 Primary Sertoli cell culture as a model system to study mRNA expression levels in Sertoli cells independent from sperm cells.

Light microscopy and immunofluorescence (IF) staining with Vimentin (Sertoli cell marker) of Sertoli cells isolated from adult TAp73KO and WT mice. Cultured Sertoli cells show comparable morphology. Magnification: 100x

The sperm pellet of the cell isolation procedure was stored for later analysis of the sperm cell fraction. To quantify mRNA expression levels of Timp1 and Serpina3n comparing primary Sertoli cells to the sperm pellet fraction, we carried out qPCR analysis. We found physiologically high expression levels of Timp1 in WT Sertoli cells. In contrast to WT sperm cells the TAp73KO sperm pellet displayed a high expression rate for Timp1 (as observed for whole testis, refer to *Figure 5.13 C*). But comparing TAp73KO sperm pellet and Sertoli cells, Timp1 expression was significantly higher in TAp73KO Sertoli cells (*Figure 5.18 A*).

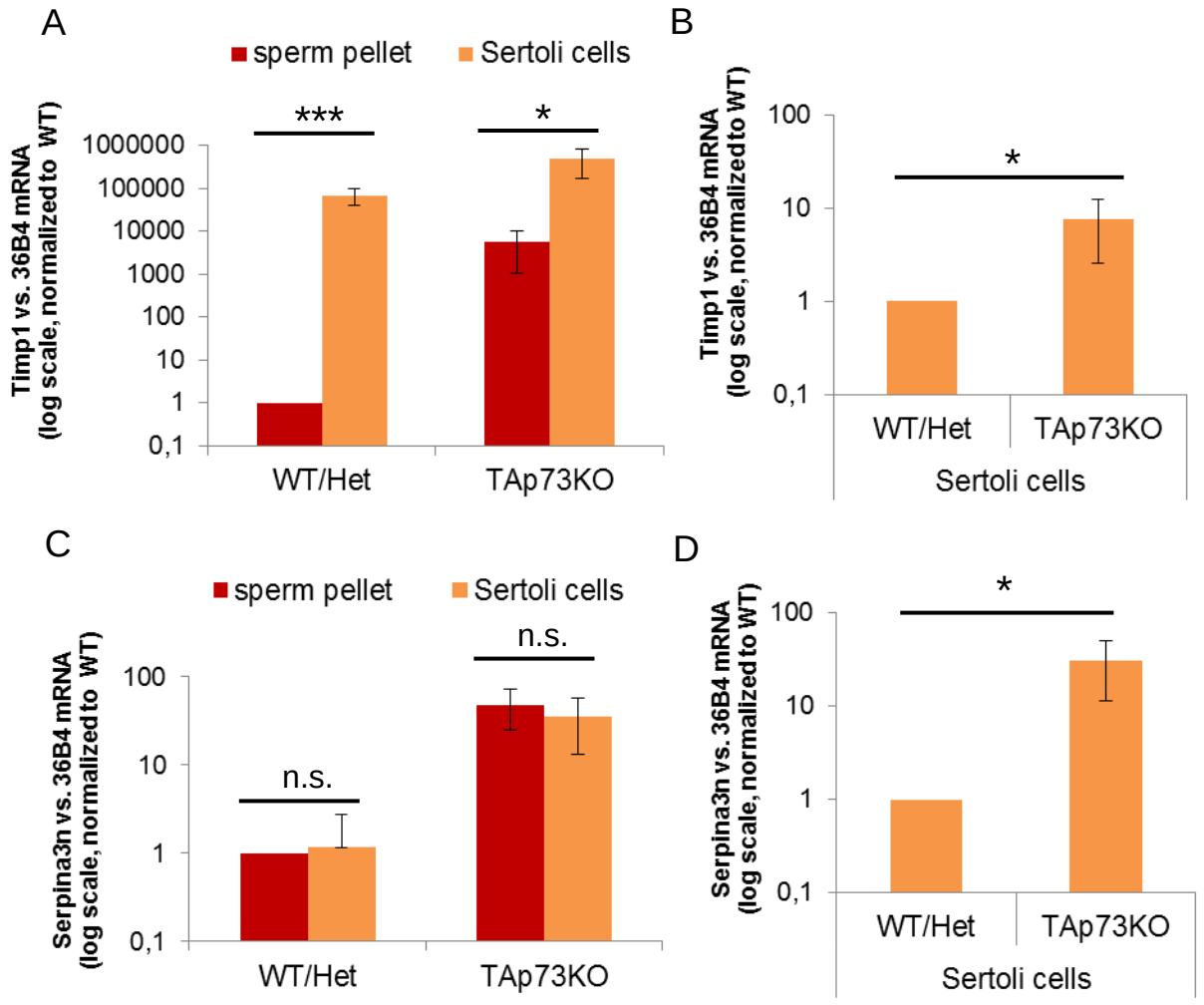

Fig. 5.18 While Timp1 is highly expressed in TAp73KO Sertoli cells, Serpina3n does not show cell specific expression.

A-D) Quantitation of mRNA isolated from TAp73KO and WT/Het Sertoli cells in comparison with expression levels in the sperm pellet via qPCR. Timp1 (B, n=3-5) as well as Serpina3n (D, n=2-3) are upregulated in TAp73KO Sertoli cells, but Serpina3n does not show specificity for the sperm or Sertoli cell population (C). Timp1 is significantly stronger expressed in Sertoli than sperm cells (A). Error bars represent the SDM. * = $p < 0.05$ and *** = $p < 0.005$; n.s. = not significant (Student´s t-test).

In comparison to the basal Timp1 expression levels in WT Sertoli cells, Timp1 was significantly upregulated in TAp73KO Sertoli cells (*Figure 5.18 B*). Serpina3n on the other hand did not show a cell specific expression pattern, but displayed similar mRNA levels for sperm and Sertoli cells (*Figure 5.18 C*). Like Timp1, it was significantly upregulated in TAp73KO Sertoli cells compared to WT (*Figure 5.18 D*). Under WT conditions Timp1 expression seems to be restricted to Sertoli cells only. TAp73KO mice show strong upregulation of both genes Timp1 and Serpina3n in sperm cells as well as in Sertoli cells. The loss of sperm cells in TAp73KO testis is therefore accompanied by a change of gene expression of proteinase inhibitors in both cell fractions of the seminiferous epithelium.

5.5.2 Integrins and metallopeptidases are differentially expressed in sperm and Sertoli cells

With the tool of primary Sertoli cell culture we also wanted to analyze expression levels of other adhesion-related genes that we could already validate to be upregulated in whole TAp73KO testis (refer to **5.4.2**). We applied qPCR analysis to mRNA isolated from Sertoli cells from WT and TAp73KO mice comparing this fraction to the sperm cell pellet, using gene specific primers for Itga5, Itgax and Adam23. While the Integrins Itga5 and Itgax show a cell-specific expression pattern (*Figure 5.19 A* and *B*), Adam23 is equally expressed in sperm and Sertoli cells and also significantly upregulated in TAp73KO Sertoli cells (*Figure 5.19 C* and *D*). Itga5 is mainly expressed in Sertoli cells of WT and TAp73KO mice (*Figure 5.19 A*). However, the upregulation of Itga5 in TAp73KO testis, as shown in the microarray and the validation qPCR of whole testis lysates (refer to **5.4.2**), is not related to Sertoli cells but to sperm cells (*Figure 5.19 A* and *D*). Itgax, on the other hand, is significantly upregulated in sperm and Sertoli cells of TAp73KO mice, but mainly expressed in the KO sperm cell fraction (*Figure 5.19 B* and *D*). Altogether, these results show that deregulation of adhesion- and migration-related genes in TAp73KO mice cannot be connected to a specific cell type of the testicular tubules. Loss of TAp73 rather affects sperm and Sertoli cells in parallel. If this is due to a direct or indirect influence of TAp73 on these cells cannot be stated.

5.5.3 TAp73 is mainly expressed in sperm cells

To gain further information, which testicular cell type could be directly affected by TAp73 action we checked for TAp73 mRNA expression in Sertoli and sperm cells of WT mice. Performing qPCR we found TAp73 strongly expressed in the sperm cell fraction. TAp73 expression in sperm cells was significantly higher compared to its expression in Sertoli cells

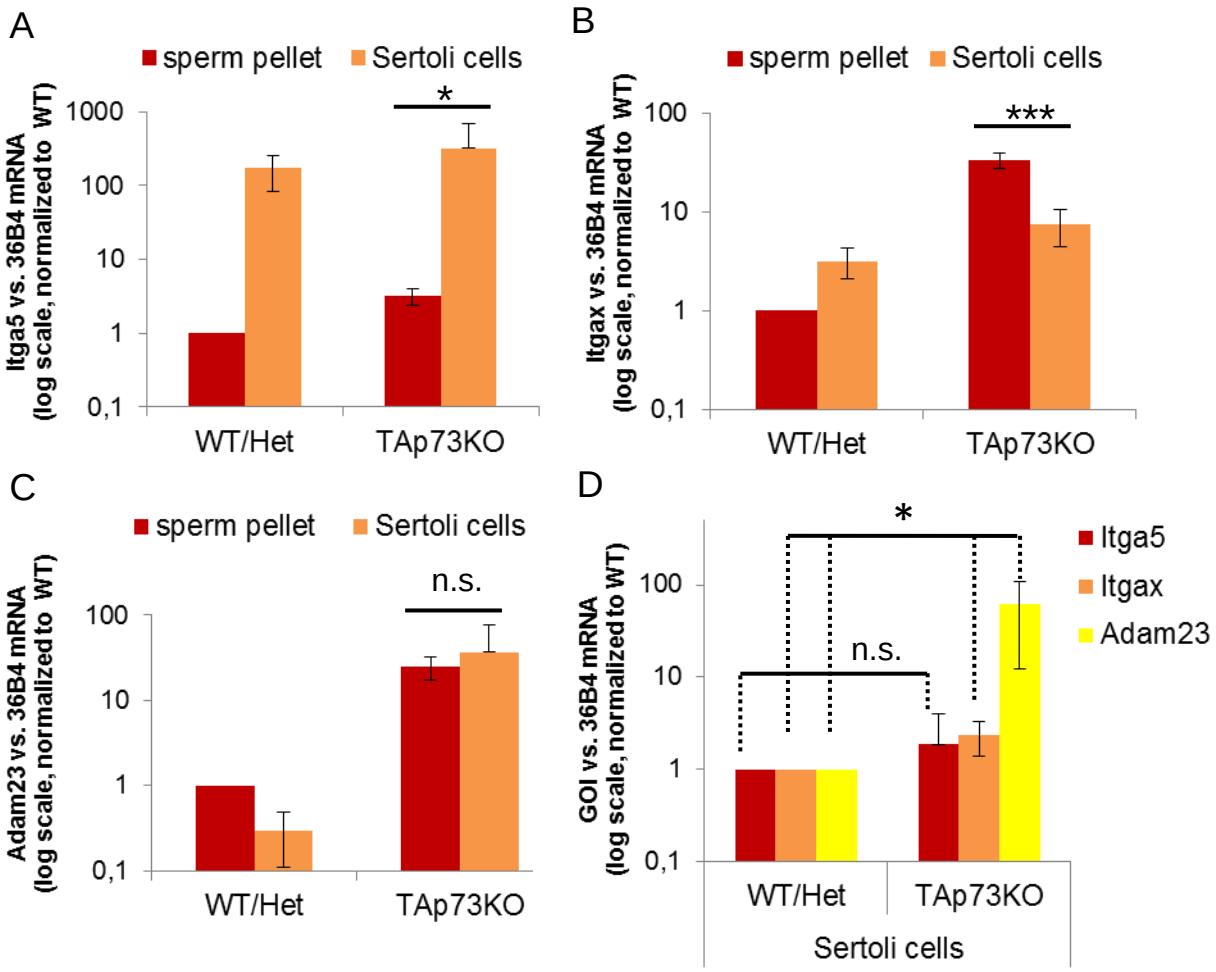

Fig. 5.19 Differential mRNA expression of adhesion- and migration related target genes in TAp73KO Sertoli and sperm cells.

A)-D) Quantitation of mRNA expression of Itga5, Itgax and Adam23 performing qPCR on TAp73KO and WT/Het Sertoli as well as sperm cells. While Itga5 (A) is mainly expressed in TAp73KO Sertoli cells and Itgax (B) in TAp73KO sperm cells, Adam23 (C) does not show a cell-specific upregulation profile for TAp73KO. Itgax and Adam23 are significantly upregulated in Sertoli cells (D). n=2-4 cell lines were analyzed per fraction and genotype. Error bars represent the SDM. * = $p < 0.05$ and *** = $p < 0.005$; n.s. = not significant (Student´s t-test).

(*Figure 5.20 A*). Additionally, we could show that after long time maintenance of Sertoli cells in culture, the upregulation of proteinase inhibitors in TAp73KO cells was dropping down to WT levels (*Figure 5.20 B*). At low cell passages (p1-p3) we could still observe the significant induction of Timp1 and Serpina3n in TAp73KO Sertoli cells. But when we checked for expression levels at higher cell passages (p5-p7), Timp1 and Serpina3n expression went down to WT level (*Figure 5.20 B*). This indicates that TAp73 might directly affect sperm cell

function and that Sertoli cell function is dependent on the surrounding sperm cells. When normal conditions of the tubule structure are changed and sperm cells are depleted from the Sertoli cell pool, the gene expression pattern of TAp73KO Sertoli cells is also affected after a while.

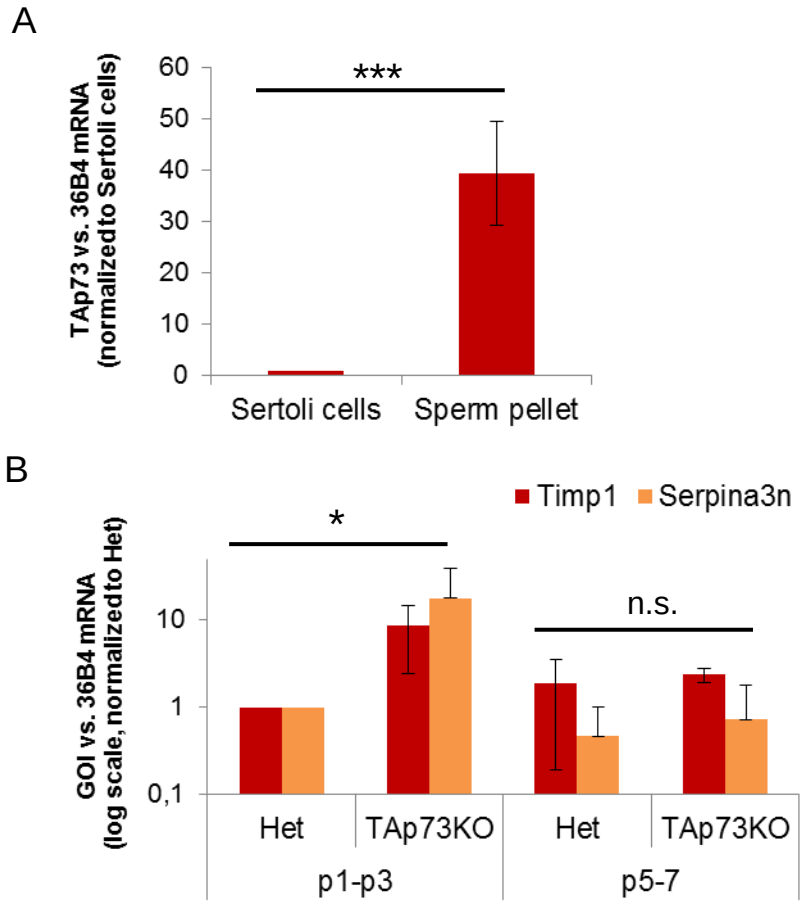

Fig. 5.20 TAp73 is primarily expressed in sperm cells. Upregulation of target genes in TAp73KO Sertoli cells is lost after frequent passaging.

A) Quantitation of TAp73 expression performing qPCR on WT Sertoli and sperm cells. TAp73 is mainly expressed in the sperm cell fraction. n=6-7 cell lines were analyzed per fraction. Error bars represent the SDM. *** = $p < 0.005$ (Student´s t-test).
B) Quantitation of mRNA isolated from TAp73KO and Het Sertoli cells of different passages. Timp1 and Serpina3n are upregulated in TAp73KO Sertoli cells at low passages (p1-p3). This upregulation is lost with frequent passaging (p5-p7). n=3 Sertoli cell lines were analyzed per genotype. Error bars represent the SDM. * = $p < 0.05$; n.s. = not significant (Student´s t-test).

5.6 The blood testis barrier is impaired in TAp73KO mice

5.6.1 TAp73KO testes have unilateral adhesions at basal Sertoli junctions

TAp73KO testes showed a strong loss of developing sperm cells accompanied by an abnormal structure of Sertoli cells, impaired Sertoli-sperm cell adhesion as well as upregulation of a group of proteinase inhibitors, proteinases and adhesion molecules. Altogether these data point towards an adhesion- and migration-defect of sperm cells in TAp73KO testis. During development and entry into meiosis sperm cells have to pass the basal junctions between Sertoli cells by a complex migration process. The basal ES and tight junctions ensure the separation of the mitotic stem cell compartment from the meiotic sperm developing compartment of the seminiferous epithelium (Yan *et al.*, 2007, Cheng *et al.*, 2011). To check for the morphology of the basal junctions of Sertoli cells we had a look on ultrathin sections of glutaraldehyde fixed testis tissue using the electron microscope. When we compared TAp73KO with WT sections we found a disorganized structure for the basal junctions in TAp73KO mice (*Figure 5.21*). To build functional tight junctions, actin bundles of two adjacent Sertoli cells have to lay directly opposite of each other. This could nicely be seen for WT Sertoli cells and the actin bundles of one cell were following each other like beads on a string (*Figure 5.21, WT, arrows*). When we looked at TAp73KO testis we frequently found the formation of a one-sided junction, the opposite actin bundles of the adjacent cell missing from the basal junctions (*Figure 5.21, TAp73KO, dashed arrow*). Additionally, we often observed big gaps between the neighbouring actin bundles of one cell, which also contributed to the disorganized structure of the basal Sertoli tight junctions in TAp73KO mice. The basal junctions of TAp73KO testis seem to be impaired and the failure of building correct junctions could contribute to the loss of sperm cells during migration and development.

5.6.2 The blood testis barrier of TAp73KO mice is defective

The sum of the described basal junctions formed between adjacent Sertoli cells, are also called the blood testis barrier (BTB). This barrier harbours the important function of protecting developing sperm cells from exogenous toxins or endogenous auto antigens. Developing sperm cells have a unique protein structure not present in any other tissue of the body. Therefore meiotic and spermiogenic sperm cells have to be protected against auto immune reactions (Xia *et al.*, 2005b). Electron microscopy already revealed an impaired structure of junctions of this barrier (refer to **5.6.1**).

Fig. 5.21 Failure of Sertoli-Sertoli cell adhesion in TAp73KO mice

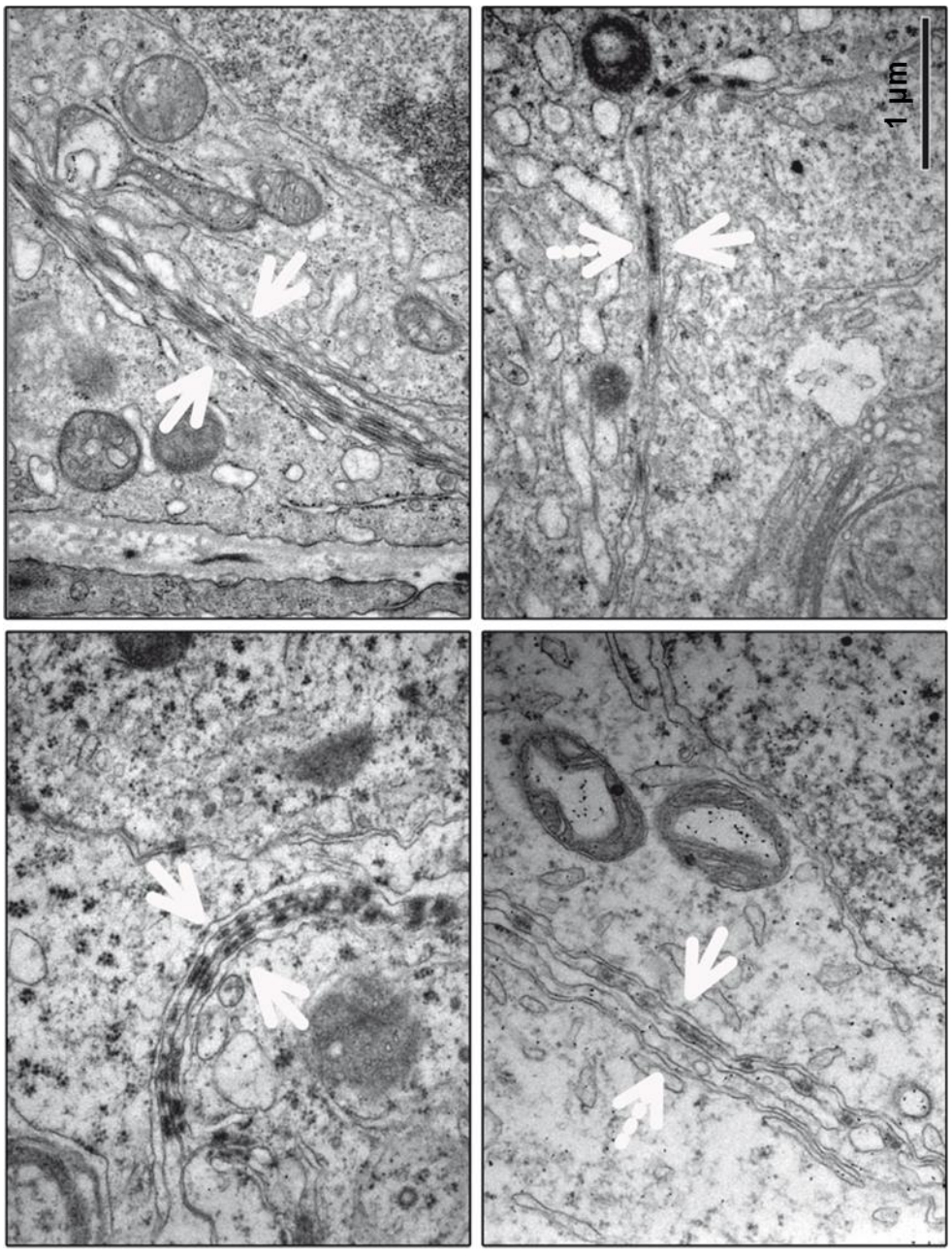

Electron microscopy of ultra thin testis sections from adult TAp73KO and WT mice. TAp73KO mice show one-sided formation of junctions as well as uneven distribution of the actin bundles (electron dense, point-like structures at the junctions) along the membrane contact. Dashed arrows indicate the missing counterpart of unilateral junctions in TAp73KO mice. Solid arrows point towards visible junctions (actin bundles). n=3-5 mice were analyze per genotype.

We next wanted to know, if also the function of the BTB could thereby be affected. For this approach we carried out an *in vivo* assay on anaesthetized mice. Testes of adult TAp73KO and WT mice were injected with 250µg EZ Link Sulfo-NHS-LC-Biotin, freshly dissolved in PBS-$CaCl_2$, and incubated for 30 minutes. Biotin reacts unspecifically with all primary amines of surface proteins, like the lysine side-chain or the amino-termini of polypeptides, forming permanent amide bonds. Biotin can be visualized by staining testis sections with Streptavidin-coupled Texas Red.

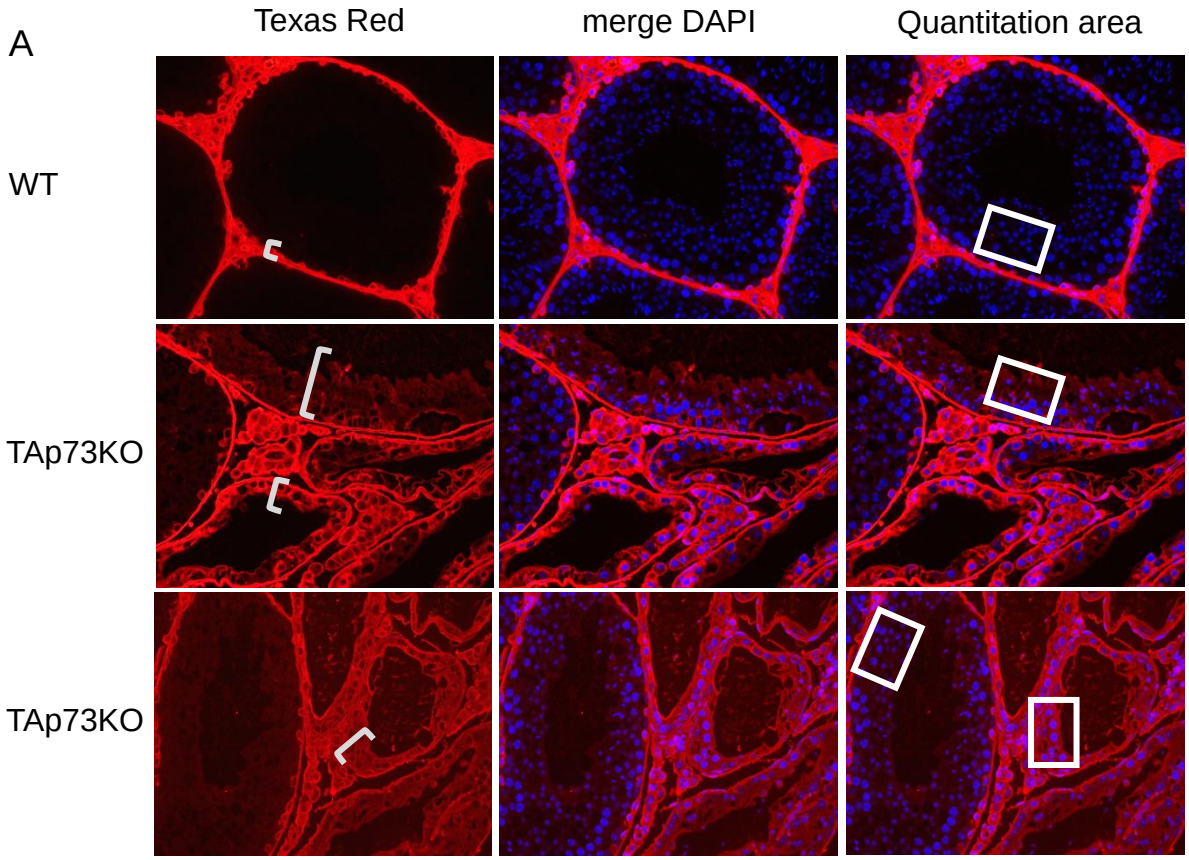

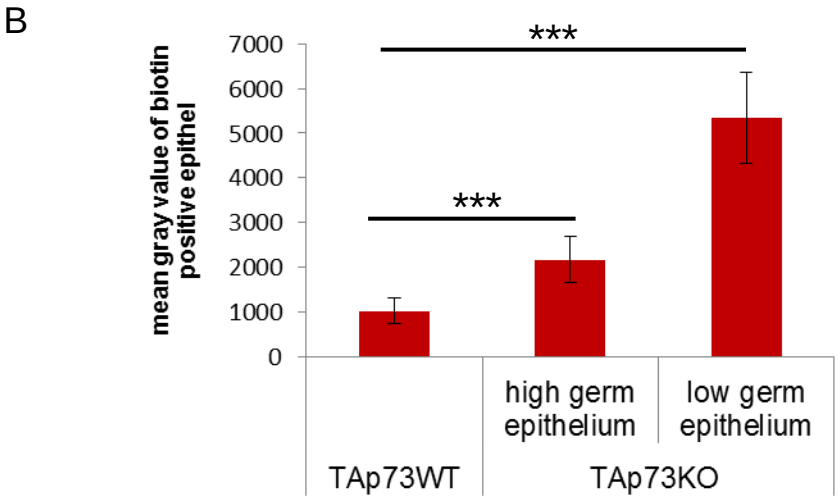

Fig. 5.22 TAp73KO mice reveal a defect of the BTB

A) *In vivo* Biotin assay was performed on adult TAp73KO and WT mice to measure the functionality of the blood testis barrier (BTB). Biotin-infiltrated tissue was visualized by Texas Red staining. WT mice only show staining of the basal layers (small bracket), because the BTB hinders the Biotin from crossing to the meiotic sperm layers. TAp73KO mice display staining of all cell layers (brackets), which implies a defect of the BTB. Magnification: 400x
B) Quantitation of Texas Red staining (A) in TAp73KO versus WT testis. Measurement was performed within the determined area of the same size (images of right column in A)). The mean gray values show a significant stronger staining for the KO sections. Thereby the intensity is increasing parallel to the decrease of the germ epithelium size (brackets in A). n=4-5 mice were analyzed per genotype. Error bars represent the SDM. *** = $p < 0.005$ (Student´s t-test).

In WT mice, all basal cells below the BTB should be labeled, while the upper sperm cells are protected against exogenous Biotin circulating through the blood stream. Besides unspecific staining of Leydig cells and the basement membrane only basal cells showed a positive staining in WT testis, indicating a working BTB in these mice (*Figure 5.22 A, WT, bracket*). In sharp contrast to that, many tubules of TAp73KO testis displayed Texas Red staining throughout the whole remaining seminiferous epithelium (*Figure 5.22 A, TAp73KO*). We additionally quantified the Texas Red positive area, using Adobe Photoshop CS5 and applying a grid of the same size to the germ epithelium of TAp73KO and WT mice (*Figure 5.22 A, sketches*). Intensities were measured as mean grey values (also refer to **4.1.7.8**). Comparing normal sized TAp73KO and WT tubules (*high germ epithelium*) the increase in Texas Red intensity per area in TAp73KO testis was strongly significant. Moreover, the intensity of Texas Red staining was increasing furthermore in TAp73KO testis, when the seminiferous epithelium was decreasing in height (*low germ epithelium*) (*Figure 5.22 B*). The observed results imply a defect in the BTB of TAp73KO mice. Disrupted Sertoli junctions fail to protect sperm cells against auto antigens or toxins. They might also inhibit proper sperm migration to the apical part of the germ epithelium. With proceeding loss of sperm cells, the structure of the seminiferous epithelium is loosening its organized shape, and this might lead to even further disruption of cell-cell junctions.

6 DISCUSSION

The process of producing viable, genetically stable sperm cells requires many steps, factors and control mechanisms. In comparison with somatic cells, it is even more crucial to maintain DNA integrity of germ cells, since mutations or the depletion of genes can lead to degenerated offspring or embryonic lethality. Furthermore, abnormal morphology and motility or impaired development of the sperm cells can decrease their number and fertilizing ability. This can subsequently lead to infertility. The male germ line produces millions of sperm cells per day, ready for fertilization. Spermatogenesis therefore has to be controlled tightly to ensure genomic stability and fertilizing ability of released mature spermatozoa.

The original function of the p53 family during evolution is thought to be the protection of the germ line and the genomic integrity of gametes (Hu *et al.*, 2011). While the focus of the research lay on the female germ line, the function of p73 in the male germ line still needed to be evaluated. In this study we intensively analyzed the role of p73 in the testis, using mouse models. Since the discovery of the different p53 family members, different mouse models for each member and also for some isoforms have been created. By examining these protein specific KO mice, the function of the p53 family members in different organ systems and tumor development could be unraveled (Donehower *et al.*, 1992, Mills *et al.*, 1999, Suh *et al.*, 2006, Tissir *et al.*, 2009, Tomasini *et al.*, 2008, Yang *et al.*, 1999, Yang *et al.*, 2000). Therefore, our approach was to gain information about the testis morphology of total as well as isoform-specific p73KO mice. In accordance with Yang et al. we found normal testis development for pre-pubertal p73KO mice, still undergoing the first wave of spermatogenesis (Yang *et al.*, 2000). However, p73 was indispensable for adult spermatogenesis, since p73KO mice showed a massive loss of developing sperm cells. Establishing an organized composition of the seminiferous epithelium and a healthy normal pool of spermatocytes and spermatids was dependent on p73. Testis development was specifically dependent on TAp73, but not ΔNp73, TAp73KO mice resembling the phenotype of total p73KO mice. TAp73 was not necessary for maintaining spermatogonial number at the basal site of the seminiferous epithelium. p73 was also dispensable for mitosis of basal cells and meiosis of developing spermatocytes, as well as for the hormonal balance of the GnRH-FSH/LH-testosterone axis. However, TAp73 expression in testis was important for retaining still developing sperm cells in the seminiferous epithelium and inhibiting premature release and loss of immature sperm. This function of TAp73 seems to be obtained by influencing Sertoli

cell morphology and function, since Vimentin-stained Sertoli arms were shortened in TAp73KO mice and electron microscopy showed thinning of Sertoli cells and increased vesicular morphology. On the molecular level, TAp73 negatively regulated a set of genes correlated to cell adhesion and migration. Especially the expression of protease inhibitors, like Timp1 and Serpina3n, was shown to be inhibited by TAp73 under WT conditions. TAp73 was shown to be mainly expressed in the sperm fraction and induced expression of protease inhibitors in TAp73KO Sertoli cells decreased after long time culture, due to the absence of sperm cells. This indicates that TAp73 might directly act on sperm cells, which in turn can influence their own as well as the Sertoli cell expression pattern. Deregulation of protease inhibitors and adhesion molecules upon loss of TAp73 could be the reason for observed Sertoli-Sertoli adhesion defects and the impermeability brake of the BTB in TAp73KO mice. The abolishment of the polarity of the seminiferous epithelium and the disruption of the two compartments, usually maintained by the BTB, could in turn lead to premature sloughing of sperm cells in the absence of TAp73.

6.1 A new developmental function for TAp73 – protection of spermatogenesis and fertility

Additionally to the protective function of the germ line by p53 family members, we could show for the first time that the TA-isoform of p73 is also involved in the physiological development of the male germ line of adult mice. Beyond its ability to protect the male germ line against genetic instability upon DNA damage, p73 is also necessary for obtaining a normal healthy pool of sperm cells during spermatogenesis. p73 was already described to be expressed in the male germ line, mainly localizing to spermatogonia and spermatocytes (Hamer *et al.*, 2001). This is in accordance with our results, which show TAp73 expression in the sperm, rather than the Sertoli cell fraction (*Figure 5.20, A*). Hamer et al. assign a sperm protective function to p73. After irradiation or etoposide treatment, p73 interacts with c-Abl, gets phosphorylated by c-Abl and removes DNA-damaged sperm in mice and rats to ensure genetic stability (Codelia *et al.*, 2010, Hamer *et al.*, 2001). Like p73, p53 and p63 were also reported to execute irradiation-induced apoptosis of sperm cells (*Figure 6.1*). Irradiation of p53 and p63KO mice lead to a decreased removal of DNA-damaged sperm cells compared to WT (Beumer *et al.*, 1998, Guerquin *et al.*, 2009). While irradiation and apoptotic studies for p53 and p63 were performed on KO mice, p73 results were obtained by *in vitro* cell culture experiments as well as analysis of irradiated WT mice. It is therefore difficult to say, whether irradiation-induced apoptosis is also dependent on p73 *in vivo* or if p53 and p63 form the

main part in protecting the male germ line against genomic instability. Whether (TA)p73 is necessary to protect sperm cells, could be tested by irradiating p73KO, TAp73KO and WT mice and comparing the rate of apoptotic sperm cells. It could well be that p73 serves as a backup of p53/p63 function, but that its physiologically occurring expression in mammalian testis rather serves as developmental regulation of spermatogenesis (*Figure 6.1*). The observed phenotype for p73 and TAp73KO testes, which display a massive loss of developing sperm cells, underlines this hypothesis (*Figure 5.1*, *5.2* and *5.4*).

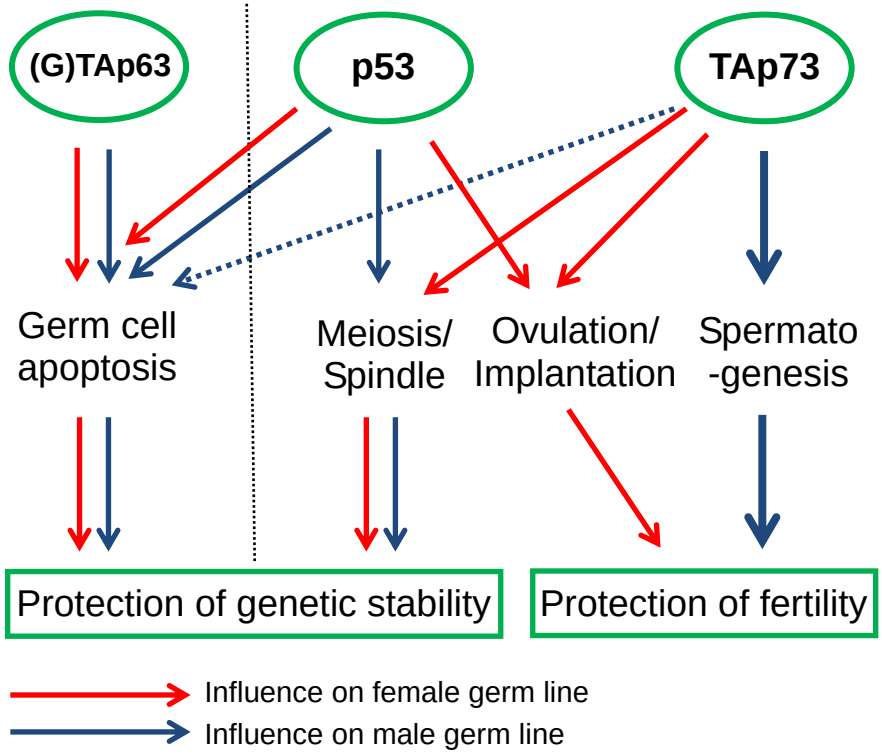

Fig. 6.1 The p53 family protects the germ line

TAp63 and GTAp63 are generally accepted as protector of the female and male germ line. Upon DNA damage, as result of irradiation or cisplatin treatment, (G)TAp63 gets activated and induces germ cell apoptosis, thereby protecting damaged cells from genetic instability (Beyer et al., 2011; Suh et al., 2006).
p53 and TAp73 are also activated upon irradiation and remove damaged germ cells (Beumer et al., 1998; Lee et al., 2008; Hamer et al., 2001). TAp73 is thought to serve as back up for TAp63- and p53-mediated apoptosis in testis (Hamer et al., 2001).
Besides their developmental regulation of the female germ line, p53 and TAp73 are also involved in sperm cell development (Hu et al., 2007; Rotter et al., 1993; Tomasini et al., 2008). Furthermore, TAp73KO mice are shown to be subfertile.

The function of p53 and p63 in the male germ line compared to p73 can also be distinguished by looking at the ability of the corresponding KO mice to produce offspring. While p53 and

TAp63KO mice (p63 total KO mice cannot be studied, since total p63 ablation is postnatal lethal) are fertile under normal conditions, p73 as well as TAp73KO males and females were reported to be infertile. The here described phenotype would explain the earlier described infertility of TAp73KO males, which do not display abnormalities in mating behavior as p73KO mice do (Tomasini *et al.*, 2008). Defects in the pheromone system of p73KO mice, accompanied by behavioral changes, do not seem to be the (only) reason for infertility, but rather impaired spermatogenesis in adult testis (Yang *et al.*, 2000).

As mentioned before, the original function of p53 family members is stated to be the protection of the germ line against genomic instability (Dotsch *et al.*, 2010). The p53-homologue Cep-1 in Caenorhabditis elegans is required for activation of apoptosis in response to DNA damage, hypoxia and starvation (Derry *et al.*, 2001, Schumacher *et al.*, 2005, Schumacher *et al.*, 2001). Similarly, the fly p63/p73 hybrid Dmp53 can drive germ cell apoptosis upon irradiation in Drosophila melanogaster to ensure genomic stability of the offspring (Brodsky *et al.*, 2004). During evolution, this primary role of p53 family members seems to be maintained in vertebrates up to mammals. In mice and humans (G)TAp63 can be stated as the protector of the male or female germ line, activated upon exogenous-induced DNA damage, but no important functions during normal development of the germ line are described (Beyer *et al.*, 2011, Suh *et al.*, 2006) (*Figure 6.1*). In contrast, in mice p53 does not only induce apoptosis upon DNA damage, but also influences meiotic recombination during spermatogenesis as well as regulates the implantation process in the female germ line (Beumer *et al.*, 1998, Hu *et al.*, 2007, Schwartz *et al.*, 1999). Likewise, p73 is also reported to possess developmental function for the female germ line, TAp73KO mice showing ovulation defects, spindle abnormalities during oocyte meiosis and multinucleated blastocysts (Tomasini *et al.*, 2008) (*Figure 6.1*). Comparable meiotic defects or morphological abnormalities could not be observed for sperm cells of TAp73KO mice. However, TAp73KO females as well as males are described to be infertile. It is therefore not surprising that TAp73 also contributes to the normal development of the testis, its depletion leading to a strong loss of developing sperm cells and subsequently to infertility. In contrast to the most ancient family member p63, p53 and p73 seem to have developed further functions in regulating the maturation of the male and female germ line of adult mammals. Additionally to its developmental regulation of the nervous system, immune system and the female germ line, our results show that p73 possesses a hitherto unknown critical function in protecting the fertility of the male germ line.

6.2 TAp73 depletion leads to hypospermatogenesis

Pre-pubertal p73 and TAp73KO mice show comparable testis morphology as WT mice. At 3 weeks of age we find normal spermatogenesis in KO animals; spermatogonia, meiotic spermatocytes and round spermatids are visible in the tubules (*Figure 5.1 A*). Like Yang et al. we do not find histologic changes in developing mice, still undergoing the first wave of spermatogenesis (Yang et al., 2000; data not shown). We can therefore exclude a prenatal developmental defect as well as a defect in undergoing spermatogenesis per se. Only with adulthood, when the cycle of spermatogenesis in the seminiferous epithelium is established, testes of p73 as well as TAp73KO mice display a visible reduction in developing sperm cells (*Figure 5.1 B* and *5.2 A*). Analysis of the different sperm stages shows that all stages up to the elongated spermatids are present, since VASA and APG1 staining reveal positive cells in KO testes (*Figure 5.4 A*). However, the layers of late meiotic and spermiogenic cells are strongly reduced (*Figure 5.4*). Since all developmental stages of sperm cells seem to be present, p73 loss is not causing a germ cell arrest phenotype. An applicable classification for the phenotype of p73 as well as TAp73KO mice is the hypospermatogenesis phenotype (also refer to **2.1.5**). This is underlined by the fact that KO mice show normal numbers of spermatogonia as well as somatic Sertoli cells (*Figure 5.5* and *5.9*). Additionally, you can find tubules unchanged in morphology in KO testes next to tubules depleted of nearly all sperm cells, which is also described to be a feature of hypospermatogenesis. Furthermore, TAp73KO males can give rise to offspring, but in reduced frequency and are therefore subfertile (around 30% in mating trials, data not shown). This stands in contradiction with the literature, where TAp73KO males are stated to be infertile (Tomasini *et al.*, 2008), but fits to the testis morphology we observe. The degree of a phenotype can vary, dependent on the genetic background of the mouse strain. In contrast to our studies, Tomasini et al., used C57BL/6J animals mixed with 129/Sv background. An obvious reduction, but not a complete loss, of developing sperm cells is found in our C57BL/6J KO males. However, the few remaining sperm cells seem to be normal in shape and can take their chances in producing healthy offspring. More precisely, the observed phenotype can be described as hypospermatogenic with decreased numbers of developing spermatocytes, spermatids and spermatozoa.

6.3 Premature sloughing of sperm cells as result of TAp73 loss

The cause for hypospermatogenic testes can be changes in germ cell development, Sertoli cell function or germ cell colonization. Defects in germ cell colonization can be excluded

since pre-pubertal KO mice do not show abnormal testis morphology and the testis morphology, shape and localization as such is not compromised (*Figure 5.1 A*).

p53 family members are known to be involved in maintaining stem ness and proliferation capacity. ΔNp63 for example is necessary to keep the stem cell pool of keratinocytes in squamous epithelia and ΔNp73 is an important survival factor in brain development (Pozniak *et al.*, 2002, Senoo *et al.*, 2007, Tissir *et al.*, 2009). Additionally, ΔNp73 and ΔNp63 are both shown to be overexpressed in several tumor types, promoting cell survival and proliferation (Hibi *et al.*, 2000, Moll *et al.*, 2004, Stiewe *et al.*, 2002a). Furthermore, p73, especially the TAp73 isoform, was recently described to ensure adult neurogenesis by promoting long-term maintenance of neural stem cells in the brain (Fujitani *et al.*, 2010, Talos *et al.*, 2010). However, in testis development TAp73 seems to be dispensable for maintaining proliferation capacity of basal cells and ensuring a stable pool of spermatogonia, because (TA)p73KO mice show comparable numbers of Ki67 and GCNA1 positive cells as WT mice (*Figure 5.5* and *5.6 A* and *C*). Since we also could show that ΔNp73 is dispensable for normal testis development (*Figure 5.2 B*), p73 isoforms do not appear to influence the testicular stem cell pool. If TAp73 does not influence the number of basal proliferating cells, it might be necessary for sperm differentiation. In contrast to the function of ΔNp63 on epithelial stem ness, the role of TAp63 in skin development is connected to keratinocyte differentiation (Candi *et al.*, 2006). TAp73 is involved in neural differentiation; TAp73KO mice display reduction in number of hippocampal neurons, TAp73 drives differentiation of cortical neurons *in vitro* and its expression increases during synaptogenesis in the postnatal brain (Agostini *et al.*, 2010, Tomasini *et al.*, 2008, Agostini *et al.*, 2011). Endogenous TAp73 levels increase during retinoic acid-induced differentiation of neuroblastoma cells as well as myeloid leukemic cells (De Laurenzi *et al.*, 2000, Tschan *et al.*, 2000). Likewise, TAp73 might also possess differentiating functions during testis development, ensuring production of mature sperm cells. In contrast to the female germ line, where depletion of TAp73 leads to spindle abnormalities during meiosis, it does not influence the meiotic process of sperm cells (Tomasini *et al.*, 2008). The meiotic rate in TAp73KO testes, determined by H3Ser10 staining, is not changed compared to WT mice (*Figure 5.6 B* and *D*). It is important to mention that a secondary effect as result of the severe neural phenotype can be largely excluded as explanation for the detected sperm cell loss. p73KO mouse models are described to show neural loss in the cortex, hippocampus and thalamic eminescence (Tissir *et al.*, 2009, Tomasini *et al.*, 2008, Yang *et al.*, 2000). The hypothalamus and therefore GnRH expression might also be affected, disturbing the entire GnRH-FSH/LH-testosterone hormone axis (also refer to **2.1.4**), and thereby causing the defect in sperm development. Analyses of

mRNA expression levels of all involved hormones of the brain (GnRH, FSH, LH) as well as serum hormone measurement do not reveal differences in (TA)p73KO mice compared to WT littermates, suggesting that TAp73 is acting directly on physiologic testis homeostasis (*Figure 5.7*).

Maturating sperm cell numbers are decreased in the seminiferous epithelium of TAp73KO testis and in parallel less mature sperm as well as increased apoptotic and immature sperm can be found in the lumen of the epididymis (*Figure 5.8*). This observation points towards a retention failure of developing sperm cells in the testis. We also describe that the seminiferous epithelium of TAp73KO mice does loose its coordinated structure, since sperm cells are usually arranged in specific layers close to each other according to their developmental stage, which is called the seminiferous cycle (also refer to **2.1.2**) (*Figure 5.2 A, 5.4 B* and *5.11 A*). The loss of maturating sperm cells is accompanied by a change in Sertoli cell morphology, Sertoli cells displaying shortened cytoplasmic arms and increased vacuolization (*Figure 5.10* and *5.11 B*). Taking these observations into account we can hypothesize that TAp73KO Sertoli cells fail to provide physical support for developing sperm cells, which therefore cannot stay in proper contact with the seminiferous epithelium. This might lead to premature detachment of developing sperm from the testicular epithelium. Some of the immature sperm cells are flushed to the epididymis, but likely the main part will be eliminated by apoptosis. Since Sertoli cells also harbour phagocytic function, this could be the reason why the lost sperm cells are not detectable anymore, but appear to “vanish” from the testis and epididymis (Chemes, 1986). The increased phagocytic activity of TAp73KO Sertoli cells could also explain their change in morphology, which is characterized by increased cytoplasmic vacuolization (*Figure 5.11 B*). The idea that sperm cells might fail to stay attached to Sertoli cells and the seminiferous epithelium is furthermore reinforced by the fact that the structure of Sertoli sperm junctions at the apical ES is impaired in TAp73KO mice (*Figure 5.16*). Elongating spermatids are attached to Sertoli cells by the apical ES (also refer to **2.1.3.3**). If they have completed their testicular maturation they will be released from the seminiferous epithelium. Restructuring of junctions by Sertoli cells is necessary for spermiation and defects in this process would support premature release of sperm cells. Premature sloughing of sperm cells is for example described in mice deficient of the enzyme α-mannosidase IIx. The carbohydrate N-glycan adhesion molecules, synthesized by this enzyme, are lost and therefore Sertoli-sperm adhesion is impaired (Akama *et al.*, 2002). It might be possible that TAp73 regulates the homeostasis of adhesion molecules, ensuring attachment of sperm to Sertoli cells. However, it cannot be said if abnormal Sertoli cell

function is the primary cause of the phenotype or a secondary effect due to abnormal sperm development.

Taken together, TAp73 loss leads to hypospermatogenesis with decreased numbers of spermatocytes and spermatids, accompanied by abnormal structure of Sertoli cells. The decrease of developing sperm numbers is explained by a retention failure and premature sloughing of sperm cells.

6.4 TAp73 – a transcriptional inhibitor in testis development?

By performing microarray analysis on whole testis lysates of TAp73KO and WT mice we had a closer look at the molecular level of TAp73 action. Surprisingly, loss of TAp73 mainly leads to mRNA upregulation of testicular genes, not downregulation (*Figure 5.12*). With regard to gene expression TAp73 seems to possess an inhibitory role in the testis. Similarly, TAp73KO ovaries also mainly displayed upregulation of p73 target genes. However, the pool of regulated genes was not comparable to induced genes in TAp73KO testes (Tomasini *et al.*, 2008).

Downregulation of mRNA levels through TAp73 could be explained by transcriptional inhibition of target genes or posttranscriptional regulation of mRNAs. TAp73 isoforms are mainly reported to activate target genes upon DNA binding (De Laurenzi *et al.*, 1998, Flores *et al.*, 2002, Jost *et al.*, 1997, Lee *et al.*, 1999). However, there are also hints that TAp73 is able to inhibit transcription. For example, TAp73β was reported to inhibit MYCN mRNA transcription in neuroblastoma cell lines. TAp73α, on the other hand, was able to downregulate MYCN mRNA level post-transcriptionally by binding to its mRNA and decreasing its stability (Horvilleur *et al.*, 2008). Besides enhancing p53 transcriptional activity on p21 and Bax reporter genes in thyroid cancer cell lines, TAp73 also antagonized p53 binding on the promoter of its negative regulator Mdm2 and inhibited transcriptional activation of Mdm2 (Malaguarnera *et al.*, 2008). Another example is the repression of the vascular endothelial growth factor (VEGF) promoter in Saos-2 cells by TAp73 (Salimath *et al.*, 2000). Furthermore, by overexpressing TAp73 isoforms in a neuroblastoma cell line and primary neurons, Notch-CBF-1 dependent transcription could be inhibited in reporter gene assays. TAp73 was able to antagonize Notch signaling by binding to Notch itself. The inhibitory ability of TAp73 was shown to be dependent on the TA domain as well as on its ability to bind DNA (Hooper *et al.*, 2006). TAp73 is able to induce retinoic acid driven neuronal differentiation of neuroblastoma cells and it does this by suppressing Notch signaling (De Laurenzi *et al.*, 2000, Hooper *et al.*, 2006).

Therefore, it might be possible that TAp73 is interacting with developmental transcription factors in sperm cells, inhibiting their transcription activity on gene promoters. This would explain the high number of upregulated genes in TAp73KO mice. Notch signaling is highly conserved in evolution and important during many developmental processes, i.e. the differentiation of the central nervous system (CNS), where it promotes maintenance of neural stem cells and oligodendrocyte differentiation (Bolos *et al.*, 2007). p73 is important for the maintenance of neural proliferation capacity, its depletion leading to downregulation of the Notch pathway (Talos *et al.*, 2010). Components of the Notch pathway, like Notch receptors 1-4 and Notch ligands Jagged 1/2, have also been reported to be expressed in sperm and Sertoli cells of mice and rats (Dirami *et al.*, 2001, Hayashi *et al.*, 2001, Mori *et al.*, 2003). It was stated that Notch 1 is necessary for sperm differentiation and spermatid survival (Hayashi *et al.*, 2001). However, the mechanism and regulated target genes in testis remain unknown. Interestingly, Notch 1, Jagged 2 and TAp63 expression increase strongly in rat testis around day 20 pp, expression levels staying unchanged in adult rats (Hayashi *et al.*, 2004). Since TAp73KO mice display loss of sperm cells only after 3 weeks of age, it could be speculated that TAp73 and Notch activity are connected. With depletion of TAp73 the control of Notch transcribed target genes during spermatogenesis would be impaired and activation of normally inhibited genes during sperm development could lead to the observed phenotype in TAp73KO mice.

6.5 TAp73 regulates adhesion and migration of sperm in the testis

TAp73-regulated genes in testis include a group of adhesion proteins and several protease inhibitors (*Table 5.4; Figure 5.13* and *5.14*). The tissue inhibitor of metalloproteinases Timp1 and the plasminogen activator (PA) inhibitor Serpina3n are highly upregulated in TAp73KO mice (*Figure 5.13*).

According to their name, Timps are able to inhibit matrix metalloproteinases (MMPs), and are implicated in regulating many processes like proliferation, apoptosis, angiogenesis, tumor growth and tissue remodelling (Bertaux *et al.*, 1991, Guedez *et al.*, 1998, Johnson *et al.*, 1994, Mruk *et al.*, 2004). Timp-1 was already described to be expressed in testis, especially in Sertoli cells, but also in sperm cells (Mruk *et al.*, 2003, Robinson *et al.*, 2001, Ulisse *et al.*, 1994). In contrast to the other family members Timp-2 and-3, Timp-1 shows a sex-dimorphic expression pattern, primarily located to the male germ line (Guyot *et al.*, 2003) 2003). Timp1 mRNA expression levels were shown to increase strongly from 40 to 60 days pp in rats. Levels remained high in adult Sertoli cells, but decreased in sperm cells (Mruk et al., 2003).

Its function during testis development is associated with adhesion and migration. Using *in vitro* primary cell culture systems Timp-1 was shown to increase during tight junction assembly in Sertoli cells as well as during adherens junction assembly between Sertoli and co-cultured sperm cells (Mruk et al., 2003). Furthermore, Timp-1 was described to be necessary for counterbalancing the TNFα-mediated activation of MMP-9 and the subsequent cleavage of collagen leading to perturbation of Sertoli tight junctions in culture (Siu *et al.*, 2003). Timp1 expression in mice was shown to peak during day 20 to 30 pp (Nothnick *et al.*, 1998). Abnormal high levels of Timp1 in adult TAp73KO mice could therefore lead to an imbalance in the junction restructuring processes, supported by MMP and Timp action. Timp1 protein is strongly secreted in TAp73KO mice and might be an indicator of increased activity of MMPs, which support cleavage of tight junctions (*Figure 5.15*) (Siu *et al.*, 2003). To address this possibility, MMP activity could be analyzed performing gelatin-zymography assays.

Serine proteases (plasminogen activators PA) and Serine proteinase inhibitors (PAIs or Serpins) are also involved in germ cell development. The original function of the plasminogen activators, which catalyze the activation of plasminogen, includes regulation of blood coagulation, platelet activation, thrombosis and fibrinolysis. Serpins form covalent, irreversible complexes with Serine proteases, inhibiting their proteolytic activity (Dellas *et al.*, 2005, Le Magueresse-Battistoni, 2007). Various PAs as well as Serpins were found to be expressed in Sertoli, Leydig and sperm cells (Odet *et al.*, 2006, Odet *et al.*, 2004). Serine protease activity was shown to increase during Sertoli-germ cell adherens junction assembly *in vitro* ((Mruk *et al.*, 1997). Components of the plasminogen activation system are known to influence several steps in migration, like cell attachment and detachment, independent of plasminogen activation by interacting with adhesion proteins like integrins or vitronectin (Dellas *et al.*, 2005, Stefansson *et al.*, 1996). Serpin 1 can disrupt cell adhesion by competing with Serine proteases for their receptor, thereby decreasing its affinity for vitronectin (Waltz *et al.*, 1997). Serpin 1 furthermore mediates internalization of adhesion receptors, leading to detachment of cells. Recycling of these receptors subsequently enables reattachment and this detachment-reattachment-cycle allows migration of cells (Czekay *et al.*, 2003). Vitronectin as well as Serpin 1 (PAI-1) are expressed in testis, locating to early spermatids and Sertoli cells (Le Magueresse-Battistoni *et al.*, 1998). Additionally, mice depleted of the nonspecific Serine proteinase inhibitor Serpina5 display sterility due to unopposed proteolytic activity of Serine proteases accompanied by detachment of immature sperm and BTB impairment (Uhrin *et al.*, 2000). Upregulated Serine proteinase inhibitors in TAp73KO testis include Serpina3n, Serpinb6b and Serping1 (*Table 5.4; Figure 5.13* and *5.14*). Serping1 so

far has not been reported to be expressed in testis. Serpinb6b, on the other hand, is known to be expressed in sperm cells and Serpina3n in Sertoli cells (Charron *et al.*, 2006, Sipione *et al.*, 2006). Regulation of proteinase inhibitors by TAp73 could be important for normal adhesion of sperm cells to Sertoli cells and might therefore affect sperm cell migration and spermiation. Even if the function of the deregulated Serpins in TAp73KO mice is not known so far, their upregulation could be an indicator for imbalanced junction assembly and disassembly. Non-physiological induction of Serpins could be the cause for premature detachment of sperm cells from the seminiferous epithelium, if for example testicular Serpins interact with and inhibit junctional proteins like integrins. On the other hand, Serpin upregulation might be a secondary effect due to increased Serine protease activity on junctions of TAp73KO mice.

Deregulation of protease inhibitors, like Timp1 and Serpins, upon TAp73 loss seems to result in imbalance of proteolysis and restructuring events on testicular junctions (*Figure 6.2*). This idea is affirmed by the observation that further adhesion- and junction-related molecules, like integrinα5, integrinαX and claudin10, are deregulated in TAp73KO testis (*Table 5.4; Figure 5.14*). Additionally, TAp73 loss leads to upregulation of Adam23, which harbours a metallopeptidase domain and was reported to interact with integrins via its disintegrin domain, thereby affecting adhesion (Cal *et al.*, 2000).

Interestingly, depletion of the retinoblastoma protein Rb in Sertoli cells leads to upregulation of similar genes as in TAp73KO testis. 10% of the TAp73-regulated genes overlap with deregulated genes of RbKO Sertoli cells, especially Timp1, Serpina3n and Adam23 being strongly induced (Nalam *et al.*, 2009). Similar to our observations, Nalam et al. find infertility, impaired tissue remodelling, defective Sertoli-germ cell interactions and increased permeability of the BTB in Sertoli cell-specific conditional KO mice of Rb. Why loss of Rb leads to a comparable phenotype as loss of TAp73, cannot be explained so far.

The structure of tight junctions at the BTB is impaired in TAp73KO mice, enabling passage of exogenous substances like Biotin into the seminiferous epithelium (*Figure 5.21* and *5.22*). This functional defect of the BTB could also be the result of deregulated protease inhibitors and adhesion molecules. Sperm cells have to cross the Sertoli-Sertoli junction barrier during development and migrate to the apical part of the seminiferous epithelium. During this migration process proteases are thought to act like scissors, opening the BTB for migrating sperm cells. To enable quick reassembly of junctions after the passage of spermatocytes and to preserve homeostasis, proteases have to be deactivated by protease inhibitors. The correct interplay between proteases and their inhibitors, resulting in disassembly and reassembly of junctions, is called the junction restructuring theory (Mruk *et al.*, 2004). TAp73

appears to regulate expression levels of proteinase inhibitors and might thereby ensure sperm migration and junction restructuring. Loss of TAp73 seems to impair the balance between proteases and inhibitors, resulting in a BTB defect and premature detachment of developing sperm cells (*Figure 6.2*).

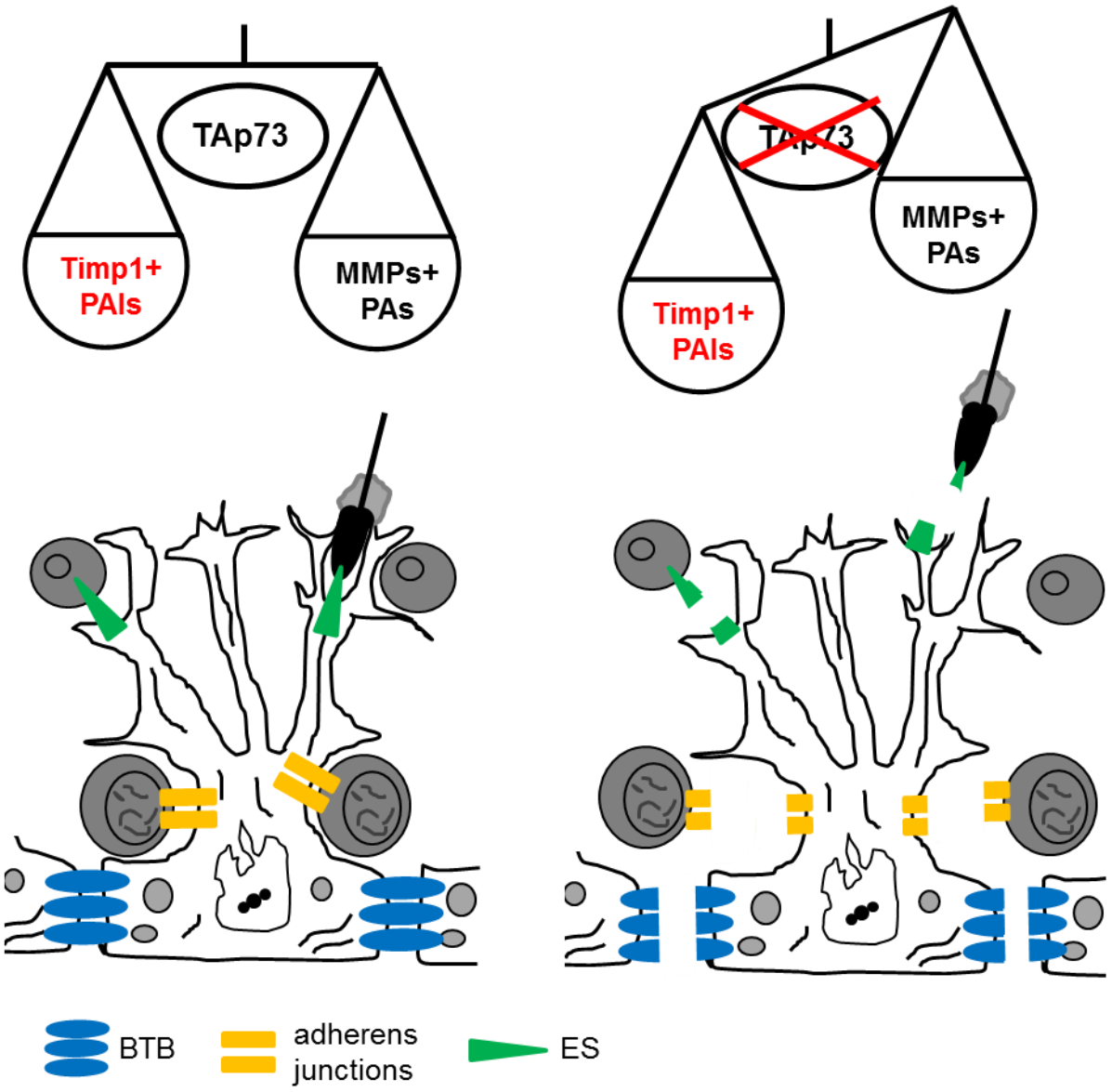

Fig. 6.2 TAp73 balances spermatogenesis

TAp73 is expressed in sperm cells of the testis. Upon loss of TAp73 the balance of protease inhibitors (Timps, PAIs) and proteases (MMPs, PAs) is lost. TAp73 depletion leads to upregulation of tissue inhibitor of metalloproteinases Timp1, several Serpins and adhesion-related molecules. These play an important role in the homeostasis of disassembly and reassembly of the BTB and Sertoli-sperm cell junctions during migration of the germ cells. Loss of TAp73 leads to an impaired BTB and junction restructuring process, resulting in detachment and premature sloughing of sperm cells from the seminiferous epithelium. TAp73 is therefore necessary to maintain normal spermatogenesis and fertility.

TAp73 is primarily located to sperm cells, but nevertheless gene expression of protease inhibitors and adhesion molecules is altered in primary Sertoli cell culture of TAp73KO testis (*Figure 5.18* and *5.19*). By acting on sperm cells TAp73 also seems to influence Sertoli cell expression. This could be explained by a crosstalk between sperm and Sertoli cells. Upregulation of target genes in KO Sertoli cells is lost during long time culture (*Figure 5.20 B*). By disrupting the interaction with sperm cells, cross-signaling is lost in primary Sertoli cells and they seem to overcome the influence of TAp73.

It might be possible that TAp73 is normally inhibiting gene expression in sperm cells, including protease inhibitors and adhesion proteins, as well as regulating a so far unknown soluble factor. Loss of TAp73 would lead to activation of this signaling molecule, which in turn is mediating gene expression in Sertoli cells. Since TGFβ3 and TNFα are involved in signaling during junction restructuring, migration and adhesion events, deregulation of these cytokines could also influence the expression of the observed target genes (Siu *et al.*, 2003, Xia *et al.*, 2005a). Both signaling molecules are described to perturb tight junctions at the BTB (Lui *et al.*, 2003b, Lui *et al.*, 2001, Lui *et al.*, 2003a, Siu *et al.*, 2003). In the seminiferous epithelium TNFα is mainly expressed in germ cells (De *et al.*, 1993). Our microarray data also show an upregulation of the TNF-receptor Tnfrsf 12a, which was reported to be expressed in Sertoli cells (*Table 5.4* and *Figure 5.14*) (Johnson *et al.*, 2007). This might resemble an increased activation of the TNF signaling pathway in sperm cells upon TAp73 depletion, acting on Sertoli cells and subsequently leading to inhibition of junction formation. Germ cells seem to signal to Sertoli cells to mediate their own detachment and migration, by inducing expression of migration related proteins. This process might be balanced by TAp73 (*Figure 6.2*).

6.6 TAp73 – a new player in spermatogenesis

During spermatogenesis sperm cells have to pass the BTB, so they can migrate towards the lumen of the testicular tubules along the Sertoli cell membrane. This process includes constant disassembly and reassembly of Sertoli-Sertoli and Sertoli-sperm junctions. If the events of junction restructuring are disrupted, spermatogenic cells fail to orientate and migration is impaired. This will lead to premature release of sperm cells from the seminiferous epithelium, resulting in infertility. Here, TAp73 is shown to be a new player in adhesion and migration processes of the seminiferous epithelium, its depletion leading to strong loss of developing sperm cells. With TAp73 a new factor in junction restructuring events is described. Especially protease inhibitors, known to be involved in sperm migration, seem to

be regulated by TAp73. Loss of TAp73 results in adhesion defects, disruption of the BTB, and premature sloughing of sperm cells. Therefore, TAp73 is not only indispensable for the female germ line, but also for the male germ line. For the first time an explanation for the reported infertility of TAp73KO males is given. However, the detailed molecular mechanisms of TAp73-mediated transcriptional inhibition in testis development and sperm migration still have to be unraveled.

7 REFERENCES

Agami R, Blandino G, Oren M, Shaul Y (1999). Interaction of c-Abl and p73alpha and their collaboration to induce apoptosis. Nature **399,** 809-813.

Agostini M, Tucci P, Chen H, Knight RA, Bano D, Nicotera P, McKeon F, Melino G (2010). p73 regulates maintenance of neural stem cell. Biochem Biophys Res Commun **403,** 13-17.

Agostini M, Tucci P, Killick R, Candi E, Sayan BS, Rivetti di Val Cervo P, Nicotera P, McKeon F, Knight RA, Mak TW, Melino G (2011). Neuronal differentiation by TAp73 is mediated by microRNA-34a regulation of synaptic protein targets. Proc Natl Acad Sci U S A **108,** 21093-21098.

Ahmed EA, Barten-van Rijbroek AD, Kal HB, Sadri-Ardekani H, Mizrak SC, van Pelt AM, de Rooij DG (2009). Proliferative activity in vitro and DNA repair indicate that adult mouse and human Sertoli cells are not terminally differentiated, quiescent cells. Biol Reprod **80,** 1084-1091.

Aitken RJ, Nixon B, Lin M, Koppers AJ, Lee YH, Baker MA (2007). Proteomic changes in mammalian spermatozoa during epididymal maturation. Asian J Androl **9,** 554-564.

Akama TO, Nakagawa H, Sugihara K, Narisawa S, Ohyama C, Nishimura S, O'Brien DA, Moremen KW, Millan JL, Fukuda MN (2002). Germ cell survival through carbohydrate-mediated interaction with Sertoli cells. Science **295,** 124-127.

Aschim EL, Saether T, Wiger R, Grotmol T, Haugen TB (2004). Differential distribution of splice variants of estrogen receptor beta in human testicular cells suggests specific functions in spermatogenesis. J Steroid Biochem Mol Biol **92,** 97-106.

Aumuller G, Steinbruck M, Krause W, Wagner HJ (1988). Distribution of vimentin-type intermediate filaments in Sertoli cells of the human testis, normal and pathologic. Anat Embryol (Berl) **178,** 129-136.

Austin CR (1952). The capacitation of the mammalian sperm. Nature **170,** 326.

Baarends WM, van der Laan R, Grootegoed JA (2001). DNA repair mechanisms and gametogenesis. Reproduction **121,** 31-39.

Baker MA, Witherdin R, Hetherington L, Cunningham-Smith K, Aitken RJ (2005). Identification of post-translational modifications that occur during sperm maturation using difference in two-dimensional gel electrophoresis. Proteomics **5,** 1003-1012.

Barakat B, O'Connor AE, Gold E, de Kretser DM, Loveland KL (2008). Inhibin, activin, follistatin and FSH serum levels and testicular production are highly modulated during the first spermatogenic wave in mice. Reproduction **136,** 345-359.

Barbieri CE, Tang LJ, Brown KA, Pietenpol JA (2006). Loss of p63 leads to increased cell migration and up-regulation of genes involved in invasion and metastasis. Cancer Res **66,** 7589-7597.

Barlow C, Liyanage M, Moens PB, Tarsounas M, Nagashima K, Brown K, Rottinghaus S, Jackson SP, Tagle D, Ried T, Wynshaw-Boris A (1998). Atm deficiency results in severe meiotic disruption as early as leptonema of prophase I. Development **125,** 4007-4017.

Bartles JR, Wierda A, Zheng L (1996). Identification and characterization of espin, an actin-binding protein localized to the F-actin-rich junctional plaques of Sertoli cell ectoplasmic specializations. J Cell Sci **109 (Pt 6),** 1229-1239.

Bellve AR, Cavicchia JC, Millette CF, O'Brien DA, Bhatnagar YM, Dym M (1977). Spermatogenic cells of the prepuberal mouse. Isolation and morphological characterization. J Cell Biol **74,** 68-85.

Belyi VA, Ak P, Markert E, Wang H, Hu W, Puzio-Kuter A, Levine AJ (2010). The origins and evolution of the p53 family of genes. Cold Spring Harb Perspect Biol **2,** a001198.

Berruti G (2006). Signaling events during male germ cell differentiation: update, 2006. Front Biosci **11,** 2144-2156.

Bertaux B, Hornebeck W, Eisen AZ, Dubertret L (1991). Growth stimulation of human keratinocytes by tissue inhibitor of metalloproteinases. J Invest Dermatol **97,** 679-685.

Beumer TL, Roepers-Gajadien HL, Gademan IS, van Buul PP, Gil-Gomez G, Rutgers DH, de Rooij DG (1998). The role of the tumor suppressor p53 in spermatogenesis. Cell Death Differ **5,** 669-677.

Beyer U, Moll-Rocek J, Moll UM, Dobbelstein M (2011). Endogenous retrovirus drives hitherto unknown proapoptotic p63 isoforms in the male germ line of humans and great apes. Proc Natl Acad Sci U S A **108,** 3624-3629.

Bicsak TA, Vale W, Vaughan J, Tucker EM, Cappel S, Hsueh AJ (1987). Hormonal regulation of inhibin production by cultured Sertoli cells. Mol Cell Endocrinol **49,** 211-217.

Blendy JA, Kaestner KH, Weinbauer GF, Nieschlag E, Schutz G (1996). Severe impairment of spermatogenesis in mice lacking the CREM gene. Nature **380,** 162-165.

Blume-Jensen P, Jiang G, Hyman R, Lee KF, O'Gorman S, Hunter T (2000). Kit/stem cell factor receptor-induced activation of phosphatidylinositol 3'-kinase is essential for male fertility. Nat Genet **24,** 157-162.

Boettger-Tong HL, Rohozinski J, Agoulnik AI, Dohmae K, Nishimune Y, Levy N, Bishop CE (2001). Identification and sequencing the juvenile spermatogonial depletion critical interval on mouse chromosome 1 reveals the presence of eight candidate genes. Biochem Biophys Res Commun **288,** 1129-1135.

Boitani C, Stefanini M, Fragale A, Morena AR (1995). Activin stimulates Sertoli cell proliferation in a defined period of rat testis development. Endocrinology **136,** 5438-5444.

Bolos V, Grego-Bessa J, de la Pompa JL (2007). Notch signaling in development and cancer. Endocr Rev **28,** 339-363.

Borg CL, Wolski KM, Gibbs GM, O'Bryan MK (2010). Phenotyping male infertility in the mouse: how to get the most out of a 'non-performer'. Hum Reprod Update **16,** 205-224.

Bourdon JC, Deguin-Chambon V, Lelong JC, Dessen P, May P, Debuire B, May E (1997). Further characterisation of the p53 responsive element--identification of new candidate genes for trans-activation by p53. Oncogene **14,** 85-94.

Bourdon JC, Fernandes K, Murray-Zmijewski F, Liu G, Diot A, Xirodimas DP, Saville MK, Lane DP (2005). p53 isoforms can regulate p53 transcriptional activity. Genes Dev **19,** 2122-2137.

Brewer LR, Corzett M, Balhorn R (1999). Protamine-induced condensation and decondensation of the same DNA molecule. Science **286,** 120-123.

Brodsky MH, Weinert BT, Tsang G, Rong YS, McGinnis NM, Golic KG, Rio DC, Rubin GM (2004). Drosophila melanogaster MNK/Chk2 and p53 regulate multiple DNA repair and apoptotic pathways following DNA damage. Mol Cell Biol **24,** 1219-1231.

Buaas FW, Kirsh AL, Sharma M, McLean DJ, Morris JL, Griswold MD, de Rooij DG, Braun RE (2004). Plzf is required in adult male germ cells for stem cell self-renewal. Nat Genet **36,** 647-652.

Buzzard JJ, Farnworth PG, De Kretser DM, O'Connor AE, Wreford NG, Morrison JR (2003). Proliferative phase sertoli cells display a developmentally regulated response to activin in vitro. Endocrinology **144,** 474-483.

Cal S, Freije JM, Lopez JM, Takada Y, Lopez-Otin C (2000). ADAM 23/MDC3, a human disintegrin that promotes cell adhesion via interaction with the alphavbeta3 integrin through an RGD-independent mechanism. Mol Biol Cell **11,** 1457-1469.

Candi E, Rufini A, Terrinoni A, Dinsdale D, Ranalli M, Paradisi A, De Laurenzi V, Spagnoli LG, Catani MV, Ramadan S, Knight RA, Melino G (2006). Differential roles of p63 isoforms in epidermal development: selective genetic complementation in p63 null mice. Cell Death Differ **13,** 1037-1047.

Carreau S, Genissel C, Bilinska B, Levallet J (1999). Sources of oestrogen in the testis and reproductive tract of the male. Int J Androl **22,** 211-223.

Casciano I, Mazzocco K, Boni L, Pagnan G, Banelli B, Allemanni G, Ponzoni M, Tonini GP, Romani M (2002). Expression of DeltaNp73 is a molecular marker for adverse outcome in neuroblastoma patients. Cell Death Differ **9,** 246-251.

Castrillon DH, Quade BJ, Wang TY, Quigley C, Crum CP (2000). The human VASA gene is specifically expressed in the germ cell lineage. Proc Natl Acad Sci U S A **97,** 9585-9590.

Celli J, Duijf P, Hamel BC, Bamshad M, Kramer B, Smits AP, Newbury-Ecob R, Hennekam RC, Van Buggenhout G, van Haeringen A, Woods CG, van Essen AJ, de Waal R, Vriend G, Haber DA, Yang A, McKeon F, Brunner HG, van Bokhoven H (1999). Heterozygous germline mutations in the p53 homolog p63 are the cause of EEC syndrome. Cell **99,** 143-153.

Chang J, Kim DH, Lee SW, Choi KY, Sung YC (1995). Transactivation ability of p53 transcriptional activation domain is directly related to the binding affinity to TATA-binding protein. J Biol Chem **270,** 25014-25019.

Charron Y, Madani R, Nef S, Combepine C, Govin J, Khochbin S, Vassalli JD (2006). Expression of serpinb6 serpins in germ and somatic cells of mouse gonads. Mol Reprod Dev **73,** 9-19.

Chemes H (1986). The phagocytic function of Sertoli cells: a morphological, biochemical, and endocrinological study of lysosomes and acid phosphatase localization in the rat testis. Endocrinology **119,** 1673-1681.

Chen C, Ouyang W, Grigura V, Zhou Q, Carnes K, Lim H, Zhao GQ, Arber S, Kurpios N, Murphy TL, Cheng AM, Hassell JA, Chandrashekar V, Hofmann MC, Hess RA, Murphy KM (2005). ERM is required for transcriptional control of the spermatogonial stem cell niche. Nature **436,** 1030-1034.

Chen PL, Chen YM, Bookstein R, Lee WH (1990). Genetic mechanisms of tumor suppression by the human p53 gene. Science **250,** 1576-1580.

Cheng CY, Wong EW, Lie PP, Li MW, Mruk DD, Yan HH, Mok KW, Mannu J, Mathur PP, Lui WY, Lee WM, Bonanomi M, Silvestrini B (2011). Regulation of blood-testis barrier dynamics by desmosome, gap junction, hemidesmosome and polarity proteins: An unexpected turn of events. Spermatogenesis **1,** 105-115.

Chi SW, Ayed A, Arrowsmith CH (1999). Solution structure of a conserved C-terminal domain of p73 with structural homology to the SAM domain. EMBO J **18,** 4438-4445.

Cho C, Willis WD, Goulding EH, Jung-Ha H, Choi YC, Hecht NB, Eddy EM (2001). Haploinsufficiency of protamine-1 or -2 causes infertility in mice. Nat Genet **28,** 82-86.

Christensen AK, Mason NR (1965). Comparative Ability of Seminiferous Tubules and Interstitial Tissue of Rat Testes to Synthesize Androgens from Progesterone-4-14c in Vitro. Endocrinology **76,** 646-656.

Chui K, Trivedi A, Cheng CY, Cherbavaz DB, Dazin PF, Huynh AL, Mitchell JB, Rabinovich GA, Noble-Haeusslein LJ, John CM (2011). Characterization and functionality of proliferative human Sertoli cells. Cell Transplant **20,** 619-635.

Chung SS, Zhu LJ, Mo MY, Silvestrini B, Lee WM, Cheng CY (1998). Evidence for cross-talk between Sertoli and germ cells using selected cathepsins as markers. J Androl **19,** 686-703.

Clermont Y (1958). Contractile elements in the limiting membrane of the seminiferous tubules of the rat. Exp Cell Res **15,** 438-440.

Cobb J, Handel MA (1998). Dynamics of meiotic prophase I during spermatogenesis: from pairing to division. Semin Cell Dev Biol **9,** 445-450.

Codelia VA, Cisterna M, Alvarez AR, Moreno RD (2010). p73 participates in male germ cells apoptosis induced by etoposide. Mol Hum Reprod **16,** 734-742.

Cohen PE, Pollack SE, Pollard JW (2006). Genetic analysis of chromosome pairing, recombination, and cell cycle control during first meiotic prophase in mammals. Endocr Rev **27,** 398-426.

Cooke HJ, Saunders PT (2002). Mouse models of male infertility. Nat Rev Genet **3,** 790-801.

Costoya JA, Hobbs RM, Barna M, Cattoretti G, Manova K, Sukhwani M, Orwig KE, Wolgemuth DJ, Pandolfi PP (2004). Essential role of Plzf in maintenance of spermatogonial stem cells. Nat Genet **36,** 653-659.

Coyne CB, Bergelson JM (2005). CAR: a virus receptor within the tight junction. Adv Drug Deliv Rev **57,** 869-882.

Czekay RP, Aertgeerts K, Curriden SA, Loskutoff DJ (2003). Plasminogen activator inhibitor-1 detaches cells from extracellular matrices by inactivating integrins. J Cell Biol **160,** 781-791.

Dadoune JP (2007). New insights into male gametogenesis: what about the spermatogonial stem cell niche? Folia Histochem Cytobiol **45,** 141-147.

de Kretser DM, Buzzard JJ, Okuma Y, O'Connor AE, Hayashi T, Lin SY, Morrison JR, Loveland KL, Hedger MP (2004). The role of activin, follistatin and inhibin in testicular physiology. Mol Cell Endocrinol **225,** 57-64.

de Kretser DM, Loveland KL, Meehan T, O'Bryan MK, Phillips DJ, Wreford NG (2001). Inhibins, activins and follistatin: actions on the testis. Mol Cell Endocrinol **180,** 87-92.

De Laurenzi V, Costanzo A, Barcaroli D, Terrinoni A, Falco M, Annicchiarico-Petruzzelli M, Levrero M, Melino G (1998). Two new p73 splice variants, gamma and delta, with different transcriptional activity. J Exp Med **188,** 1763-1768.

De Laurenzi V, Raschella G, Barcaroli D, Annicchiarico-Petruzzelli M, Ranalli M, Catani MV, Tanno B, Costanzo A, Levrero M, Melino G (2000). Induction of neuronal differentiation by p73 in a neuroblastoma cell line. J Biol Chem **275,** 15226-15231.

De Laurenzi VD, Catani MV, Terrinoni A, Corazzari M, Melino G, Costanzo A, Levrero M, Knight RA (1999). Additional complexity in p73: induction by mitogens in lymphoid cells and identification of two new splicing variants epsilon and zeta. Cell Death Differ **6,** 389-390.

de Rooij DG (2001). Proliferation and differentiation of spermatogonial stem cells. Reproduction **121,** 347-354.

De SK, Chen HL, Pace JL, Hunt JS, Terranova PF, Enders GC (1993). Expression of tumor necrosis factor-alpha in mouse spermatogenic cells. Endocrinology **133,** 389-396.

Dellas C, Loskutoff DJ (2005). Historical analysis of PAI-1 from its discovery to its potential role in cell motility and disease. Thromb Haemost **93,** 631-640.

Derry WB, Putzke AP, Rothman JH (2001). Caenorhabditis elegans p53: role in apoptosis, meiosis, and stress resistance. Science **294,** 591-595.

Deutsch GB, Zielonka EM, Coutandin D, Dotsch V (2011). Quality control in oocytes: domain-domain interactions regulate the activity of p63. Cell Cycle **10,** 1884-1885.

Di Como CJ, Gaiddon C, Prives C (1999). p73 function is inhibited by tumor-derived p53 mutants in mammalian cells. Mol Cell Biol **19,** 1438-1449.

Dirami G, Ravindranath N, Achi MV, Dym M (2001). Expression of Notch pathway components in spermatogonia and Sertoli cells of neonatal mice. J Androl **22,** 944-952.

Donehower LA, Harvey M, Slagle BL, McArthur MJ, Montgomery CA, Jr., Butel JS, Bradley A (1992). Mice deficient for p53 are developmentally normal but susceptible to spontaneous tumours. Nature **356,** 215-221.

Dotsch V, Bernassola F, Coutandin D, Candi E, Melino G (2010). p63 and p73, the ancestors of p53. Cold Spring Harb Perspect Biol **2,** a004887.

el-Deiry WS, Kern SE, Pietenpol JA, Kinzler KW, Vogelstein B (1992). Definition of a consensus binding site for p53. Nat Genet **1,** 45-49.

Enders GC, May JJ, 2nd (1994). Developmentally regulated expression of a mouse germ cell nuclear antigen examined from embryonic day 11 to adult in male and female mice. Dev Biol **163,** 331-340.

Falender AE, Freiman RN, Geles KG, Lo KC, Hwang K, Lamb DJ, Morris PL, Tjian R, Richards JS (2005). Maintenance of spermatogenesis requires TAF4b, a gonad-specific subunit of TFIID. Genes Dev **19,** 794-803.

Finlay CA, Hinds PW, Levine AJ (1989). The p53 proto-oncogene can act as a suppressor of transformation. Cell **57,** 1083-1093.

Flaman JM, Waridel F, Estreicher A, Vannier A, Limacher JM, Gilbert D, Iggo R, Frebourg T (1996). The human tumour suppressor gene p53 is alternatively spliced in normal cells. Oncogene **12,** 813-818.

Flores ER, Sengupta S, Miller JB, Newman JJ, Bronson R, Crowley D, Yang A, McKeon F, Jacks T (2005). Tumor predisposition in mice mutant for p63 and p73: evidence for broader tumor suppressor functions for the p53 family. Cancer Cell **7,** 363-373.

Flores ER, Tsai KY, Crowley D, Sengupta S, Yang A, McKeon F, Jacks T (2002). p63 and p73 are required for p53-dependent apoptosis in response to DNA damage. Nature **416,** 560-564.

Fujitani M, Cancino GI, Dugani CB, Weaver IC, Gauthier-Fisher A, Paquin A, Mak TW, Wojtowicz MJ, Miller FD, Kaplan DR (2010). TAp73 acts via the bHLH Hey2 to promote long-term maintenance of neural precursors. Curr Biol **20,** 2058-2065.

Gao F, Maiti S, Alam N, Zhang Z, Deng JM, Behringer RR, Lecureuil C, Guillou F, Huff V (2006). The Wilms tumor gene, Wt1, is required for Sox9 expression and maintenance of tubular architecture in the developing testis. Proc Natl Acad Sci U S A **103,** 11987-11992.

Gartel AL, Tyner AL (2002). The role of the cyclin-dependent kinase inhibitor p21 in apoptosis. Mol Cancer Ther **1,** 639-649.

Gerdes J, Lemke H, Baisch H, Wacker HH, Schwab U, Stein H (1984). Cell cycle analysis of a cell proliferation-associated human nuclear antigen defined by the monoclonal antibody Ki-67. J Immunol **133,** 1710-1715.

Ghafari F, Pelengaris S, Walters E, Hartshorne GM (2009). Influence of p53 and genetic background on prenatal oogenesis and oocyte attrition in mice. Hum Reprod **24,** 1460-1472.

Ghosh A, Stewart D, Matlashewski G (2004). Regulation of human p53 activity and cell localization by alternative splicing. Mol Cell Biol **24,** 7987-7997.

Giebel J, Loster K, Rune GM (1997). Localization of integrin beta 1, alpha 1, alpha 5 and alpha 9 subunits in the rat testis. Int J Androl **20,** 3-9.

Gliki G, Ebnet K, Aurrand-Lions M, Imhof BA, Adams RH (2004). Spermatid differentiation requires the assembly of a cell polarity complex downstream of junctional adhesion molecule-C. Nature **431,** 320-324.

Gonfloni S, Di Tella L, Caldarola S, Cannata SM, Klinger FG, Di Bartolomeo C, Mattei M, Candi E, De Felici M, Melino G, Cesareni G (2009). Inhibition of the c-Abl-TAp63 pathway protects mouse oocytes from chemotherapy-induced death. Nat Med **15,** 1179-1185.

Griswold MD (1998). The central role of Sertoli cells in spermatogenesis. Semin Cell Dev Biol **9,** 411-416.

Grob TJ, Novak U, Maisse C, Barcaroli D, Luthi AU, Pirnia F, Hugli B, Graber HU, De Laurenzi V, Fey MF, Melino G, Tobler A (2001). Human delta Np73 regulates a dominant negative feedback loop for TAp73 and p53. Cell Death Differ **8,** 1213-1223.

Guedez L, Stetler-Stevenson WG, Wolff L, Wang J, Fukushima P, Mansoor A, Stetler-Stevenson M (1998). In vitro suppression of programmed cell death of B cells by tissue inhibitor of metalloproteinases-1. J Clin Invest **102,** 2002-2010.

Guerquin MJ, Duquenne C, Coffigny H, Rouiller-Fabre V, Lambrot R, Bakalska M, Frydman R, Habert R, Livera G (2009). Sex-specific differences in fetal germ cell apoptosis induced by ionizing radiation. Hum Reprod **24,** 670-678.

Guglielmino MR, Santonocito M, Vento M, Ragusa M, Barbagallo D, Borzi P, Casciano I, Banelli B, Barbieri O, Astigiano S, Scollo P, Romani M, Purrello M, Di Pietro C (2011). TAp73 is

downregulated in oocytes from women of advanced reproductive age. Cell Cycle **10,** 3253-3256.

Guo X, Keyes WM, Papazoglu C, Zuber J, Li W, Lowe SW, Vogel H, Mills AA (2009). TAp63 induces senescence and suppresses tumorigenesis in vivo. Nat Cell Biol **11,** 1451-1457.

Guyot R, Magre S, Leduque P, Le Magueresse-Battistoni B (2003). Differential expression of tissue inhibitor of metalloproteinases type 1 (TIMP-1) during mouse gonad development. Dev Dyn **227,** 357-366.

Ha H, van Wijnen AJ, Hecht NB (1997). Tissue-specific protein-DNA interactions of the mouse protamine 2 gene promoter. J Cell Biochem **64,** 94-105.

Hamer G, Gademan IS, Kal HB, de Rooij DG (2001). Role for c-Abl and p73 in the radiation response of male germ cells. Oncogene **20,** 4298-4304.

Han S, Semba S, Abe T, Makino N, Furukawa T, Fukushige S, Takahashi H, Sakurada A, Sato M, Shiiba K, Matsuno S, Nimura Y, Nakagawara A, Horii A (1999). Infrequent somatic mutations of the p73 gene in various human cancers. Eur J Surg Oncol **25,** 194-198.

Handel MA, Cobb J, Eaker S (1999). What are the spermatocyte's requirements for successful meiotic division? J Exp Zool **285,** 243-250.

Hashimoto O, Nakamura T, Shoji H, Shimasaki S, Hayashi Y, Sugino H (1997). A novel role of follistatin, an activin-binding protein, in the inhibition of activin action in rat pituitary cells. Endocytotic degradation of activin and its acceleration by follistatin associated with cell-surface heparan sulfate. J Biol Chem **272,** 13835-13842.

Hayashi T, Kageyama Y, Ishizaka K, Xia G, Kihara K, Oshima H (2001). Requirement of Notch 1 and its ligand jagged 2 expressions for spermatogenesis in rat and human testes. J Androl **22,** 999-1011.

Hayashi T, Yoshinaga A, Ohno R, Ishii N, Kamata S, Yamada T (2004). Expression of the p63 and Notch signaling systems in rat testes during postnatal development: comparison with their expression levels in the epididymis and vas deferens. J Androl **25,** 692-698.

Hayrabedyan S, Todorova K, Pashova S, Mollova M, Fernandez N (2012). Sertoli cell quiescence - new insights. Am J Reprod Immunol **68,** 451-455.

Held T, Paprotta I, Khulan J, Hemmerlein B, Binder L, Wolf S, Schubert S, Meinhardt A, Engel W, Adham IM (2006). Hspa4l-deficient mice display increased incidence of male infertility and hydronephrosis development. Mol Cell Biol **26,** 8099-8108.

Hendzel MJ, Wei Y, Mancini MA, Van Hooser A, Ranalli T, Brinkley BR, Bazett-Jones DP, Allis CD (1997). Mitosis-specific phosphorylation of histone H3 initiates primarily within pericentromeric heterochromatin during G2 and spreads in an ordered fashion coincident with mitotic chromosome condensation. Chromosoma **106,** 348-360.

Hermo L, Clermont Y (1976). Light cells within the limiting membrane of rat seminiferous tubules. Am J Anat **145,** 467-483.

Hermo L, Pelletier RM, Cyr DG, Smith CE (2010). Surfing the wave, cycle, life history, and genes/proteins expressed by testicular germ cells. Part 1: background to spermatogenesis, spermatogonia, and spermatocytes. Microsc Res Tech **73,** 241-278.

Herr D, Keck C, Tempfer C, Pietrowski D (2004). Chorionic gonadotropin regulates the transcript level of VHL, p53, and HIF-2alpha in human granulosa lutein cells. Mol Reprod Dev **69,** 397-401.

Hibi K, Trink B, Patturajan M, Westra WH, Caballero OL, Hill DE, Ratovitski EA, Jen J, Sidransky D (2000). AIS is an oncogene amplified in squamous cell carcinoma. Proc Natl Acad Sci U S A **97,** 5462-5467.

Hollstein M, Shomer B, Greenblatt M, Soussi T, Hovig E, Montesano R, Harris CC (1996). Somatic point mutations in the p53 gene of human tumors and cell lines: updated compilation. Nucleic Acids Res **24,** 141-146.

Hollstein M, Sidransky D, Vogelstein B, Harris CC (1991). p53 mutations in human cancers. Science **253,** 49-53.

Hooper C, Tavassoli M, Chapple JP, Uwanogho D, Goodyear R, Melino G, Lovestone S, Killick R (2006). TAp73 isoforms antagonize Notch signalling in SH-SY5Y neuroblastomas and in primary neurones. J Neurochem **99,** 989-999.

Horvilleur E, Bauer M, Goldschneider D, Mergui X, de la Motte A, Benard J, Douc-Rasy S, Cappellen D (2008). p73alpha isoforms drive opposite transcriptional and post-transcriptional regulation of MYCN expression in neuroblastoma cells. Nucleic Acids Res **36,** 4222-4232.

Hu W, Feng Z, Atwal GS, Levine AJ (2008). p53: a new player in reproduction. Cell Cycle **7,** 848-852.

Hu W, Feng Z, Teresky AK, Levine AJ (2007). p53 regulates maternal reproduction through LIF. Nature **450,** 721-724.

Hu W, Zheng T, Wang J (2011). Regulation of Fertility by the p53 Family Members. Genes Cancer **2,** 420-430.

Hussein MR, Bedaiwy MA, Falcone T (2006). Analysis of apoptotic cell death, Bcl-2, and p53 protein expression in freshly fixed and cryopreserved ovarian tissue after exposure to warm ischemia. Fertil Steril **85 Suppl 1,** 1082-1092.

Hutson JC (1994). Testicular macrophages. Int Rev Cytol **149,** 99-143.

Ichimiya S, Kojima T, Momota H, Kondo N, Ozaki T, Nakagawara A, Toribio ML, Imamura M, Sato N (2002). p73 is expressed in human thymic epithelial cells. J Histochem Cytochem **50,** 455-462.

Jacobs WB, Govoni G, Ho D, Atwal JK, Barnabe-Heider F, Keyes WM, Mills AA, Miller FD, Kaplan DR (2005). p63 is an essential proapoptotic protein during neural development. Neuron **48,** 743-756.

Jacobs WB, Walsh GS, Miller FD (2004). Neuronal survival and p73/p63/p53: a family affair. Neuroscientist **10,** 443-455.

Jeffrey PD, Gorina S, Pavletich NP (1995). Crystal structure of the tetramerization domain of the p53 tumor suppressor at 1.7 angstroms. Science **267,** 1498-1502.

Jin S, Martinek S, Joo WS, Wortman JR, Mirkovic N, Sali A, Yandell MD, Pavletich NP, Young MW, Levine AJ (2000). Identification and characterization of a p53 homologue in Drosophila melanogaster. Proc Natl Acad Sci U S A **97,** 7301-7306.

Johnson KJ, Hensley JB, Kelso MD, Wallace DG, Gaido KW (2007). Mapping gene expression changes in the fetal rat testis following acute dibutyl phthalate exposure defines a complex temporal cascade of responding cell types. Biol Reprod **77,** 978-989.

Johnson MD, Kim HR, Chesler L, Tsao-Wu G, Bouck N, Polverini PJ (1994). Inhibition of angiogenesis by tissue inhibitor of metalloproteinase. J Cell Physiol **160,** 194-202.

Jones RC (1999). To store or mature spermatozoa? The primary role of the epididymis. Int J Androl **22,** 57-67.

Jost CA, Marin MC, Kaelin WG, Jr. (1997). p73 is a simian [correction of human] p53-related protein that can induce apoptosis. Nature **389,** 191-194.

Kaghad M, Bonnet H, Yang A, Creancier L, Biscan JC, Valent A, Minty A, Chalon P, Lelias JM, Dumont X, Ferrara P, McKeon F, Caput D (1997). Monoallelically expressed gene related to p53 at 1p36, a region frequently deleted in neuroblastoma and other human cancers. Cell **90,** 809-819.

Kang HJ, Feng Z, Sun Y, Atwal G, Murphy ME, Rebbeck TR, Rosenwaks Z, Levine AJ, Hu W (2009). Single-nucleotide polymorphisms in the p53 pathway regulate fertility in humans. Proc Natl Acad Sci U S A **106,** 9761-9766.

Kay C, Jeyendran RS, Coulam CB (2006). p53 tumour suppressor gene polymorphism is associated with recurrent implantation failure. Reprod Biomed Online **13,** 492-496.

Keyes WM, Pecoraro M, Aranda V, Vernersson-Lindahl E, Li W, Vogel H, Guo X, Garcia EL, Michurina TV, Enikolopov G, Muthuswamy SK, Mills AA (2011). DeltaNp63alpha is an oncogene that

targets chromatin remodeler Lsh to drive skin stem cell proliferation and tumorigenesis. Cell Stem Cell **8,** 164-176.

Keyes WM, Wu Y, Vogel H, Guo X, Lowe SW, Mills AA (2005). p63 deficiency activates a program of cellular senescence and leads to accelerated aging. Genes Dev **19,** 1986-1999.

Kitayner M, Rozenberg H, Kessler N, Rabinovich D, Shaulov L, Haran TE, Shakked Z (2006). Structural basis of DNA recognition by p53 tetramers. Mol Cell **22,** 741-753.

Kluin PM, Kramer MF, de Rooij DG (1984). Proliferation of spermatogonia and Sertoli cells in maturing mice. Anat Embryol (Berl) **169,** 73-78.

Koch M, Olson PF, Albus A, Jin W, Hunter DD, Brunken WJ, Burgeson RE, Champliaud MF (1999). Characterization and expression of the laminin gamma3 chain: a novel, non-basement membrane-associated, laminin chain. J Cell Biol **145,** 605-618.

Kovalev S, Marchenko N, Swendeman S, LaQuaglia M, Moll UM (1998). Expression level, allelic origin, and mutation analysis of the p73 gene in neuroblastoma tumors and cell lines. Cell Growth Differ **9,** 897-903.

Kramer JM, Erickson RP (1981). Developmental program of PGK-1 and PGK-2 isozymes in spermatogenic cells of the mouse: specific activities and rates of synthesis. Dev Biol **87,** 37-45.

Kress M, May E, Cassingena R, May P (1979). Simian virus 40-transformed cells express new species of proteins precipitable by anti-simian virus 40 tumor serum. J Virol **31,** 472-483.

Krishnamurthy H, Danilovich N, Morales CR, Sairam MR (2000). Qualitative and quantitative decline in spermatogenesis of the follicle-stimulating hormone receptor knockout (FORKO) mouse. Biol Reprod **62,** 1146-1159.

Kurita T, Cunha GR, Robboy SJ, Mills AA, Medina RT (2005). Differential expression of p63 isoforms in female reproductive organs. Mech Dev **122,** 1043-1055.

Lane DP (1992). Cancer. p53, guardian of the genome. Nature **358,** 15-16.

Lane DP, Crawford LV (1979). T antigen is bound to a host protein in SV40-transformed cells. Nature **278,** 261-263.

Le Magueresse-Battistoni B (2007). Serine proteases and serine protease inhibitors in testicular physiology: the plasminogen activation system. Reproduction **134,** 721-729.

Le Magueresse-Battistoni B, Pernod G, Sigillo F, Kolodie L, Benahmed M (1998). Plasminogen activator inhibitor-1 is expressed in cultured rat Sertoli cells. Biol Reprod **59,** 591-598.

Leblond CP, Clermont Y (1952). Definition of the stages of the cycle of the seminiferous epithelium in the rat. Ann N Y Acad Sci **55,** 548-573.

Lee AF, Ho DK, Zanassi P, Walsh GS, Kaplan DR, Miller FD (2004a). Evidence that DeltaNp73 promotes neuronal survival by p53-dependent and p53-independent mechanisms. J Neurosci **24,** 9174-9184.

Lee CJ, Kim HT, Song KW, Kim SS, Park HH, Yoon YD (2008). Ovarian expression of p53 and p21 apoptosis regulators in gamma-irradiated mice. Mol Reprod Dev **75,** 383-391.

Lee CW, La Thangue NB (1999). Promoter specificity and stability control of the p53-related protein p73. Oncogene **18,** 4171-4181.

Lee NP, Cheng CY (2004b). Ectoplasmic specialization, a testis-specific cell-cell actin-based adherens junction type: is this a potential target for male contraceptive development? Hum Reprod Update **10,** 349-369.

Lee NP, Mruk D, Lee WM, Cheng CY (2003). Is the cadherin/catenin complex a functional unit of cell-cell actin-based adherens junctions in the rat testis? Biol Reprod **68,** 489-508.

Levine AJ, Tomasini R, McKeon FD, Mak TW, Melino G (2011). The p53 family: guardians of maternal reproduction. Nat Rev Mol Cell Biol **12,** 259-265.

Lewis KA, Gray PC, Blount AL, MacConell LA, Wiater E, Bilezikjian LM, Vale W (2000). Betaglycan binds inhibin and can mediate functional antagonism of activin signalling. Nature **404,** 411-414.

Lin J, Chen J, Elenbaas B, Levine AJ (1994). Several hydrophobic amino acids in the p53 amino-terminal domain are required for transcriptional activation, binding to mdm-2 and the adenovirus 5 E1B 55-kD protein. Genes Dev **8,** 1235-1246.

Linzer DI, Levine AJ (1979). Characterization of a 54K dalton cellular SV40 tumor antigen present in SV40-transformed cells and uninfected embryonal carcinoma cells. Cell **17,** 43-52.

Liu G, Nozell S, Xiao H, Chen X (2004). DeltaNp73beta is active in transactivation and growth suppression. Mol Cell Biol **24,** 487-501.

Livera G, Petre-Lazar B, Guerquin MJ, Trautmann E, Coffigny H, Habert R (2008). p63 null mutation protects mouse oocytes from radio-induced apoptosis. Reproduction **135,** 3-12.

Lui WY, Lee WM, Cheng CY (2001). Transforming growth factor-beta3 perturbs the inter-Sertoli tight junction permeability barrier in vitro possibly mediated via its effects on occludin, zonula occludens-1, and claudin-11. Endocrinology **142,** 1865-1877.

Lui WY, Lee WM, Cheng CY (2003a). Transforming growth factor beta3 regulates the dynamics of Sertoli cell tight junctions via the p38 mitogen-activated protein kinase pathway. Biol Reprod **68,** 1597-1612.

Lui WY, Wong CH, Mruk DD, Cheng CY (2003b). TGF-beta3 regulates the blood-testis barrier dynamics via the p38 mitogen activated protein (MAP) kinase pathway: an in vivo study. Endocrinology **144,** 1139-1142.

Malaguarnera R, Vella V, Pandini G, Sanfilippo M, Pezzino V, Vigneri R, Frasca F (2008). TAp73 alpha increases p53 tumor suppressor activity in thyroid cancer cells via the inhibition of Mdm2-mediated degradation. Mol Cancer Res **6,** 64-77.

Matsui Y, Nagano R, Obinata M (2000). Apoptosis of fetal testicular cells is regulated by both p53-dependent and independent mechanisms. Mol Reprod Dev **55,** 399-405.

Melero JA, Stitt DT, Mangel WF, Carroll RB (1979). Identification of new polypeptide species (48-55K) immunoprecipitable by antiserum to purified large T antigen and present in SV40-infected and -transformed cells. Virology **93,** 466-480.

Melino G, Bernassola F, Ranalli M, Yee K, Zong WX, Corazzari M, Knight RA, Green DR, Thompson C, Vousden KH (2004). p73 Induces apoptosis via PUMA transactivation and Bax mitochondrial translocation. J Biol Chem **279,** 8076-8083.

Meng J, Holdcraft RW, Shima JE, Griswold MD, Braun RE (2005). Androgens regulate the permeability of the blood-testis barrier. Proc Natl Acad Sci U S A **102,** 16696-16700.

Meng X, Lindahl M, Hyvonen ME, Parvinen M, de Rooij DG, Hess MW, Raatikainen-Ahokas A, Sainio K, Rauvala H, Lakso M, Pichel JG, Westphal H, Saarma M, Sariola H (2000). Regulation of cell fate decision of undifferentiated spermatogonia by GDNF. Science **287,** 1489-1493.

Mills AA, Zheng B, Wang XJ, Vogel H, Roop DR, Bradley A (1999). p63 is a p53 homologue required for limb and epidermal morphogenesis. Nature **398,** 708-713.

Mirza M, Hreinsson J, Strand ML, Hovatta O, Soder O, Philipson L, Pettersson RF, Sollerbrant K (2006). Coxsackievirus and adenovirus receptor (CAR) is expressed in male germ cells and forms a complex with the differentiation factor JAM-C in mouse testis. Exp Cell Res **312,** 817-830.

Mita M, Price JM, Hall PF (1982). Stimulation by follicle-stimulating hormone of synthesis of lactate by Sertoli cells from rat testis. Endocrinology **110,** 1535-1541.

Miyashita T, Krajewski S, Krajewska M, Wang HG, Lin HK, Liebermann DA, Hoffman B, Reed JC (1994). Tumor suppressor p53 is a regulator of bcl-2 and bax gene expression in vitro and in vivo. Oncogene **9,** 1799-1805.

Moll UM, Slade N (2004). p63 and p73: roles in development and tumor formation. Mol Cancer Res **2,** 371-386.

Mori S, Kadokawa Y, Hoshinaga K, Marunouchi T (2003). Sequential activation of Notch family receptors during mouse spermatogenesis. Dev Growth Differ **45,** 7-13.

Mruk D, Zhu LJ, Silvestrini B, Lee WM, Cheng CY (1997). Interactions of proteases and protease inhibitors in Sertoli-germ cell cocultures preceding the formation of specialized Sertoli-germ cell junctions in vitro. J Androl **18,** 612-622.

Mruk DD, Cheng CY (2004). Sertoli-Sertoli and Sertoli-germ cell interactions and their significance in germ cell movement in the seminiferous epithelium during spermatogenesis. Endocr Rev **25,** 747-806.

Mruk DD, Siu MK, Conway AM, Lee NP, Lau AS, Cheng CY (2003). Role of tissue inhibitor of metalloproteases-1 in junction dynamics in the testis. J Androl **24,** 510-523.

Murray-Zmijewski F, Lane DP, Bourdon JC (2006). p53/p63/p73 isoforms: an orchestra of isoforms to harmonise cell differentiation and response to stress. Cell Death Differ **13,** 962-972.

Nakamuta N, Kobayashi S (2003). Expression of p63 in the testis of mouse embryos. J Vet Med Sci **65,** 853-856.

Nakamuta N, Kobayashi S (2004). Developmental expression of p63 in the mouse testis. J Vet Med Sci **66,** 681-687.

Nalam RL, Andreu-Vieyra C, Braun RE, Akiyama H, Matzuk MM (2009). Retinoblastoma protein plays multiple essential roles in the terminal differentiation of Sertoli cells. Mol Endocrinol **23,** 1900-1913.

Naughton CK, Jain S, Strickland AM, Gupta A, Milbrandt J (2006). Glial cell-line derived neurotrophic factor-mediated RET signaling regulates spermatogonial stem cell fate. Biol Reprod **74,** 314-321.

Nebel BR, Amarose AP, Hacket EM (1961). Calendar of gametogenic development in the prepuberal male mouse. Science **134,** 832-833.

Nemajerova A, Palacios G, Nowak NJ, Matsui S, Petrenko O (2009). Targeted deletion of p73 in mice reveals its role in T cell development and lymphomagenesis. PLoS One **4,** e7784.

Nemajerova A, Petrenko O, Trumper L, Palacios G, Moll UM (2010). Loss of p73 promotes dissemination of Myc-induced B cell lymphomas in mice. J Clin Invest **120,** 2070-2080.

Nothnick WB, Soloway PD, Curry TE, Jr. (1998). Pattern of messenger ribonucleic acid expression of tissue inhibitors of metalloproteinases (TIMPs) during testicular maturation in male mice lacking a functional TIMP-1 gene. Biol Reprod **59,** 364-370.

O'Bryan MK, Takada S, Kennedy CL, Scott G, Harada S, Ray MK, Dai Q, Wilhelm D, de Kretser DM, Eddy EM, Koopman P, Mishina Y (2008). Sox8 is a critical regulator of adult Sertoli cell function and male fertility. Dev Biol **316,** 359-370.

O'Donnell L, Nicholls PK, O'Bryan MK, McLachlan RI, Stanton PG (2011). Spermiation: The process of sperm release. Spermatogenesis **1,** 14-35.

Oakberg EF (1956). Duration of spermatogenesis in the mouse and timing of stages of the cycle of the seminiferous epithelium. Am J Anat **99,** 507-516.

Oakberg EF (1957). Duration of spermatogenesis in the mouse. Nature **180,** 1137-1138.

Oatley JM, Brinster RL (2006). Spermatogonial stem cells. Methods Enzymol **419,** 259-282.

Odet F, Guyot R, Leduque P, Le Magueresse-Battistoni B (2004). Evidence for similar expression of protein C inhibitor and the urokinase-type plasminogen activator system during mouse testis development. Endocrinology **145,** 1481-1489.

Odet F, Verot A, Le Magueresse-Battistoni B (2006). The mouse testis is the source of various serine proteases and serine proteinase inhibitors (SERPINs): Serine proteases and SERPINs identified in Leydig cells are under gonadotropin regulation. Endocrinology **147,** 4374-4383.

Odorisio T, Rodriguez TA, Evans EP, Clarke AR, Burgoyne PS (1998). The meiotic checkpoint monitoring synapsis eliminates spermatocytes via p53-independent apoptosis. Nat Genet **18,** 257-261.

Ogawa T, Ohmura M, Ohbo K (2005). The niche for spermatogonial stem cells in the mammalian testis. Int J Hematol **82,** 381-388.

Ohta H, Yomogida K, Dohmae K, Nishimune Y (2000). Regulation of proliferation and differentiation in spermatogonial stem cells: the role of c-kit and its ligand SCF. Development **127,** 2125-2131.

Osada M, Park HL, Nagakawa Y, Yamashita K, Fomenkov A, Kim MS, Wu G, Nomoto S, Trink B, Sidransky D (2005). Differential recognition of response elements determines target gene specificity for p53 and p63. Mol Cell Biol **25,** 6077-6089.

Ozaki-Kuroda K, Nakanishi H, Ohta H, Tanaka H, Kurihara H, Mueller S, Irie K, Ikeda W, Sakai T, Wimmer E, Nishimune Y, Takai Y (2002). Nectin couples cell-cell adhesion and the actin scaffold at heterotypic testicular junctions. Curr Biol **12,** 1145-1150.

Pankow S, Bamberger C (2007). The p53 tumor suppressor-like protein nvp63 mediates selective germ cell death in the sea anemone Nematostella vectensis. PLoS One **2,** e782.

Paranko J, Kallajoki M, Pelliniemi LJ, Lehto VP, Virtanen I (1986). Transient coexpression of cytokeratin and vimentin in differentiating rat Sertoli cells. Dev Biol **117,** 35-44.

Pentikainen V, Erkkila K, Suomalainen L, Otala M, Pentikainen MO, Parvinen M, Dunkel L (2001). TNFalpha down-regulates the Fas ligand and inhibits germ cell apoptosis in the human testis. J Clin Endocrinol Metab **86,** 4480-4488.

Petersen C, Boitani C, Froysa B, Soder O (2001). Transforming growth factor-alpha stimulates proliferation of rat Sertoli cells. Mol Cell Endocrinol **181,** 221-227.

Petre-Lazar B, Livera G, Moreno SG, Trautmann E, Duquenne C, Hanoux V, Habert R, Coffigny H (2007). The role of p63 in germ cell apoptosis in the developing testis. J Cell Physiol **210,** 87-98.

Pittman DL, Cobb J, Schimenti KJ, Wilson LA, Cooper DM, Brignull E, Handel MA, Schimenti JC (1998). Meiotic prophase arrest with failure of chromosome synapsis in mice deficient for Dmc1, a germline-specific RecA homolog. Mol Cell **1,** 697-705.

Pozniak CD, Barnabe-Heider F, Rymar VV, Lee AF, Sadikot AF, Miller FD (2002). p73 is required for survival and maintenance of CNS neurons. J Neurosci **22,** 9800-9809.

Pozniak CD, Radinovic S, Yang A, McKeon F, Kaplan DR, Miller FD (2000). An anti-apoptotic role for the p53 family member, p73, during developmental neuron death. Science **289,** 304-306.

Pozzi S, Zambelli F, Merico D, Pavesi G, Robert A, Maltere P, Gidrol X, Mantovani R, Vigano MA (2009). Transcriptional network of p63 in human keratinocytes. PLoS One **4,** e5008.

Rao MK, Pham J, Imam JS, MacLean JA, Murali D, Furuta Y, Sinha-Hikim AP, Wilkinson MF (2006). Tissue-specific RNAi reveals that WT1 expression in nurse cells controls germ cell survival and spermatogenesis. Genes Dev **20,** 147-152.

Robertson KM, O'Donnell L, Jones ME, Meachem SJ, Boon WC, Fisher CR, Graves KH, McLachlan RI, Simpson ER (1999). Impairment of spermatogenesis in mice lacking a functional aromatase (cyp 19) gene. Proc Natl Acad Sci U S A **96,** 7986-7991.

Robinson LL, Sznajder NA, Riley SC, Anderson RA (2001). Matrix metalloproteinases and tissue inhibitors of metalloproteinases in human fetal testis and ovary. Mol Hum Reprod **7,** 641-648.

Robinson R, Fritz IB (1981). Metabolism of glucose by Sertoli cells in culture. Biol Reprod **24,** 1032-1041.

Rommerts FF, de Jong FH, Brinkmann AO, van der Molen HJ (1982). Development and cellular localization of rat testicular aromatase activity. J Reprod Fertil **65,** 281-288.

Roosen-Runge EC (1962). The process of spermatogenesis in mammals. Biol Rev Camb Philos Soc **37,** 343-377.

Rotter V, Schwartz D, Almon E, Goldfinger N, Kapon A, Meshorer A, Donehower LA, Levine AJ (1993). Mice with reduced levels of p53 protein exhibit the testicular giant-cell degenerative syndrome. Proc Natl Acad Sci U S A **90,** 9075-9079.

Russell L (1977). Movement of spermatocytes from the basal to the adluminal compartment of the rat testis. Am J Anat **148,** 313-328.

Russell LD (1979a). Further observations on tubulobulbar complexes formed by late spermatids and Sertoli cells in the rat testis. Anat Rec **194,** 213-232.

Russell LD (1979b). Spermatid-Sertoli tubulobulbar complexes as devices for elimination of cytoplasm from the head region late spermatids of the rat. Anat Rec **194,** 233-246.

Salanova M, Stefanini M, De Curtis I, Palombi F (1995). Integrin receptor alpha 6 beta 1 is localized at specific sites of cell-to-cell contact in rat seminiferous epithelium. Biol Reprod **52,** 79-87.

Salimath B, Marme D, Finkenzeller G (2000). Expression of the vascular endothelial growth factor gene is inhibited by p73. Oncogene **19,** 3470-3476.

Sariola H, Saarma M (2003). Novel functions and signalling pathways for GDNF. J Cell Sci **116,** 3855-3862.

Scarabelli L, Caviglia D, Bottazzi C, Palmero S (2003). Prolactin effect on pre-pubertal Sertoli cell proliferation and metabolism. J Endocrinol Invest **26,** 718-722.

Schlegel RA, Hammerstedt R, Cofer GP, Kozarsky K, Freidus D, Williamson P (1986). Changes in the organization of the lipid bilayer of the plasma membrane during spermatogenesis and epididymal maturation. Biol Reprod **34,** 379-391.

Schmale H, Bamberger C (1997). A novel protein with strong homology to the tumor suppressor p53. Oncogene **15,** 1363-1367.

Schumacher B, Hofmann K, Boulton S, Gartner A (2001). The C. elegans homolog of the p53 tumor suppressor is required for DNA damage-induced apoptosis. Curr Biol **11,** 1722-1727.

Schumacher B, Schertel C, Wittenburg N, Tuck S, Mitani S, Gartner A, Conradt B, Shaham S (2005). C. elegans ced-13 can promote apoptosis and is induced in response to DNA damage. Cell Death Differ **12,** 153-161.

Schwartz D, Goldfinger N, Kam Z, Rotter V (1999). p53 controls low DNA damage-dependent premeiotic checkpoint and facilitates DNA repair during spermatogenesis. Cell Growth Differ **10,** 665-675.

Senoo M, Pinto F, Crum CP, McKeon F (2007). p63 Is essential for the proliferative potential of stem cells in stratified epithelia. Cell **129,** 523-536.

Serber Z, Lai HC, Yang A, Ou HD, Sigal MS, Kelly AE, Darimont BD, Duijf PH, Van Bokhoven H, McKeon F, Dotsch V (2002). A C-terminal inhibitory domain controls the activity of p63 by an intramolecular mechanism. Mol Cell Biol **22,** 8601-8611.

Sharpe RM, McKinnell C, Kivlin C, Fisher JS (2003). Proliferation and functional maturation of Sertoli cells, and their relevance to disorders of testis function in adulthood. Reproduction **125,** 769-784.

Shinohara T, Orwig KE, Avarbock MR, Brinster RL (2003). Restoration of spermatogenesis in infertile mice by Sertoli cell transplantation. Biol Reprod **68,** 1064-1071.

Sipione S, Simmen KC, Lord SJ, Motyka B, Ewen C, Shostak I, Rayat GR, Dufour JM, Korbutt GS, Rajotte RV, Bleackley RC (2006). Identification of a novel human granzyme B inhibitor secreted by cultured sertoli cells. J Immunol **177,** 5051-5058.

Siu MK, Lee WM, Cheng CY (2003). The interplay of collagen IV, tumor necrosis factor-alpha, gelatinase B (matrix metalloprotease-9), and tissue inhibitor of metalloproteases-1 in the basal lamina regulates Sertoli cell-tight junction dynamics in the rat testis. Endocrinology **144,** 371-387.

Sjoblom T, Lahdetie J (1996). Expression of p53 in normal and gamma-irradiated rat testis suggests a role for p53 in meiotic recombination and repair. Oncogene **12,** 2499-2505.

Skinner MK, Schlitz SM, Anthony CT (1989). Regulation of Sertoli cell differentiated function: testicular transferrin and androgen-binding protein expression. Endocrinology **124,** 3015-3024.

Soranzo L, Dadoune JP, Fain-Maurel MA (1982). [Segmentation of the epididymal duct in mouse: an ultrastructural study]. Reprod Nutr Dev **22,** 999-1012.

Stefansson S, Lawrence DA (1996). The serpin PAI-1 inhibits cell migration by blocking integrin alpha V beta 3 binding to vitronectin. Nature **383,** 441-443.

Stiewe T, Putzer BM (2002a). Role of p73 in malignancy: tumor suppressor or oncogene? Cell Death Differ **9,** 237-245.

Stiewe T, Theseling CC, Putzer BM (2002b). Transactivation-deficient Delta TA-p73 inhibits p53 by direct competition for DNA binding: implications for tumorigenesis. J Biol Chem **277,** 14177-14185.

Straub WE, Weber TA, Schafer B, Candi E, Durst F, Ou HD, Rajalingam K, Melino G, Dotsch V (2010). The C-terminus of p63 contains multiple regulatory elements with different functions. Cell Death Dis **1,** e5.

Sturzbecher HW, Donzelmann B, Henning W, Knippschild U, Buchhop S (1996). p53 is linked directly to homologous recombination processes via RAD51/RecA protein interaction. EMBO J **15,** 1992-2002.

Su X, Paris M, Gi YJ, Tsai KY, Cho MS, Lin YL, Biernaskie JA, Sinha S, Prives C, Pevny LH, Miller FD, Flores ER (2009). TAp63 prevents premature aging by promoting adult stem cell maintenance. Cell Stem Cell **5,** 64-75.

Suh EK, Yang A, Kettenbach A, Bamberger C, Michaelis AH, Zhu Z, Elvin JA, Bronson RT, Crum CP, McKeon F (2006). p63 protects the female germ line during meiotic arrest. Nature **444,** 624-628.

Sunahara M, Ichimiya S, Nimura Y, Takada N, Sakiyama S, Sato Y, Todo S, Adachi W, Amano J, Nakagawara A (1998). Mutational analysis of the p73 gene localized at chromosome 1p36.3 in colorectal carcinomas. Int J Oncol **13,** 319-323.

Takai Y, Nakanishi H (2003). Nectin and afadin: novel organizers of intercellular junctions. J Cell Sci **116,** 17-27.

Takano H (1980). [Qualitative and quantitative histology and histogenesis of the mouse epididymis, with special emphasis on the regional difference (author's transl)]. Kaibogaku Zasshi **55,** 573-587.

Talos F, Abraham A, Vaseva AV, Holembowski L, Tsirka SE, Scheel A, Bode D, Dobbelstein M, Bruck W, Moll UM (2010). p73 is an essential regulator of neural stem cell maintenance in embryonal and adult CNS neurogenesis. Cell Death Differ **17,** 1816-1829.

Tan KA, De Gendt K, Atanassova N, Walker M, Sharpe RM, Saunders PT, Denolet E, Verhoeven G (2005). The role of androgens in sertoli cell proliferation and functional maturation: studies in mice with total or Sertoli cell-selective ablation of the androgen receptor. Endocrinology **146,** 2674-2683.

Tapanainen JS, Aittomaki K, Min J, Vaskivuo T, Huhtaniemi IT (1997). Men homozygous for an inactivating mutation of the follicle-stimulating hormone (FSH) receptor gene present variable suppression of spermatogenesis and fertility. Nat Genet **15,** 205-206.

Teufel DP, Freund SM, Bycroft M, Fersht AR (2007). Four domains of p300 each bind tightly to a sequence spanning both transactivation subdomains of p53. Proc Natl Acad Sci U S A **104,** 7009-7014.

Thanos CD, Bowie JU (1999). p53 Family members p63 and p73 are SAM domain-containing proteins. Protein Sci **8,** 1708-1710.

Tissir F, Ravni A, Achouri Y, Riethmacher D, Meyer G, Goffinet AM (2009). DeltaNp73 regulates neuronal survival in vivo. Proc Natl Acad Sci U S A **106,** 16871-16876.

Tomasini R, Tsuchihara K, Tsuda C, Lau SK, Wilhelm M, Ruffini A, Tsao MS, Iovanna JL, Jurisicova A, Melino G, Mak TW (2009). TAp73 regulates the spindle assembly checkpoint by modulating BubR1 activity. Proc Natl Acad Sci U S A **106,** 797-802.

Tomasini R, Tsuchihara K, Wilhelm M, Fujitani M, Rufini A, Cheung CC, Khan F, Itie-Youten A, Wakeham A, Tsao MS, Iovanna JL, Squire J, Jurisica I, Kaplan D, Melino G, Jurisicova A, Mak

TW (2008). TAp73 knockout shows genomic instability with infertility and tumor suppressor functions. Genes Dev **22,** 2677-2691.

Tompkins AB, Hutchinson P, de Kretser DM, Hedger MP (1998). Characterization of lymphocytes in the adult rat testis by flow cytometry: effects of activin and transforming growth factor beta on lymphocyte subsets in vitro. Biol Reprod **58,** 943-951.

Trink B, Okami K, Wu L, Sriuranpong V, Jen J, Sidransky D (1998). A new human p53 homologue. Nat Med **4,** 747-748.

Tschan MP, Grob TJ, Peters UR, Laurenzi VD, Huegli B, Kreuzer KA, Schmidt CA, Melino G, Fey MF, Tobler A, Cajot JF (2000). Enhanced p73 expression during differentiation and complex p73 isoforms in myeloid leukemia. Biochem Biophys Res Commun **277,** 62-65.

Uhrin P, Dewerchin M, Hilpert M, Chrenek P, Schofer C, Zechmeister-Machhart M, Kronke G, Vales A, Carmeliet P, Binder BR, Geiger M (2000). Disruption of the protein C inhibitor gene results in impaired spermatogenesis and male infertility. J Clin Invest **106,** 1531-1539.

Ulisse S, Farina AR, Piersanti D, Tiberio A, Cappabianca L, D'Orazi G, Jannini EA, Malykh O, Stetler-Stevenson WG, D'Armiento M, et al. (1994). Follicle-stimulating hormone increases the expression of tissue inhibitors of metalloproteinases TIMP-1 and TIMP-2 and induces TIMP-1 AP-1 site binding complex(es) in prepubertal rat Sertoli cells. Endocrinology **135,** 2479-2487.

Upadhyay RD, Kumar AV, Ganeshan M, Balasinor NH (2012). Tubulobulbar complex: cytoskeletal remodeling to release spermatozoa. Reprod Biol Endocrinol **10,** 27.

Van Haaster LH, De Jong FH, Docter R, De Rooij DG (1992). The effect of hypothyroidism on Sertoli cell proliferation and differentiation and hormone levels during testicular development in the rat. Endocrinology **131,** 1574-1576.

Vernole P, Neale MH, Barcaroli D, Munarriz E, Knight RA, Tomasini R, Mak TW, Melino G, De Laurenzi V (2009). TAp73alpha binds the kinetochore proteins Bub1 and Bub3 resulting in polyploidy. Cell Cycle **8,** 421-429.

Waltz DA, Natkin LR, Fujita RM, Wei Y, Chapman HA (1997). Plasmin and plasminogen activator inhibitor type 1 promote cellular motility by regulating the interaction between the urokinase receptor and vitronectin. J Clin Invest **100,** 58-67.

Ward WS, Coffey DS (1991). DNA packaging and organization in mammalian spermatozoa: comparison with somatic cells. Biol Reprod **44,** 569-574.

Wei Y, Yu L, Bowen J, Gorovsky MA, Allis CD (1999). Phosphorylation of histone H3 is required for proper chromosome condensation and segregation. Cell **97,** 99-109.

Wilhelm MT, Rufini A, Wetzel MK, Tsuchihara K, Inoue S, Tomasini R, Itie-Youten A, Wakeham A, Arsenian-Henriksson M, Melino G, Kaplan DR, Miller FD, Mak TW (2010). Isoform-specific p73 knockout mice reveal a novel role for delta Np73 in the DNA damage response pathway. Genes Dev **24,** 549-560.

Wolski KM, Perrault C, Tran-Son-Tay R, Cameron DF (2005). Strength measurement of the Sertoli-spermatid junctional complex. J Androl **26,** 354-359.

Wright WW, Zabludoff SD, Erickson-Lawrence M, Karzai AW (1989). Germ cell-Sertoli cell interactions. Studies of cyclic protein-2 in the seminiferous tubule. Ann N Y Acad Sci **564,** 173-185.

Wu G, Nomoto S, Hoque MO, Dracheva T, Osada M, Lee CC, Dong SM, Guo Z, Benoit N, Cohen Y, Rechthand P, Califano J, Moon CS, Ratovitski E, Jen J, Sidransky D, Trink B (2003). DeltaNp63alpha and TAp63alpha regulate transcription of genes with distinct biological functions in cancer and development. Cancer Res **63,** 2351-2357.

Xia W, Cheng CY (2005a). TGF-beta3 regulates anchoring junction dynamics in the seminiferous epithelium of the rat testis via the Ras/ERK signaling pathway: An in vivo study. Dev Biol **280,** 321-343.

Xia W, Mruk DD, Lee WM, Cheng CY (2005b). Cytokines and junction restructuring during spermatogenesis--a lesson to learn from the testis. Cytokine Growth Factor Rev **16,** 469-493.

Yamaguchi K, Wu L, Caballero OL, Hibi K, Trink B, Resto V, Cairns P, Okami K, Koch WM, Sidransky D, Jen J (2000). Frequent gain of the p40/p51/p63 gene locus in primary head and neck squamous cell carcinoma. Int J Cancer **86,** 684-689.

Yan HH, Cheng CY (2005). Blood-testis barrier dynamics are regulated by an engagement/disengagement mechanism between tight and adherens junctions via peripheral adaptors. Proc Natl Acad Sci U S A **102,** 11722-11727.

Yan HH, Cheng CY (2006). Laminin alpha 3 forms a complex with beta3 and gamma3 chains that serves as the ligand for alpha 6beta1-integrin at the apical ectoplasmic specialization in adult rat testes. J Biol Chem **281,** 17286-17303.

Yan HH, Mruk DD, Lee WM, Cheng CY (2007). Ectoplasmic specialization: a friend or a foe of spermatogenesis? Bioessays **29,** 36-48.

Yang A, Kaghad M, Wang Y, Gillett E, Fleming MD, Dotsch V, Andrews NC, Caput D, McKeon F (1998). p63, a p53 homolog at 3q27-29, encodes multiple products with transactivating, death-inducing, and dominant-negative activities. Mol Cell **2,** 305-316.

Yang A, Schweitzer R, Sun D, Kaghad M, Walker N, Bronson RT, Tabin C, Sharpe A, Caput D, Crum C, McKeon F (1999). p63 is essential for regenerative proliferation in limb, craniofacial and epithelial development. Nature **398,** 714-718.

Yang A, Walker N, Bronson R, Kaghad M, Oosterwegel M, Bonnin J, Vagner C, Bonnet H, Dikkes P, Sharpe A, McKeon F, Caput D (2000). p73-deficient mice have neurological, pheromonal and inflammatory defects but lack spontaneous tumours. Nature **404,** 99-103.

Yoshida K, Kondoh G, Matsuda Y, Habu T, Nishimune Y, Morita T (1998). The mouse RecA-like gene Dmc1 is required for homologous chromosome synapsis during meiosis. Mol Cell **1,** 707-718.

Zaika AI, Kovalev S, Marchenko ND, Moll UM (1999). Overexpression of the wild type p73 gene in breast cancer tissues and cell lines. Cancer Res **59,** 3257-3263.

Zaika AI, Slade N, Erster SH, Sansome C, Joseph TW, Pearl M, Chalas E, Moll UM (2002). DeltaNp73, a dominant-negative inhibitor of wild-type p53 and TAp73, is up-regulated in human tumors. J Exp Med **196,** 765-780.

Zhu J, Jiang J, Zhou W, Chen X (1998a). The potential tumor suppressor p73 differentially regulates cellular p53 target genes. Cancer Res **58,** 5061-5065.

Zhu J, Zhou W, Jiang J, Chen X (1998b). Identification of a novel p53 functional domain that is necessary for mediating apoptosis. J Biol Chem **273,** 13030-13036.

APPENDIX

List of TAp73-regulated genes in testis – Microarray results: TAp73KO relative to WT

The table includes the name of the upregulated gene, as well as its NCBI gene number. Induction of expression in TAp73KO testis relative to WT is depicted as log2, since the threshold is set at 2. Therefore a positive number indicates upregulation in TAp73KO mice, as compared to WT mice.

The fold induction can be calculated by 2^x.

Symbol	Description	Gene	logFC	P.Value
Trp73	transformation related protein 73	22062	5,96	1,56E-05
Tas1r1	taste receptor, type 1, member 1	110326	-5,58	4,76E-06
Timp1	tissue inhibitor of metalloproteinase 1	21857	3,82	1,44E-07
Aqp5	aquaporin 5	11830	3,79	1,57E-03
Gpnmb	glycoprotein (transmembrane) nmb	93695	3,77	1,45E-03
Gm13969	predicted gene 13969	667481	3,55	1,57E-04
A_55_P1998737 probe			3,40	7,80E-08
Scrg1	scrapie responsive gene 1	20284	3,34	8,03E-05
Mpzl2	myelin protein zero-like 2	14012	3,33	1,30E-05
Olfr776	olfactory receptor 776	404321	3,30	1,51E-03
A_66_P139703 probe			3,20	3,92E-05
Cd83	CD83 antigen	12522	3,18	1,88E-05
Wnt4	wingless-related MMTV integration site 4	22417	3,18	3,79E-07
Trp73	transformation related protein 73	22062	3,17	2,72E-07
Lrg1	leucine-rich alpha-2-glycoprotein 1	76905	3,06	3,15E-04
Serpina3n	serine (or cysteine) peptidase inhibitor, clade A, member 3N	20716	3,01	1,73E-06
A_55_P2089219 probe			3,00	1,32E-08
4930486L24Rik	RIKEN cDNA 4930486L24 gene	214639	2,89	6,38E-07
Expi	extracellular proteinase inhibitor	14038	2,87	4,13E-04
Dab1	disabled homolog 1 (Drosophila)	13131	-2,84	2,63E-04
Robo4	roundabout homolog 4 (Drosophila)	74144	2,77	6,70E-06
A_51_P472879 probe			2,76	1,10E-06
Igfbp3	insulin-like growth factor binding protein 3	16009	2,72	1,79E-05
Ccl9	chemokine (C-C motif) ligand 9	20308	2,67	7,78E-04
Ccl6	chemokine (C-C motif) ligand 6	20305	2,59	1,63E-04
Aqp5	aquaporin 5	11830	2,57	2,47E-07
Tnfrsf12a	tumor necrosis factor receptor superfamily, member 12a	27279	2,44	7,02E-06
Hspb8	heat shock protein 8	80888	2,34	5,39E-07
Ly6d	lymphocyte antigen 6 complex, locus D	17068	2,29	6,92E-06
Lbh	limb-bud and heart	77889	2,26	4,16E-05
Ttr	transthyretin	22139	2,06	9,52E-04
Atf3	activating transcription factor 3	11910	2,04	4,06E-05
Mtx3	metaxin 3	382793	-1,93	8,25E-05
Fst	follistatin	14313	1,92	1,95E-04
Myoz2	myozenin 2	59006	1,92	2,04E-05

C3	complement component 3	12266	1,87	1,32E-05
Itgax	integrin alpha X	16411	1,86	1,01E-05
A_55_P2158577	probe		-1,80	6,90E-05
Casp4	caspase 4, apoptosis-related cysteine peptidase	12363	1,74	1,26E-03
Fam65c	family with sequence similarity 65, member C	69553	1,72	1,35E-03
Arl5c	ADP-ribosylation factor-like 5C	217151	1,70	1,44E-05
Gm11428	predicted gene 11428	100034251	1,69	3,86E-05
A_55_P2142232	probe		1,68	6,69E-06
Ldhd	lactate dehydrogenase D	52815	1,67	5,63E-07
Fam78b	family with sequence similarity 78, member B	226610	1,66	1,32E-03
Casp4	caspase 4, apoptosis-related cysteine peptidase	12363	1,64	1,12E-03
Psg16	pregnancy specific glycoprotein 16	26436	1,64	3,14E-07
Fos	FBJ osteosarcoma oncogene	14281	1,64	1,00E-03
Cntfr	ciliary neurotrophic factor receptor	12804	-1,62	5,53E-04
Tnni1	troponin I, skeletal, slow 1	21952	1,58	5,23E-05
Eomes	eomesodermin homolog (Xenopus laevis)	13813	-1,58	8,98E-05
Sykb	spleen tyrosine kinase	20963	1,57	1,69E-05
Aplp1	amyloid beta (A4) precursor-like protein 1	11803	1,55	3,51E-05
Plekhh3	pleckstrin homology domain containing, family H 3	217198	1,54	1,08E-05
Fam155a	family with sequence similarity 155, member A	270028	1,51	3,26E-06
Krtap11-1	keratin associated protein 11-1	16693	1,51	2,44E-05
Egr2	early growth response 2	13654	1,51	7,61E-04
5430435G22Rik	RIKEN cDNA 5430435G22 gene	226421	1,48	3,56E-06
Padi2	peptidyl arginine deiminase, type II	18600	1,48	6,56E-05
Rasl11a	RAS-like, family 11, member A	68895	1,48	2,00E-04
Lrrc2	leucine rich repeat containing 2	74249	1,47	1,92E-06
Chst8	carbohydrate (N-acetylgalactosamine 4-0) sulfotransferase 8	68947	1,47	4,70E-04
Padi2	peptidyl arginine deiminase, type II	18600	1,47	1,18E-04
C3	complement component 3	12266	1,46	4,43E-06
Gm1078	predicted gene 1078	381835	1,46	1,83E-05
Itih3	inter-alpha trypsin inhibitor, heavy chain 3	16426	1,46	8,60E-06
Serpinb6b	serine (or cysteine) peptidase inhibitor, clade B, member 6b	20708	1,45	1,40E-04
Ephb1	Eph receptor B1	270190	1,44	1,15E-05
Ddr1	discoidin domain receptor family, member 1	12305	1,41	6,00E-06
A_55_P2082854	probe		1,41	2,31E-05
Clec7a	C-type lectin domain family 7, member a	56644	1,41	8,71E-06
Gm1631	predicted gene 1631	381371	1,40	2,34E-04
S100z	S100 calcium binding protein, zeta	268686	1,40	1,47E-04
P2ry2	purinergic receptor P2Y, G-protein coupled 2	18442	1,39	6,73E-06
Gabrb3	gamma-aminobutyric acid (GABA) A receptor, subunit beta 3	14402	-1,39	6,55E-04
S100a4	S100 calcium binding protein A4	20198	1,37	2,75E-04
Fas	Fas (TNF receptor superfamily member 6)	14102	1,35	6,80E-05
Mpeg1	macrophage expressed gene 1	17476	1,35	8,61E-05
Tspan4	tetraspanin 4	64540	1,33	7,37E-06
Lcp1	lymphocyte cytosolic protein 1	18826	1,33	9,72E-06
Gad1	glutamic acid decarboxylase 1	14415	1,31	2,24E-04
Scin	scinderin	20259	1,31	2,28E-05
Vsig4	V-set and immunoglobulin domain containing 4	278180	1,31	6,01E-04
Plxnb3	plexin B3	140571	1,30	4,29E-04
Lcp1	lymphocyte cytosolic protein 1	18826	1,29	7,09E-06

Slc6a8	solute carrier family 6 (neurotransmitter transporter, creatine), 8	102857	1,29	2,11E-04
Srrm4	serine/arginine repetitive matrix 4	68955	1,26	4,04E-05
Il13ra1	interleukin 13 receptor, alpha 1	16164	1,26	1,72E-03
Phlda3	pleckstrin homology-like domain, family A, member 3	27280	1,26	6,01E-05
Serping1	serine (or cysteine) peptidase inhibitor, clade G, member 1	12258	1,25	5,80E-06
A_51_P462428 probe			1,25	9,16E-05
Zfp704	zinc finger protein 704	170753	1,24	1,61E-04
Adam23	a disintegrin and metallopeptidase domain 23	23792	1,24	1,89E-06
Nbl1	neuroblastoma, suppression of tumorigenicity 1	17965	1,23	3,56E-06
Gm3502	predicted gene 3502	100041765	1,23	1,57E-04
Ccr5	chemokine (C-C motif) receptor 5	12774	1,23	2,34E-05
Rab3b	RAB3B, member RAS oncogene family	69908	1,23	2,47E-05
Itga5	integrin alpha 5 (fibronectin receptor alpha)	16402	1,23	5,32E-06
Whrn	whirlin	73750	-1,22	1,44E-03
Cnn3	calponin 3, acidic	71994	1,22	6,86E-06
Slc6a4	solute carrier family 6 (neurotransmitter transporter, serotonin), 4	15567	1,22	4,36E-06
Ltbp1	latent transforming growth factor beta binding protein 1	268977	1,22	3,26E-04
Stk32a	serine/threonine kinase 32A	269019	1,21	4,61E-05
Myb	myeloblastosis oncogene	17863	-1,21	2,59E-04
Trim2	tripartite motif-containing 2	80890	1,20	4,11E-05
Stk32a	serine/threonine kinase 32A	269019	1,20	1,02E-04
Tspan8	tetraspanin 8	216350	1,20	8,30E-05
Serping1	serine (or cysteine) peptidase inhibitor, clade G, member 1	12258	1,19	3,31E-06
Ttc34	tetratricopeptide repeat domain 34	242800	-1,19	9,72E-06
Lilrb3	leukocyte immunoglobulin-like receptor, subfamily B	18733	1,18	5,99E-06
Cadps	Ca2+-dependent secretion activator	27062	1,18	2,90E-06
Tnfrsf1b	tumor necrosis factor receptor superfamily, member 1b	21938	1,18	2,48E-04
Tlr12	toll-like receptor 12	384059	1,16	6,24E-04
2610002J02Rik	RIKEN cDNA 2610002J02 gene	67513	-1,16	7,26E-06
Gm2737	predicted gene 2737	100040368	1,15	3,03E-05
Klrb1a	killer cell lectin-like receptor subfamily B member 1A	17057	1,14	2,88E-06
Ermap	erythroblast membrane-associated protein	27028	1,14	6,38E-04
4931406P16Rik	RIKEN cDNA 4931406P16 gene	233103	1,13	1,24E-05
Dpt	dermatopontin	56429	1,13	1,64E-03
Emp1	epithelial membrane protein 1	13730	1,13	3,10E-04
Cpe	carboxypeptidase E	12876	1,13	1,95E-06
Defa1	defensin, alpha 1	13216	1,13	3,21E-04
Spnb1	spectrin beta 1	20741	1,12	6,87E-05
Wnt10a	wingless related MMTV integration site 10a	22409	1,12	2,50E-04
2610002J02Rik	RIKEN cDNA 2610002J02 gene	67513	-1,12	1,36E-05
Slc4a3	solute carrier family 4 (anion exchanger), member 3	20536	1,12	4,08E-06
Rbp1	retinol binding protein 1, cellular	19659	1,12	2,69E-04
Mpeg1	macrophage expressed gene 1	17476	1,12	2,27E-05
Accn1	amiloride-sensitive cation channel 1, neuronal (degenerin)	11418	1,12	1,96E-04
Cldn10	claudin 10	58187	-1,11	1,19E-03
Il1rl1	interleukin 1 receptor-like 1	17082	1,11	8,97E-04
Cd74	CD74 antigen, invariant polypeptide of MHC	16149	1,11	9,86E-05
Il1r1	interleukin 1 receptor, type I	16177	1,10	6,75E-05
Evi2a	ecotropic viral integration site 2a	14017	1,10	1,24E-04
Nfkb2	nuclear factor of kappa light polypeptide gene enhancer in B-cells	18034	1,09	1,13E-05

	2			
Psen2	presenilin 2	19165	1,09	3,74E-05
Inf2	inverted formin, FH2 and WH2 domain containing	70435	1,08	1,03E-04
Cmtm3	CKLF-like MARVEL transmembrane domain containing 3	68119	1,08	4,48E-06
Il17ra	interleukin 17 receptor A	16172	1,08	6,56E-05
Apoc1	apolipoprotein C-I	11812	1,07	9,27E-05
Eda	ectodysplasin-A	13607	1,07	3,92E-05
A630023P12Rik	RIKEN cDNA A630023P12 gene	231603	1,06	3,44E-04
Spink8	serine peptidase inhibitor, Kazal type 8	78709	1,05	3,00E-04
Lilrb4	leukocyte immunoglobulin-like receptor, subfamily B, member 4	14728	1,05	5,93E-04
Cpe	carboxypeptidase E	12876	1,05	3,14E-06
Slc4a3	solute carrier family 4 (anion exchanger), member 3	20536	1,05	5,16E-06
Pdpn	podoplanin	14726	1,05	1,19E-04
Mmp23	matrix metallopeptidase 23	26561	1,04	9,40E-04
Lipa	lysosomal acid lipase A	16889	1,04	3,95E-05
Mgp	matrix Gla protein	17313	1,03	3,34E-06
Cnn3	calponin 3, acidic	71994	1,03	7,36E-06
Aqp8	aquaporin 8	11833	1,03	1,25E-04
Cfi	complement component factor i	12630	1,03	2,12E-05
Gpr137b	G protein-coupled receptor 137B	83924	1,02	1,56E-05
Gbx1	gastrulation brain homeobox 1	231044	1,01	2,18E-04
Clec4a3	C-type lectin domain family 4, member a3	73149	1,01	4,49E-05
Fosl2	fos-like antigen 2	14284	1,01	1,07E-03
Osmr	oncostatin M receptor	18414	1,01	3,19E-04
Car11	carbonic anhydrase 11	12348	1,00	1,59E-04